Production and Characterization of Bio-oil and Its Utilization in the Synthesis of Bio-based Epoxy Resin

by

Yusuf Celikbag

A dissertation submitted to the Graduate Faculty of
Auburn University
in partial fulfillment of the
requirements for the Degree of
Doctor of Philosophy

Auburn, Alabama
December 10, 2016

Keywords: hydrothermal liquefaction, bio-oil, ^{31}P-NMR, hydroxyl number, bio-based epoxy

Approved by

Brian K. Via, Chair, Associate Professor, School of Forestry and Wildlife Sciences
Sushil Adhikari, Associate Professor, Department of Biosystem Engineering
Maria L. Auad, Associate Professor, Department of Chemical Engineering
Gisela Buschle-Diller, Professor, Department of Biosystem Engineering

Abstract

Epoxy resins (ERs) are one of the most versatile thermoset polymers which are widely used in variety of applications from electrical and electronics (insulation and circuit boards) to construction and civil engineering works (coating of concrete floors), automotive (structural glue), and aircraft (carbon fiber reinforced composites) industries due to their superior properties such as toughness, mechanical strength, flexibility, chemical and thermal resistance and adhesion. The global epoxy production is projected to be 3 million tons by 2017 with a market size of USD 21.5 billion. Today epoxy and other plastic production processes rely on petroleum-based chemicals. Current petroleum use is large and creates significant problems such as air pollution, promotion of the greenhouse effect, and depletion of petroleum reserves. Therefore, environmental concerns, as well as instability in the petrochemical market, have recently increased in using more sustainable and renewable chemical resources.

Bio-oil is a liquefied biomass produced by decomposition of lignocellulosic biomass through thermomechanical liquefaction processes, and it could be used as a biopolyol to synthesize bio-based epoxy resin due to its high hydroxyl number (OHN). The main hypothesis was that the reaction behavior and the consequent physical, mechanical, and thermal properties of resulting epoxy resin depend on the interaction between OH group availability in bio-oil and epoxy group in epichlorohydrin Therefore, the objectives of this dissertation were to (i) produce a high quality bio-oil via thermomechanical liquefaction of lignocellulosic biomass, (ii)

investigate the source and variation of hydroxyl (OH) groups in bio-oil, and (iii) utilize the bio-oil as an alternative to petroleum-based polyols for the synthesis of bio-based epoxy resin.

Bio-oils from different thermomechanical liquefaction processes, organic solvent liquefaction (OSL) and hydrothermal liquefaction (HTL), were studied. In Chapters 3 and 4, OSL of loblolly pine in ethylene glycol (EG) using atmospheric reactor and Parr® reactor at different liquefaction time and temperature was studied, respectively. It was found that bio-oil from OSL process (OSL-bio-oil) had a high hydroxyl number (11.3 – 26.4 mmol/g); however, gas chromatography–mass spectrometry (GC-MS) results revealed that unreacted liquefying solvent (EG) left in the OSL-bio-oil was the major source of the high OHN, and accounted for the 70 – 95% of the total OHN. ^{31}P-NMR analysis of OSL-bio-oils showed that the majority of OH groups was aliphatic type. The focus of Chapter 5 was on the HTL process of loblolly pine. HTL was performed in water and water/ethanol medium at different temperatures. For the first time, ^{31}P-NMR and ^{19}F-NMR were employed to understand the effect of ethanol on the formation bio-oil. It was found that addition of ethanol significantly increased the yield of bio-oil (from 25 to 68 wt.%) and decreased the residue yield (from 39 to 2 wt.%), increased the hydroxyl concentration (from 3.91 to 7.42 mmol/g), and decreased the carbonyl concentration (from 3.46 to 2.53 mmol/g). Analysis showed that more aliphatic and less phenolic type OH was obtained when ethanol was used as a co-solvent in HTL process.

Utilization of bio-oil in ER systems was studied in Chapters 6 and 7. A commercial epoxy resin (EPON828) was cured using a pyrolysis bio-oil (Chapter 6). The resulting cured ER exhibited superior thermal and mechanical properties. The glass transition temperature (Tg),

crosslink density, and storage modulus at room temperature was found to be 120 ℃, 1891

mol/m^3, and 2.55 GPa, respectively, using dynamic mechanical analysis (DMA). In the last

chapter, Chapter 7, synthesis and characterization of a novel bio-oil-based self-curing epoxy

resin was presented. For the first time, HTL-bio-oil was utilized as an alternative to bisphenol-A

(BPA) in epoxy synthesis. It was found that the resulting bio-oil-based epoxy resin could be

cured without using a curing agent. Differential Scanning Calorimetry (DSC) analysis proved the

self-curing phenomena, and the activation energy for curing was calculated to be 95 – 98 kJ/mol,

using Kissinger model of kinetic analysis. Self-curing phenomena of bio-oil-based epoxy resin

was attributed to etherification reaction based on the evidences obtained from Fourier Transform

Infrared Spectroscopy (FT-IR) and curing kinetic analysis. Tg, crosslinking density, and the

storage modulus of self-cured epoxy resin were obtained from DMA to be 96 ℃, 58.7 mol/m^3,

and 845 MPa, respectively.

Acknowledgments

All praises and thanks be to Allah, the most merciful, the most companionate.

I would like to start expressing my sincere gratitude to my major advisor, Dr. Brian K. Via, for giving me the opportunity to pursue a doctorate degree. This work would not have been possible without his guidance and help. I would also thank to my dissertation committee, Dr. Sushil Adhikari, Dr. Maria Auad and Dr. Gisela Buschle-Diller, for their support, encouragement and help. Special thanks to Dr. Mario Eden for accepting to be the outside reader of my dissertation, and giving me the opportunity to be a member of NSF-IGERT team. I deeply appreciate the NSF-IGERT team for their financial support for my studies. I would like to thank Forest Product Development Center at Auburn University for providing me a welcoming environment. I must also recognize my friends in Auburn for their continues motivation.

Finally, I would like to express my deepest gratitude to my dear family, my mother Nahide Celikbag, and sisters Semanur Ekinci and Esmanur Nazli, for their unconditional love and support. I would like to dedicate this dissertation to my beloved father, Huseyin Celikbag (1955 – 2001).

Table of Contents

List of Tables

List of Figures

xvi

Chapter 1

Introduction

Epoxy resins (ERs) are thermosetting polymers that contain one or more epoxide groups in its structure. Using a proper curing agent or a catalyst, ERs are crosslinked to create a network structure. Crosslinked epoxy resins exhibit high toughness, mechanical strength, flexibility, chemical and thermal resistance and adhesion. Therefore, ERs have wide range applications in electrical and electronics (insulation and circuit boards), construction and civil engineering works (coating of concrete floors), automotive (structural glue), and aircraft (carbon fiber reinforced composites) industries. The North America, the epoxy resin market was amounted to approximately USD 1.0 billion in 2015, and is predicted to be USD 1.4 billion by 2020 (Research 2016); the global epoxy production, on the other hand, is projected to be 3 million tons by 2017 with a market size of USD 21.5 billion (Auvergne et al. 2014).

Theoretically, two components are needed to synthesize an ER, namely: (i) a component for a source of an epoxide functionality, and (ii) a polyol that undergoes condensation reaction with epoxide groups in the presence of a catalyst. The most widely used ER is the diglycidyl ether of bisphenol A (DGEBA) which accounts for approximately 75% of the ER in the market today (Pham and Marks 2000). Epichlorohydrin (ECH) and bisphenol A (BPA) are used as the source of an epoxide and a polyol, respectively, in the synthesis of DGEBA. One of the

challenges that epoxy market is facing today is the toxicity issue of BPA. The toxicity of BPA has raised questions and concerns regarding its use in epoxy resins. The U.S. Food and Drug Administration (FDA) and European Union (EU) have banned the use of BPA-based epoxy resins as coatings in infant formula packaging in 2013 and 2011, respectively (EU 2011, FDA 2013). In addition, today ERs as well as the other plastic production rely on the petroleum resources. Using petroleum in such a large volume creates significant problems such as air pollution, promoting the greenhouse effect, and depleting petroleum reserves (Naik et al. 2010). Therefore, there is an increasing effort to explore bio-based polyol to be used in epoxy synthesis as an alternative to BPA. Moreover, the uncertainty in the price of petroleum as well as the social tendency toward materials from renewable and sustainable resources have also motivated researchers to focus on bio-based materials.

Bio-oil is defined as "liquefied biomass" produced by decomposition of lignocellulosic biomass through thermomechanical liquefaction processes (organic solvent liquefaction, fast pyrolysis and hydrothermal liquefaction), and it could be used as a biopolyol and alternative to BPA to synthesize bio-based epoxy resin due to its high hydroxyl number (OHN). Lignocellulosic biomass, on the other hand, is an abundant natural resource with an annual production of 1.3 billion dry tons in the USA (Perlack et al. 2005), and has attracted interests to be used as a feedstock to manufacture industrial polymer and plastics. The U.S. Department of Energy (DOE) and the U.S. Department of Agriculture (USDA) have prioritized the development of bioenergy and bioproducts, and they have a goal to produce 18% of the current U.S. chemical commodities from lignocellulosic biomass by 2020, and 25% by 2030 (Perlack et al. 2005). In addition, the Dutch Ministry of Economic Affairs in Europe also set a long term

goal to replace 30% of the chemicals produced from fossil resources with bio-based alternatives by 2030 (Ree and Annevelink 2007).

1.1. Rationale and Significance

U.S. Department of Energy (DOE) and U.S. Department of Agriculture (USDA) have priority for the development of bioenergy and bioproducts for the U.S to reduce our dependency on foreign petroleum. This dissertation will contribute to initiate this development plan. A procedure to produce high quality bio-oil via liquefaction of loblolly pine (*Pinus taeda*) as a renewable and sustainable alternative resource to petroleum has been developed. Utilization of bio-oil in epoxy synthesis is a challenge due to the complex chemical composition of bio-oil and lack of understanding of decomposition mechanism of lignocellulosic biomass. As a result of this dissertation: **(i)** a comprehensive hydroxyl (OH) and carbonyl (C=O) group characterization protocol using ^{31}P-NMR and ^{19}F-NMR analysis, **(ii)** fundamental understanding of the source and variation of hydroxyl groups within bio-oil, and **(iii)** a novel bio-oil based self-curing epoxy resin have been developed.

1.2. Research Plan

The main hypothesis of this dissertation was that the reaction behavior and the consequent physical, mechanical, and thermal properties of bio-oil-based epoxy resin depend on the interaction between OH group availability in the bio-oil and epoxy group in the epichlorohydrin. The overall objective of this project, on the other hand, was to synthesize and characterize bio-oil-based epoxy resin that is comparable in mechanical and thermal properties to the conventional petroleum-based epoxy resin. One challenge in the utilization of bio-oil as a

3

bio-based polyol is to determine the source and variation of OH and C=O groups in bio-oil due to the complex nature of lignocellulosic biomass. Characterization of the OH groups as well as C=O groups is a must to be able to engineer the properties of bio-based polymers synthesized using bio-oil since the bio-oil reacts with other monomers through its OH groups. C=O groups, on the other hand, such as aldehydes, ketones and quinones play a major role in the aging of bio-oil during storage and equipment corrosion. Therefore, this dissertation consisted of two main sections: **(Section-i)** production and characterization of bio-oil produced by thermomechanical liquefaction of lignocellulosic biomass, and **(Section-ii)** utilization of bio-oil in the synthesis and curing of an epoxy resin.

1.3. Organization of the Dissertation

Sections i and ii were divided into five specific objectives. Section-i was studied in Chapters 3, 4 and 5; and the Section-ii resulted in Chapters 6 and 7. A detailed literature review about epoxy resins, thermomechanical liquefaction of biomass, bio-oil and bio-oil characterization has been given in Chapter 2.

In Chapter 3, liquefaction of loblolly pine in ethylene glycol (EG) at different reaction time using atmospheric glass reactor was studied. OHN of resulting bio-oil and chemical analysis of the residue was investigated using phthalic esterification, X-Ray diffractograms (XRD), and Attenuated total reflection Fourier Transform (ATR-FTIR) Infrared analysis.

In Chapter 4, liquefaction of loblolly pine in ethylene glycol (EG) at different reaction temperature using Parr® reactor was studied. The source and variation of OH groups depending

on the reaction temperature has been investigated performing phthalic esterification, Gas chromatography–mass spectrometry (GC-MS), and ^{31}P-NMR. A fundamental understanding about the decomposition of lignocellulosic biomass was provided.

In Chapter 5, hydrothermal liquefaction (HTL) of loblolly pine at different liquefying solvents and temperature was studied. The effect of reaction conditions on the formation of OH and C=O groups was investigated using ^{31}P-NMR and ^{19}F-NMR.

In Chapter 6, utilization of bio-oil as a bio-based curing agent in a commercial epoxy resin was investigated. Compatibility of bio-oil in an epoxy resin was studied using Dynamic mechanical analysis (DMA).

In Chapter 7, a novel self-curing epoxy resin was developed using bio-oil. Chemistry and curing kinetics of resulting epoxy resin was investigated by Differential scanning calorimetry (DSC), and ATR-FTIR. Thermomechanical properties of the epoxy resin were studied by DMA.

References

1. Auvergne, R., S. Caillol, G. David, B. Boutevin, and J. P. Pascault. 2014. Biobased Thermosetting Epoxy: Present and Future. Chemical Reviews **114**:1082-1115.

2. EU. 2011. The restriction of use of Bisphenol A in plastic infant feeding bottles. Official Journal of the European Union, http://eur-lex.europa.eu/LexUriServ/LexUriServ.do?uri=OJ:L:2011:026:0011:0014:EN:PDF (accessed September 2016).

3. FDA. 2013. Indirect Food Additives: Adhesives and Components of Coatings. Food and Drug Administration, https://www.gpo.gov/fdsys/pkg/FR-2013-07-12/pdf/2013-16684.pdf (accessed September 2016).

4. Naik, S. N., V. V. Goud, P. K. Rout, and A. K. Dalai. 2010. Production of first and second generation biofuels: A comprehensive review. Renewable and Sustainable Energy Reviews **14**:578-597.

5. Perlack, R. D., L. L. Wright, A. F. Turhollow, R. L. Graham, B. J. Stokes, and D. C. Erbach. 2005. Biomass as feedstock for a bioenergy and bioproducts industry: the technical feasibility of a billion-ton annual supply. DTIC Document.

6. Pham, H. Q. and M. J. Marks. 2000. Epoxy Resins. Ullmann's Encyclopedia of Industrial Chemistry. Wiley-VCH Verlag GmbH & Co. KGaA.

7. Ree, R. v. and B. Annevelink. 2007. Status Report Biorefinery 2007. Agrotechnology and Food Sciences Group.

8. Research, G. V. 2016. Epoxy Resin Market Analysis By Application (Paints & Coatings, Wind Turbine, Composites, Construction, Electrical & Electronics, Adhesives) And Segment Forecasts To 2024, http://www.grandviewresearch.com/industry-analysis/epoxy-resins-market, (accessed September 2016).

Chapter 2

Literature Review

2.1. Epoxy Resin

Epoxy resin (ER) is a term which is used to describe a compound that contains one or more epoxide functional groups in its structure. An epoxide, also called glycidyl or oxirane group, is a three-membered cyclic ether as illustrated in Fig. 2.1. The first ER was synthesized in 1891, patented in 1930, and commercially produced in 1940 (Ellis 2012). ERs are traditionally synthesized by condensation reaction of an epoxide containing compound with a polyhdyroxyl compound (polyol). Various types of ERs have been synthesized using different types of polyols since the invention of ERs. The three most common ERs in the market are diglycidyl ether of bisphenol-A (DGEBA), diglycidyl ether of bisphenol-F (DGEBF), and epoxy novolac resin (ENR) which are synthesized using polyols of bisphenol-A (BPA), bisphenol-F (BPF), and novolac, respectively (Fig. 2.2).
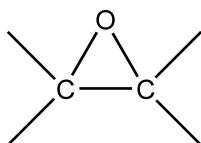
Fig. 2.1. Epoxide (glycidyl or oxirane) functional group.
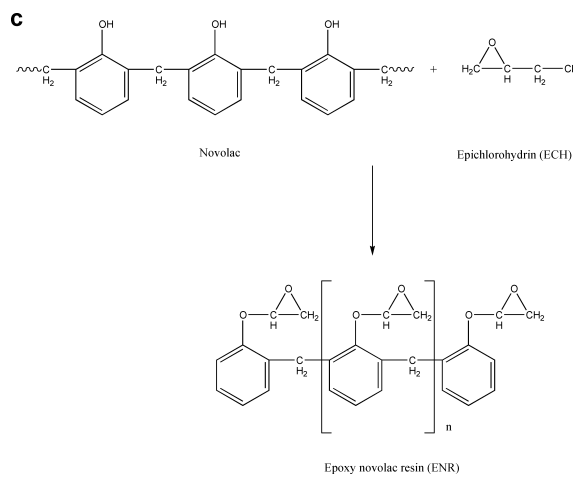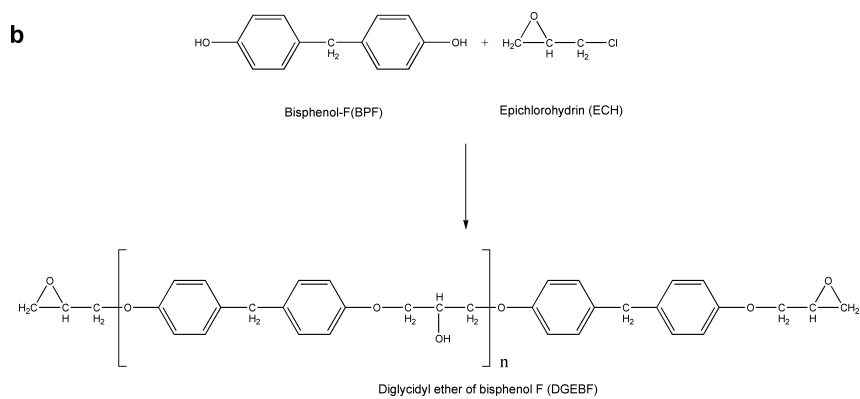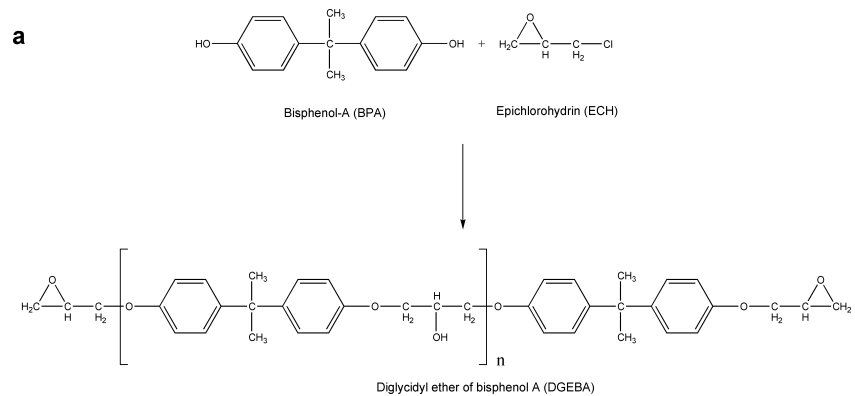
Fig. 2.2. The most common ERs in the market; **(a)** diglycidyl ether of bisphenol A (DGEBA), **(b)** diglycidyl ether of bisphenol F (DGEBF), and **(c)** epoxy novolac resin (ENR).

Due to the different chemical structure of the polyols, these ERs exhibit different chemical and physical properties as summarized in Table 2.1. BPA and BPF have similar chemical structure except the methyl groups. However, methyl groups in BPA increased the molecular weight which resulted in higher viscosity of DGEBA as compared to DGEBF. Moreover, lower epoxy equivalent weight (EEW) of DGEBF was also attributed to the missing methyl groups in BPF (Durig 2000). As can be seen in Table 2.1, ENR had the highest viscosity and functionality values which makes it a good candidate to be used in the applications where high thermal and chemical resistance are required. Heat deflection temperature of an ENR with a 2.5 – 3 functionality was reported to be 30 – 40 °C higher than DGEBA (Lee and Neville 1957).

Table 2.1. Key properties of DGEBA, DGEBF, and ENR (Kuo 2016).

	n*	Viscosity (cps, at 25 °C)	EEW (g/eq)	Functionality
DGEBA	0.1-12	11,000 - 15,000	188 - 3200	1.9
DGEBF	0.15	2,500 - 5,000	165	2.1
ENR	0.2-1.8	20,000 - 50,000	175 - 200	1.6 - 3.5

*n is the number of repeating units in the ER backbone.

2.1.1. Synthesis of ER

In general, aromatic types of polyols (**1**) are used in the synthesis of ER since aromatics provide thermal resistance, toughness and rigidity (Pham and Marks 2000). The synthesis of ER starts with the formation of phenate ion (**3**) by the reaction of sodium hydroxide (NaOH) (**2**) and aromatic polyol as illustrated in Fig. 2.3. Early studies showed that phenate ion may react with ECH (**4**) in two different mechanisms: (i) one-step nucleophilic substitution (S_N2), and/or (ii) ring opening reactions (Bradley et al. 1951). In the case of S_N2 reaction, Cl–C bond is attacked by the phenate ion, and ER (**5**) is produced by the introduction of epoxide group in ECH to the

aromatic polyol. The other possible reaction is the ring opening of ECH which yields an intermediate compound of **6**. ER (**5**) is produced as a result of dehydrochlorination of compound **6** by NaOH. However, incomplete dehydrochlorination may also occur which yields a side product, 1-chloro-3-aryloxypropan-2-ols (**7**).
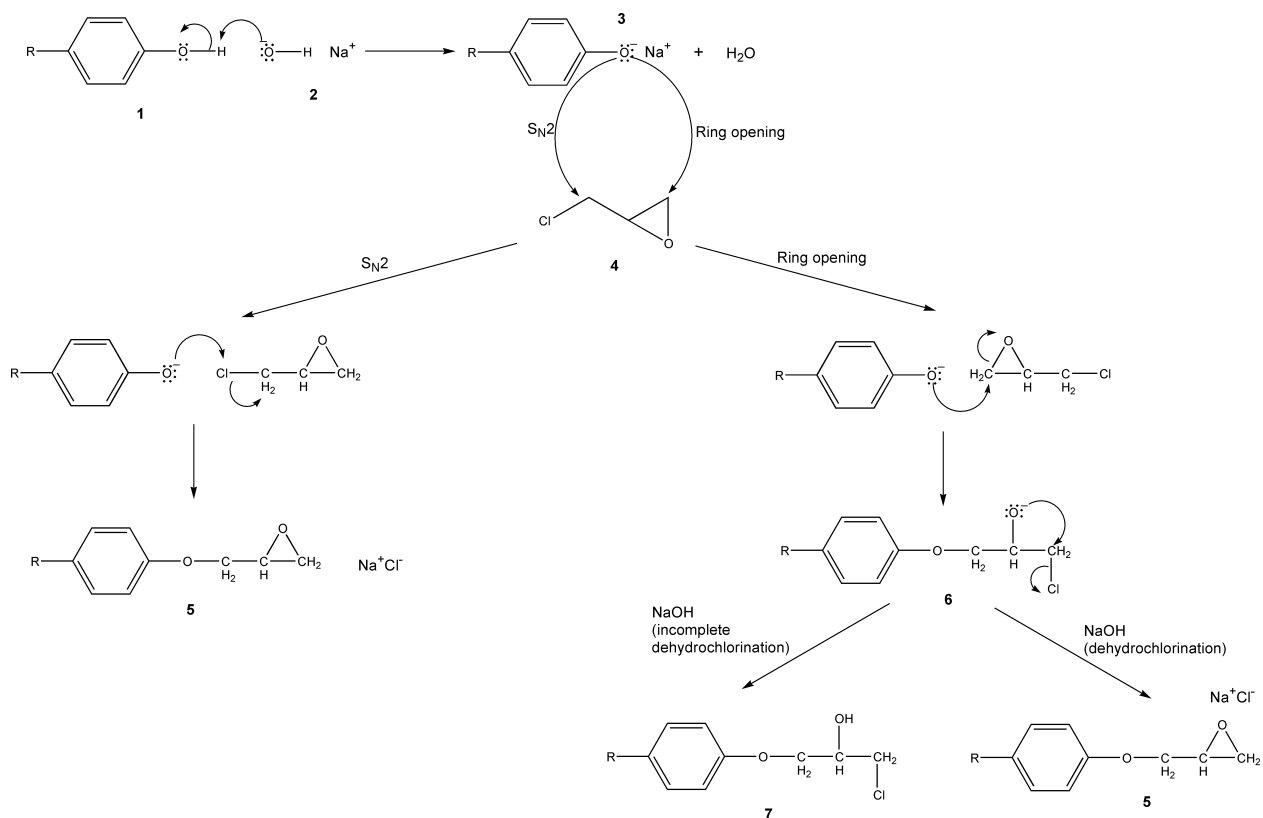
Fig. 2.3. Reaction mechanisms of ER.

The molecular weight (MW) of ER depends on the ratio of ECH and aromatic polyol in the reaction mixture. For example, when using BPA as an aromatic polyol, if the ratio of ECH/BPA is 2, the other ECH left in the reaction mixture reacts with the other anion side of the BPA, and monomeric DGEBA is obtained. However, when the ratio of ECH/BPA was 2, the yield of monomeric DGEBA has been reported to be less than 10% (Lee and Neville 1957).

10

Therefore, usually excess ECH is used to obtain high yield of monomeric DGEBA. In practice, liquid epoxy resin (molecular weight ≈ 380) is synthesized using the ratio of ECH/BPA of 10. When the ratio of ECH/BPA gets closer to 1, higher molecular weight epoxy resin is obtained. For example, if the ratio of ECH/BPA is 3/2, one anion side of the BPA attacks to epoxide ring, then yields to a dimer, as illustrated in Figure 2.4.
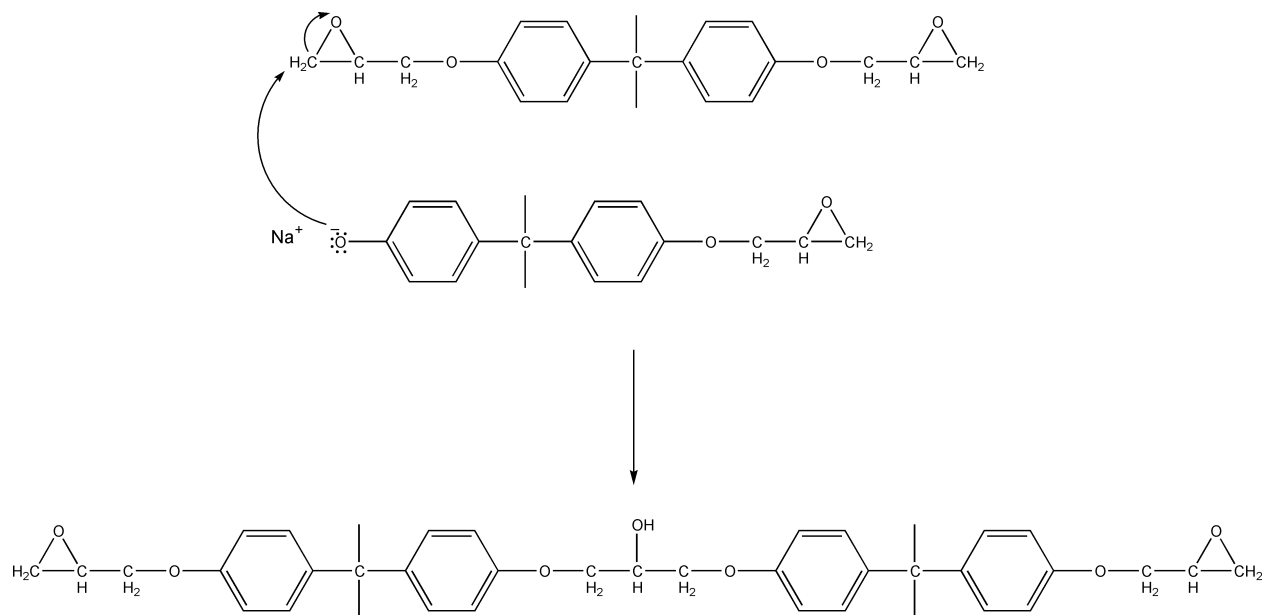
Fig. 2.4. Formation of dimer of DGEBA.

It is clear that the ratio of ECH/BPA is an important factor to control the molecular weight and the degree of polymerization of DGBEA. In the synthesis of ER, molecular weight is adjusted by the amount of ECH. Higher ratio of ECH/BPA produces shorter chains with ECH on both ends. Fewer ratios give longer DGEBA chains which means more viscous epoxy resin. Table 2.2 shows effect of ECH/BPA ratio on molecular weight of resulting epoxy resin.

Table 2.2. The effect of ECH/BPA ratio on molecular weight (MW) and epoxy equivalent weight (EEW) (Lee and Neville 1957).

Molar ratio of ECH/BPA	MW (g/mol)	EEW (g/eq)
2.0	451	314
1.4	84	592
1.33	90	730
1.25	100	862
1.2	112	1176

Besides the reaction mechanisms shown in Fig. 2.3, there are also some unavoidable side reactions take place during the synthesis of ER such as hydrolysis and abnormal addition of ECH, and formation of bound chlorides (Fig. 2.5). α-glycol can be observed in the ER as a result of hydrolysis of ECH in small quantities (0.1 – 5%), and reported to increase the curing yield of ER with diamines which could be attributable to the additional OH groups (Pham and Marks 2000). Abnormal addition of ECH occurs when the central carbon of ECH is cleaved by the phenate ion (Fig. 2.5b). Formation of bound chlorides is observed when ECH and OH groups reacts each other in the polymer backbone (Fig. 2.5c).
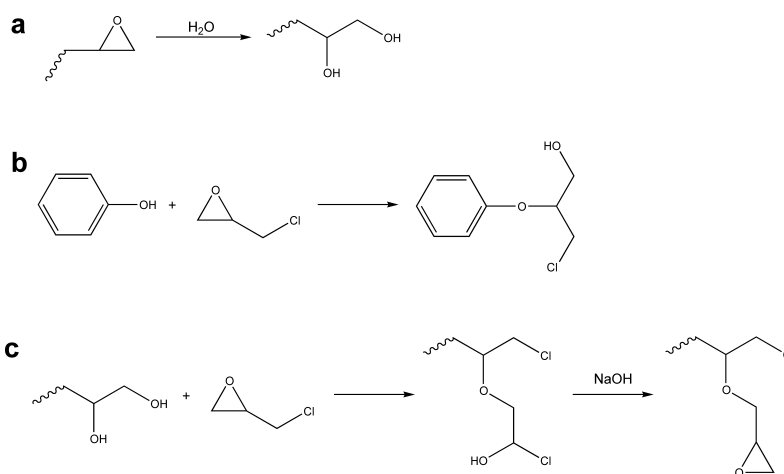
Fig. 2.5. Possible side reactions take place during the synthesis of ER: **(a)** hydrolysis of ECH and formation of α-glycol, **(b)** abnormal addition of ECH, and **(c)** formation of bound chlorides.

12

The use of catalyst is crucial in ER synthesis as the yield and other properties of ER depend on the type and amount of catalyst. Traditionally, NaOH has been widely used in the synthesis of ER due to its low price and high reactivity since the invention of ERs. As can be seen in Fig. 2.3, the role of NaOH could be summarized as (i) to form phenate ions, and (ii) to dehydrochlorinate the intermediates to yield ER. The amount of NaOH was found to be critical because insufficient amount of NaOH resulted in a decrease in phenate yield which ultimately decreased the yield of ER. Incomplete dehydrochlorination may also be attributable to the insufficient amount of NaOH in the reaction (Reinking 1960). An excess amount of NaOH, on the other hand, caused hydrolysis of ECH and increased the side reactions which again resulted in a decrease in the yield of ER (Pielichowski and Czub 1997).

In order to avoid the hydrolysis of ECH and side reaction caused by NaOH, phase transfer catalysts (PTCs) have been developed for the synthesis of ER by Reinking et al. (1960). They proposed two step synthesis where in the first step quaternary ammonium salts (tetramethyl ammonium chloride, benzyl trimethyl ammonium chloride, tetraethanol ammonium chloride, tetraethanol ammonium hydroxide and dodecyl dimethylbenzyl ammonium naphthenate) were used as a catalyst to form phenate ion. And in the second step, since PTSCs are not a strong enough base for dehydrochlorination (Pham and Marks 2000), NaOH was used at room temperature to dehydrochlorinate the intermediates to yield ER. Moreover, the use of PTC was found to make the low-molecular weight ER relatively easier than NaOH (Pielichowski and Czub 1997). Therefore, two step synthesis using PTC and NaOH has attracted great interest in the field of ER.

2.1.2. Application of ER

Liquid ER (i.e. DGEBA) exhibits good adhesion properties. Due to the high reactivity of epoxide group, ERs can also react each other (homopolymerization) or with a variety of curing agents to create a crosslinked structure. Once an ER is cured, it exhibits superior thermal/mechanical properties and chemical resistance. The thermal resistance, toughness and rigidity could be attributable to the aromatic ring in polyol, good adhesion properties is due to the epoxide group of ECH and hydroxyl (OH) groups, and ER owes its chemical resistance to the ether linkages (Pham and Marks 2000). Therefore, ERs are being used in variety of application areas including coatings, construction, composites and electrical/electronic field (Fig. 2.6). The market size of the ERs also demonstrates their importance: The North America, the epoxy resin market was amounted to approximately USD 1.0 billion in 2015, and is predicted to be USD 1.4 billion by 2020 (Research 2016); the global epoxy production, on the other hand, is projected to be 3 million tons by 2017 with a market size of USD 21.5 billion (Auvergne et al. 2014).
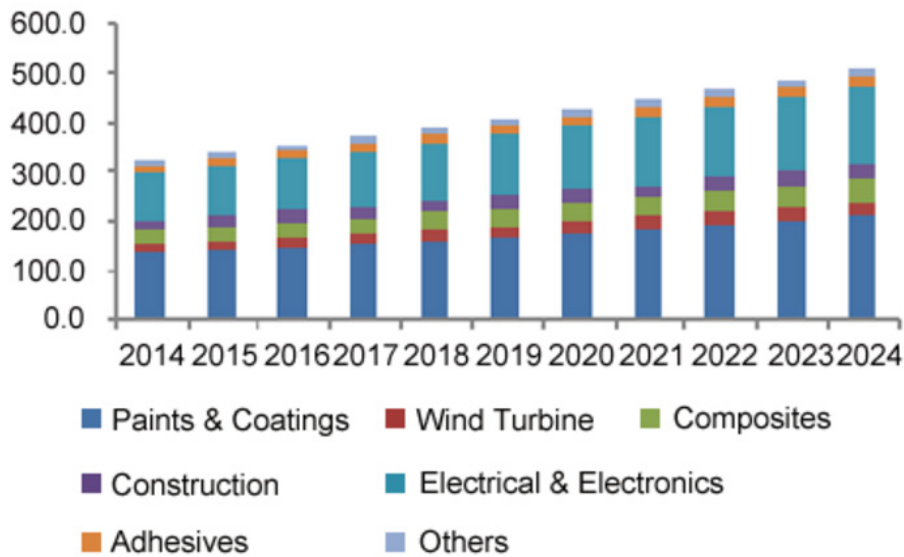
Fig. 2.6. U.S. Epoxy resin market volume by application, 2014 – 2024 (kilo tons) (Research 2016).

14

Among the ERs mentioned above, the most widely used ER is the DGEBA which accounts for approximately 75% of the ER in the market today (Pham and Marks 2000). As illustrated in Fig. 2.2, DGEBA is derived from condensation reaction of bisphenol A (BPA) and epichlorohydrin (ECH) in the presence of sodium hydroxide (NaOH). However, the toxicity of BPA has raised questions and concerns regarding its use in epoxy resins. The negative effects of BPA on hormones and brain chemistry have been previously documented in the literature (vom Saal and Hughes 2005, Okada et al. 2008, vom Saal and Myers 2008). The use of BPA in ER to be used in coatings for drinking water pipelines was recently banned (Auvergne et al. 2014). Moreover, the U.S. Food and Drug Administration (FDA) and European Union (EU) have also banned the use of BPA-based epoxy resins as coatings in infant formula packaging in 2013 and 2011, respectively (EU 2011, FDA 2013). Therefore, there is an increasing effort to explore bio-based aromatic polyol resources to be used in epoxy synthesis as an alternative to BPA. Moreover, the uncertainty in the price of petroleum as well as the social tendency toward materials from renewable and sustainable resources have also motivated researchers to focus on bio-based materials.

Bio-oil could be used as a biopolyol and alternative to BPA to synthesize bio-based epoxy resins due to its high hydroxyl number (OHN). The production techniques, chemistry and properties of bio-oil is discussed in detailed in the next section.

2.2. Bio-oil

Bio-oil is a term used in the literature for "liquefied biomass" produced by decomposition of lignocellulosic biomass through thermomechanical liquefaction processes. There are mainly

three liquefaction processes to produce bio-oil: (i) organic solvent liquefaction (OSL) – the liquefaction of lignocellulosic biomass using organic solvents such as ethylene glycol at moderate temperature, (ii) fast pyrolysis (FP) – the liquefaction in the absence of oxygen and solvent at elevated temperatures, and (iii) hydrothermal liquefaction (HTL) – the liquefaction using water at high temperature and pressure. It is very important to note that even if the liquid product from OSL, FP and HTL processes is defined as bio-oil, the properties of the bio-oils (OHN, molecular weight and chemical composition) are different from each other. A detailed literature about FP process and FP-bio-oil elsewhere (Mohan et al. 2006); therefore, only OSL and HTL processes have been reviewed in this section. Bio-oil obtained from OSL, FP, and HTL processes are termed as OSL-bio-oil, FP-bio-oil, and HTL-bio-oil, respectively, in this chapter.

2.2.1. Organic Solvent Liquefaction (OSL)

OSL is a thermomechanical liquefaction process in where lignocellulosic biomass is converted into bio-oil using an organic solvent at moderate temperature (100 – 250 °C) in the presence of a catalyst. OSL-bio-oil yield was found to be in the range of 25 – 75 wt.% depending on the solvent type, solvent/biomass weight ratio, liquefaction temperature and time. A typical OSL process is illustrated in Fig. 2.7.

2.2.1.1. Effect of OSL Solvent

The solvent type plays a crucial role in the OSL process. An effective solvent is needed to convert lignocellulosic biomass into OSL-bio-oil. Different types of organic solvents have been previously studied. Phenol has been reported as the best liquefying solvent for lignocellulosic biomass in terms of OSL-bio-oil yield (Zhang et al. 2006); however, owing to the

16

toxicity of phenol, more environmental friendly solvents, such as ethylene glycol (EG), diethylene glycol (DEG), and glycerol, have gained more attention for liquefaction. Liquefaction of bagasse with EG (Zhang et al. 2007), spruce with DEG-glycerol (Jasiukaityte et al. 2010), pine with EG (Rezzoug and Capart 2002), switchgrass with DEG (Wei et al. 2014), bamboo with EG (Ye et al. 2014), and bark with PEG/glycerol (D'Souza and Yan 2013) have been previously reported. The optimum liquefaction time was reported to be approximately 30 – 60 min when using EG, DEG, PEG by many researchers.
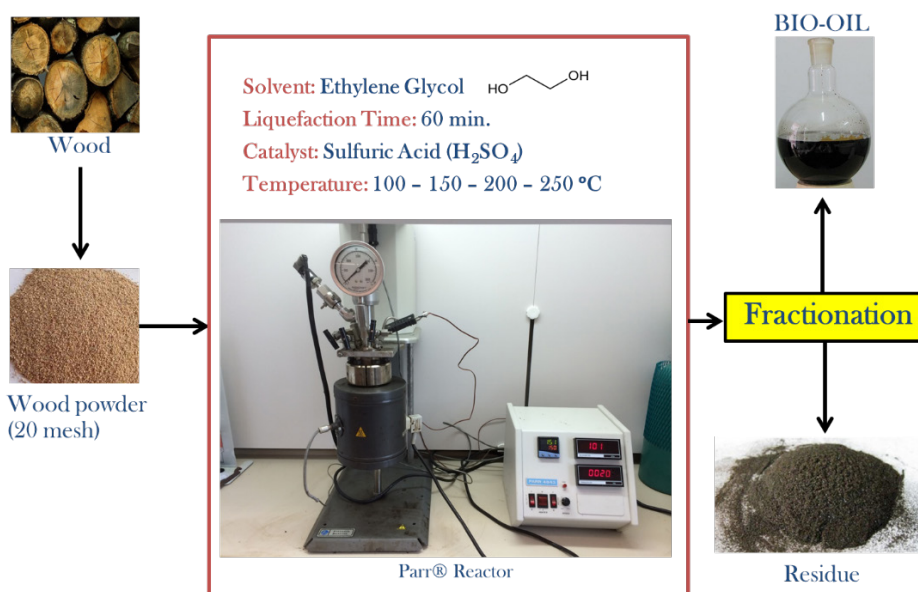
Fig. 2.7. Flow chart of OSL-bio-oil production using Parr® reactor in the presence of EG and sulfuric acid.

Yamada and Ono (1999) proposed that cyclic carbonates such as ethylene carbonate (EC) and propylene carbonate (PC) could provide rapid liquefaction, and they reported that EC gave 28 times faster liquefaction as compared to EG. The rapid liquefaction using EC was attributed to the lower dielectric constant which is 90.5 at 40 °C while dielectric constant of EG is 38.4 (Liang et al. 2007). However, one problem with using EC in the liquefaction of lignocellulosic

biomass was the high amount of insoluble lignin formation; therefore, mixture of EC/EG was suggested for the liquefaction of biomass (Yamada and Ono 1999).

Solvent/biomass weight ratio is another important consideration in OSL process. A study of Guo et al. (2014) showed there was a critical point for solvent/biomass weight ratio. For example, the liquefaction rate increased 75% when the solvent/biomass increased from 1/1 to 1/3 (wt./wt.); however, only 3.5% increase in OSL-bio-oil yield was observed when solvent/biomass ratio increased from 3/1 to 7/1 (Guo et al. 2014). Therefore, many studies suggest that $1/3 - 1/5$ (wt./wt.) is optimum weight ratio for lignocellulosic biomass when using EG, DEG and PEG as the liquefying solvent (Hu et al. 2014). Higher bio-oil yield when using higher solvent/biomass ratio was attributed to the fact that the rate of the liquefaction of biomass became higher than recondensation reaction as more solvent used in the OSL process (Yip et al. 2009).

After liquefaction, OSL-bio-oil is obtained followed by fractionation process which includes vacuum filtering and rotary evaporation to remove the solid residue and the solvents used to dilute the liquefied biomass. One of the biggest challenge in OSL process is to remove the unreacted liquefying solvents left in the OSL-bio-oil due to their high boiling point; i.e., boiling point of EG, DEG, PEG, and glycerol is 197, 245, 290 and 290 °C, respectively. The unreacted solvent left in the OSL-bio-oils becomes a problem when they are utilized as a polyol in the synthesis of rigid polymers due to the plasticizer effect of glycols (Lourdin et al. 1997). For example, Wei et al. (2014) used OSL-bio-oil to cure a commercial epoxy resin, and they found that the cured epoxy resin suffered from thermal and mechanical properties. However,

OSL-bio-oils may be considered as a good candidate for the synthesis of polymers where rigidity is not desired such as polyester (Kunaver et al. 2010).

2.2.1.2. Effect of OSL Temperature and Time

The liquefaction temperature and time have significant effect on OSL-bio-oil yield and composition. Many studies could be found in the literature that investigated the effect of OSL temperature and time on OSL-bio-oil (Rezzoug and Capart 2002, Zhang et al. 2006, Zhang et al. 2007, Jasiukaityte et al. 2010, Guo et al. 2014, Hu et al. 2014, Wei et al. 2014). The optimum OSL temperature in terms of OSL-bio-oil yield were found to be in the range of 130 – 250 ℃ depending on the presence or absence of catalyst. The use of catalyst such as sulfuric acid was found to lower the OSL temperature from 250 ℃ to 150 ℃ (Kishi et al. 2006). Many of the OSL studies reported a trend that OSL-bio-oil yield begins to drop after a critical temperature. The decrease in the OSL-bio-oil yield at high temperatures was attributed to the re-condensation reaction of the degradation products of lignocellulosic biomass (D'Souza and Yan 2013). Moreover, OSL at lower temperature than critical temperature also resulted in low OSL-bio-oil yield which is due to the low permeability and fluidity of the liquefying solvent (Zou et al. 2009).

Kinetics studies of OSL process showed that a rapid degradation of lignocellulosic biomass occurred in the early stage of the liquefaction, mostly the first 15 – 30 min (Yamada and Ono 1999, Xie and Chen 2005). Similar to the effect of temperature, longer OSL was reported to cause a decrease in bio-oil yield. Due to the complex nature of lignocellulosic biomass, variety of reactions take place during the OSL process which was discussed in the next section. Among

these reactions, alcoholysis of biomass occurs when the optimum conditions are reached while re-condensation reaction between highly reactive degradation products occurs at prolonged OSL. The optimum OSL time varies depending on the type of liquefying solvent and biomass type as summarized in Table 2.3.

Table 2.3. Optimum OSL conditions based on the biomass in the presence of acid or base catalyst.

Biomass	Solvent	Time (min)	Temp (^{o}C)	Reference
Cellulose	PEG400	60	150	(Yamada et al. 2007)
Lignin	Furfuryl alcohol	15	170	(Li et al. 2013)
Corn stover	EC	20	160	(Liang et al. 2007)
Corn stover	PEG/glycerol	60	160	(Liang et al. 2007)
Corn stover	EG	60	160	(Liang et al. 2007)
Chinese eucalyptus	EG/glycerol	60	160	(Zhang et al. 2012)
Black poplar	DEG	95	150	(Budija et al. 2009)
Birch	Phenol	120	160	(Lin et al. 1994)
Cellulose	Phenol	60	150	(Zhang et al. 2006)
Bagasse	EC	18	150	(Xie and Chen 2005)
White birch	EC	15	150	(Yamada and Ono 1999)
Lignin	DEG/glycerol	240	150	(Jasiukaityte et al. 2010)
Spruce	Resorcinol	120	150	(Kishi et al. 2006)
Bamboo	Phenol	60	130	(Wu and Lee 2010)
Bamboo	PEG/glycerol	75	150	(Wu and Lee 2010)
Spruce	DEG/glycerol	120	180	(Kunaver et al. 2010)

2.2.1.2. Reaction Mechanism of OSL Process

Zou et al. (2009) provided valuable information about the reaction mechanism of OSL process. Their DSC analysis of biomass/solvent mixture revealed that there were three stages during biomass liquefaction: (i) biomass dehydration, (ii) solvent volatilization, and (iii) biomass alcoholysis. Biomass dehydration and solvent volatilization were found to be endothermic reaction which were attributed to the removal of moisture and volatilization of solvent. Biomass

alcoholysis is simply the main liquefaction step of lignocellulosic biomass. Their studies suggested that OSL temperature should be higher than solvent volatilization for a successful biomass alcoholysis. This finding explained the reason why 150 – 160 °C was the optimum OSL temperature when EG was used as the liquefying solvent. The solvent volatilization temperature of EG was found to be 156 °C by the TGA experiments.

During the alcoholysis of lignocellulosic biomass, there were mainly two competitive reactions take place: (i) decomposition of biomass, and (ii) re-condensation of degraded biomass (Demirbaş 2000, Zhang et al. 2006, Xiao et al. 2013). Lignocellulosic biomass (cellulose, hemicellulose and lignin) is degraded to its monomers by the liquefying solvent, then a recombination of degraded fragments takes place. In the presence of excess solvent, these fragments could create high molecular weight components via condensation reaction with solvent (Zou et al. 2009).

Alcoholysis of biomass in OSL process begins with the decomposition of hemicellulose since hemicellulose is the first depolymerized wood polymer under heat (Via et al. 2013). Degradation of lignin and amorphous cellulose occurs at higher temperature than the solvent volatilization temperature. Decomposition of crystalline cellulose was found to be the rate-limiting step in OSL process because liquefying solvent cannot easily reach the cellulose matrix due to the well-packed structure (Hu et al. 2014).
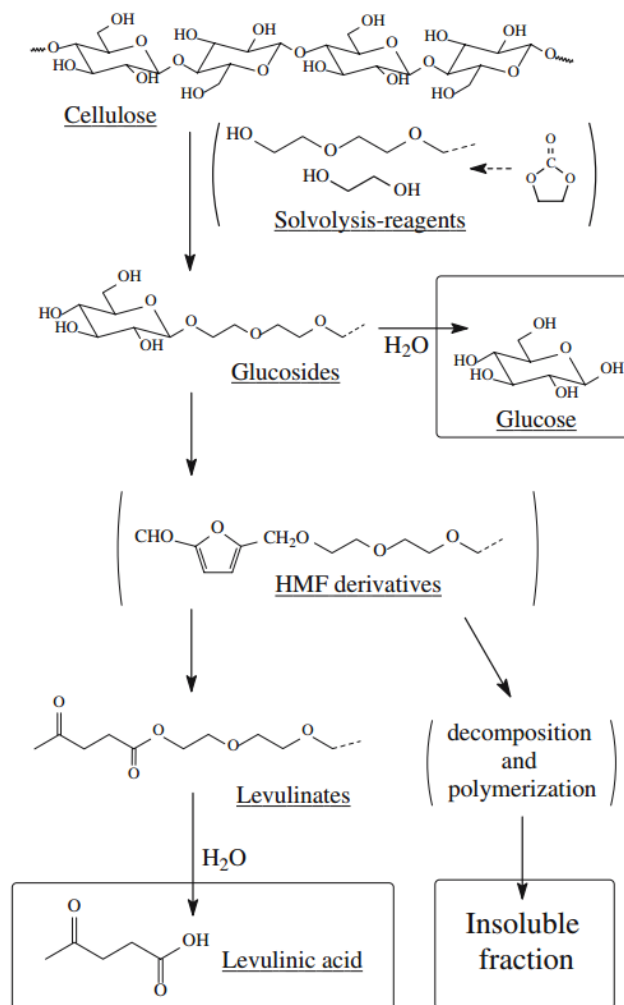
Fig. 2.8. Proposed reaction mechanism of solvolysis of cellulose using PEG in OSL

process (Yamada et al. 2007).

Yamada et al. (2007) studied the cellulose degradation in PEG and EC in order to

understand the liquefaction mechanism of cellulose. They observed the formation of glucosides

as a result of solvolysis of cellulose. When liquefaction was prolonged, authors found that

degradation of glucosides resulted in levulinic acid (Fig. 2.8). The reaction rate of the formation

of glucosides and levulinic acid was reported to be depended on the reaction conditions.

Lignin is a three-dimensional amorphous polymer composed of phenylpropane building blocks: p-coumaryl alcohol, coniferyl alcohol, and sinapyl alcohol (Sjostrom 1993). Degradation of lignin provides valuable aromatic chemicals to the OSL-bio-oil. However, phenolic type of OH groups were not observed in the OSL-bio-oil due to the condensation reaction of lignin fragment with alcoholic solvents (EG, DEG, PEG, and glycerol) (D'Souza and Yan 2013) which limits the utilization of OSL-bio-oil as a polyol in polymer synthesis.

2.2.2. *Hydrothermal Liquefaction (HTL)*

Hydrothermal liquefaction (HTL), also known as direct liquefaction, is a thermomechanical conversion technique to produce bio-oil where lignocellulosic biomass is converted into liquid (bio-oil), gas and solid products using subcritical or supercritical water at elevated temperature (250 – 370 °C) and pressure (2 – 24 MPa). Bio-oil produced by the HTL process has a significant potential for commercialization in terms of price and life cycle assessment (Elliott et al. 2015). The effect of process parameters such as temperature, pressure, reaction time and feedstock type on the bio-oil yield in HTL process has been intensively studied and valuable literature reviews can be found elsewhere (Akhtar and Amin 2011, Toor et al. 2011). Approximately 30 – 40 wt.% bio-oil (based on dry mass of biomass) is obtained from the hydrothermal liquefaction of lignocellulosic biomass (Akhtar and Amin 2011).

Recently, ethanol has received attention to be used as a co-solvent in the HTL process due to its high hydrogen solvent capability. Yuan et al. (2007) proposed that the highly reactive free radicals generated from the HTL of biomass were stabilized by the ethanol which acts as a hydrogen-donor solvent, and Cheng et al. (2010) reported that bio-oil yield could be increased

from 40 to 65 wt.% when ethanol was used along with water in a sub-critical condition. In another study, alkaline lignin was liquefied in hot compressed water/ethanol medium, and found that addition of ethanol increased the degradation of lignin which resulted in a lower amount of solid residue (Yuan et al. 2010). This improvement may be due to the low dielectric constant of ethanol which facilitates dissolving of high molecular weight lignin at supercritical temperatures (Krammer and Vogel 2000). The synergistic effect of water/ethanol mixture in the liquefaction of rice husk for bio-oil production via the HTL process was also observed by Liu et al. (2013). Besides the high bio-oil yield, the addition of ethanol to water also affects the distribution of phenolics such as phenol, ethylphenol and guaiacols, ethylguaiacol and syringol in the bio-oil as well (Ye et al. 2012, Ouyang et al. 2015). Recently, Kosinkova et al. (2015) reported that aqueous ethanol improved the higher heating value (HHV) of bio-oil to be used in the field of biodiesel applications. Moreover, the addition of medical stone as a catalyst into aqueous ethanol could further increase the yield of bio-oil produced by HTL of cotton seed (Yan et al. 2015).

During the HTL, lignocellulosic biomass is degraded to fragments and free radicals are generated. When there is no hydrogen donor solvent, these reactive free radicals recombine and forms high molecular weight products called solid residue or char. In case a sufficiently high amount of a hydrogen donor solvent such as ethanol is introduced to the HTL, free radicals can be stabilized and the formation of solid residue is decreased as illustrated in Fig. 2.9 (Vasilakos and Austgen 1985). Thus, lower residue content when ethanol is used as a co-solvent in HTL process was attributed to the hydrogen donor capability of ethanol. As Liu et al. (2013) summarized the synergetic effect of water/ethanol, the high bio-oil and low residue yield could be attributed to (i) enhanced hydrogen donor capability of ethanol at subcritical and supercritical

24

conditions and acting as a reaction substrate, (ii) high ability of ethanol to dissolve oily products, (iii) ability of ethanol to stabilize the free radicals resulting in lower residue content, and (iv) the increased solubility of high molecular weight products in water/ethanol mixture at subcritical conditions. In addition to the synergistic effects mentioned above, conversion of highly reactive carbonyl groups in the bio-oil to more stable acetal groups by ethanol could be another reason for the low residue content in ethanol/water HTL process. Compounds containing carbonyl groups such as aldehydes and ketones are primarily responsible for the repolymerization of bio-oil due to their high reactivity and consequently result in the generation of solid residue as well as an increase in the viscosity of bio-oil (Czernik et al. 1994).

Biomass $\xrightarrow{\text{HTL}}$ n(R·)

no hydrogen donation → $(R)_n$ high molecular weight products (solid residue)

free radical

hydrogen donor, H· → n(RH) lower molecular weight product
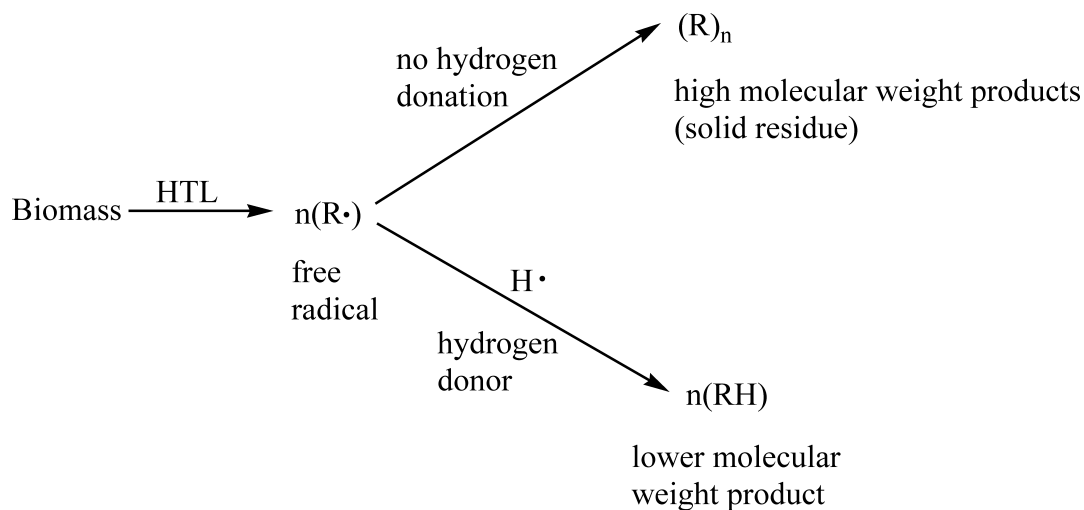
Fig. 2.9. Schematic representation of residue formation in the presence and absence of hydrogen donor solvent.

The studies on OSL and HTL processes mainly focused on the effect of liquefaction parameters on bio-oil yield and bio-oil composition; however, information is sparse on residue formation and OH analysis of bio-oil, which are important considerations because they positively

impact the financial feasibility for use as bioenergy or bioproducts. Source and variation of OH groups in OSL-bio-oil and the residue analysis will be addressed in Chapters 3 and 4.

2.2.3. Characterization of Hydroxyl (OH) Groups in Bio-oil

The reaction behavior of bio-oil based polymers depends on the interaction between hydroxyl groups the bio-oil and the formaldehyde (CH_2O) for phenol formaldehyde resin, isocyanate (R–N=C=O) for the polyurethane, epoxide (C_2H_4O) group for epoxy resin, and ester (-COOH) groups for polyester production. Therefore, characterization of OH group plays crucial role in process optimization of bio-oil based polymer synthesis.

Bio-oil contains different type of OH groups in the composition such as aliphatic OH, phenolic OH, guaiacyl phenolic OH and catechol type OH. The variation in OH groups arises from the highly complex structure of lignocellulosic biomass. Determination of the source of OH groups as well as characterization is a challenge in bio-oil field. In this section, OH group characterization techniques including ^{31}P-NMR and phthalation titration (ASTM D4274-11) were reviewed.

2.2.3.1. ^{31}P-NMR

Nuclear Magnetic Resonance (NMR) is a strong analytical technique used in various fields for structural characterization of chemical compounds. In the field of bio-oil, ^{13}C-NMR and ^{1}H-NMR are widely used to analyze the carbon and hydrogen atoms in different functional groups in the bio-oil (Mullen et al. 2009) as well as the decomposition pathway of biomass in thermomechanical conversion processes (Yamada and Ono 1999, Ben and Ragauskas 2011). [31]P-

NMR provides great deal of information to determine the content of OH groups present in the bio-oil. In this technique, OH groups belonging to aliphatic, phenolic, carboxylic units are phosphitylated by a phosphorous-containing derivatizing reagent followed by quantitative ^{31}P-NMR.

For ^{31}P-NMR analysis, mixture of pyridine and deuterated chloroform (1.6/1.0, v/v) is used as the solvent system. In the phosphitylation reaction (Fig. 2.10), 2-Chloro-4,4,5,5-tetramethyl-1,3,2-dioxaphospholane (TMDP) reacts with the free OH groups in the bio-oil, and yields to derivatized compound and hydrochloric acid (HCl). Since HCl may cause to decomposition of derivatized compound, pyridine is used in the solvent system as the base to capture HCl. The reasons for using deuterated chloroform (CDCl$_3$) in the solvent system are (i) to dissolve derivatized sample, (ii) to inhibit precipitation of pyridine-HCl salt, and (iii) to get a deuterium signal for NMR experiment (Pu et al. 2011). In some cases, N,N-dimethylformamide (DMF) is additionally used in the solvent system in order to improve the solubility of the sample (Pu et al. 2011).
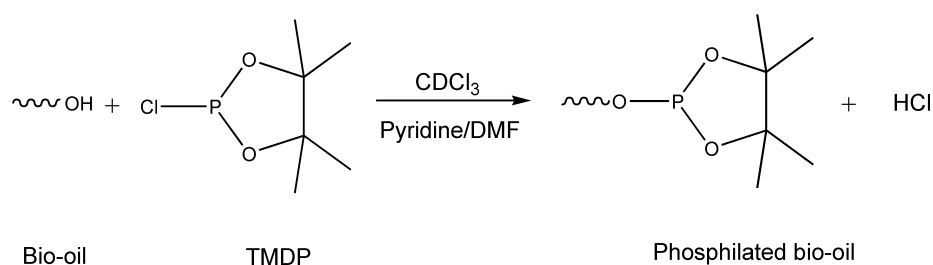
Fig. 2.10. Phosphitylation of free OH group with TMDP in the solvent system of CDCl3/Pyridine/DMF.

The most common phosphorous reagent used in ^{31}P-NMR analysis is TMDP. Wroblewski et al. (1988) compared five different phosphorous reagents (Fig. 2.11) to derivatize model organic compounds including phenols, aliphatic alcohols, aromatic acids, aliphatic acids,

27

amines, and thiols in the coal pyrolysis condensates, and reported that TMDP is the best reagent in order to identify different types of OH groups.
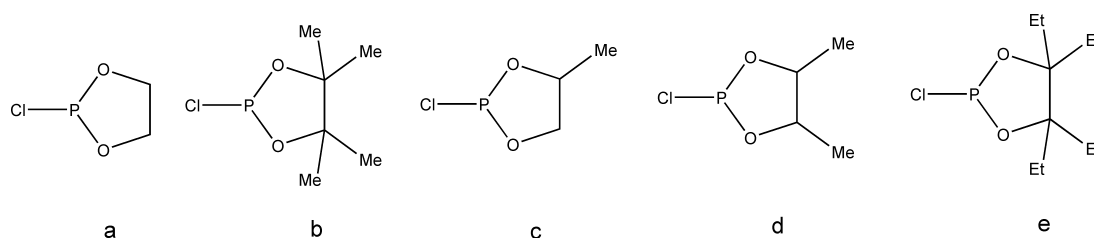
Fig. 2.11. Phosphorus-containing reagents used to derivatize the OH groups: **(a)** 2-Chloro-1,3,2-dioxaphospholane, **(b)** 2-Chloro-4,4,5,5-tetramethyl-1,3,2-dioxaphospholane (TMDP), **(c)** cis/trans-2-Chloro-4-methyl-1,3,2-dioxaphospholane, **(d)** meso-2-Chloro-4,5-dimethyl-1,3,2-dioxaphospholane-meso, and **(e)** 2-Chloro-4,4,5,5-tetraethyl-1,3,2-dioxaphospholane.

In most cases, N-hydroxy compounds are used as an internal standard in ^{31}P-NMR analysis in the field of bio-oil. Zawadzki and Ragauskas (2001) studied some N-hydroxy compounds and cyclohexanols as an internal standard to determine OH groups in lignin structure. They observed some signals of cyclohexanol–phosphite product overlap with and aliphatic and phenolic lignin structures while N-hydroxy compounds were better in terms of signal separation. In the same study (Zawadzki and Ragauskas 2001), four different N-hydroxy compounds including N-hydroxyphthalimide, 1-hydroxy-7-azabenzotriazole, N-hydroxy-5-norbornene-2,3-dicarboximide, and N-hydroxy-1,8-naphthalimide (Fig. 2.12) have been compared, and reported that N-hydroxy-5-norborene-2,3-dicarboximide (Fig. 2.12c) was the most suitable internal standard for ^{31}P-NMR analysis of lignin.
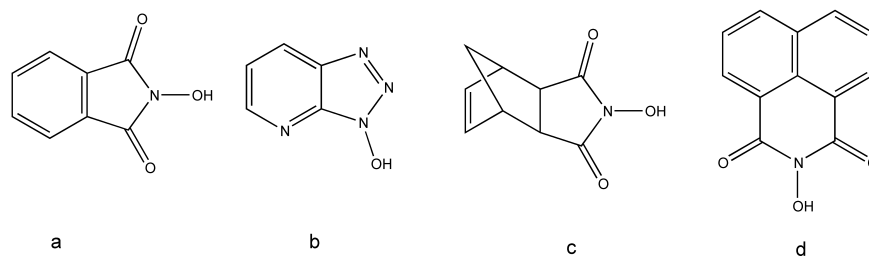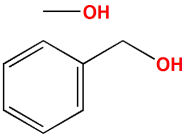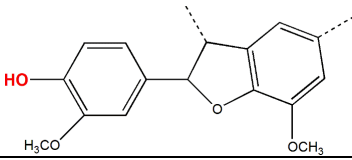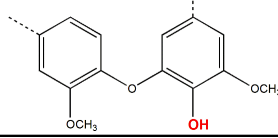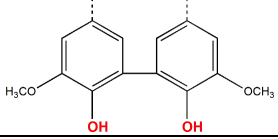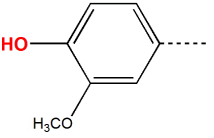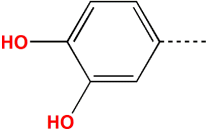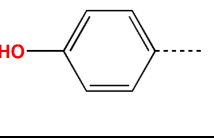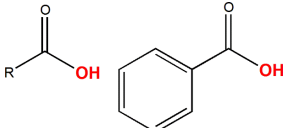
Fig. 2.12. N-hydroxy compounds used as an internal standard in ^{31}P-NMR analysis: **(a)** N-hydroxyphthalimide, **(b)** 1-hydroxy-7-azabenzotriazole, **(c)** N-hydroxy-5-norbornene-2,3-dicarboximide, and **(d)** N-hydroxy-1,8-naphthalimide.

The type of the OH in bio-oil could be easily determined from the ^{31}P-NMR spectra. Table 2.4 shows 31P-NMR chemical shifts and integration regions of the phosphilated OH groups with TMDP.

2.2.3.2. Phtahalic Anhydride Esterification

Phtahalic anhydride esterification is a wet chemistry technique used to measure the OH number in the bio-oil. This technique is based on esterification of OH groups in the bio-oil. Acetic anhydride, phthalic anhydride, pyromellitic dianhydride, phenyl isocyanate have been studied as an esterification agent (Carey et al. 1984). The most recent ASTM D4274-11 test method for determination of hydroxyl numbers of polyols has accepted the use of acetic anhydride or phthalic anhydride for the esterification. Today ASTM D4274-11 is the most common standard followed by researchers to measure the OH number in the bio-oil. This test method is originally developed to measure the polyesters and polyethers polyols containing primary and secondary OH groups; however, it is suitable for many other hydroxyl-containing compounds as well.

Table 2.4. Chemical shifts and integration regions of bio-oil phosphilated by TMDP.

Type of OH group			Example of Chemical Structure	Integration Region (ppm)
Aliphatic OH				150.0 - 145.5
Phenolic OH	C5 substituded Condensed phenolic OH	β-5		144.7 - 142.8
		4-O-5		142.8 - 141.7
		5-5		141.7 - 140.2
	Guaiacyl phenolic OH			140.2 - 139.0
	Catechol type OH			139.0 - 138.2
	p-hydroxy-phenyl OH			138.2 - 137.3
Acidic OH				136.6 - 133.6

In the esterification technique described by ASTM D4274-11, esterification reagent is prepared by dissolving phthalic anhydride in pyridine. Esterification of the bio-oil with phthalic anhydride/pyridine solution requires 2 hours. Carey et al. (1984) suggested that use of imidazole

as a catalyst in the esterification reagent could reduce esterification time from 2 hours to 15 minutes. Reaction mechanism of esterification reagent with OH groups in bio-oil is illustrated in Fig. 2.13.

(a)   (b)
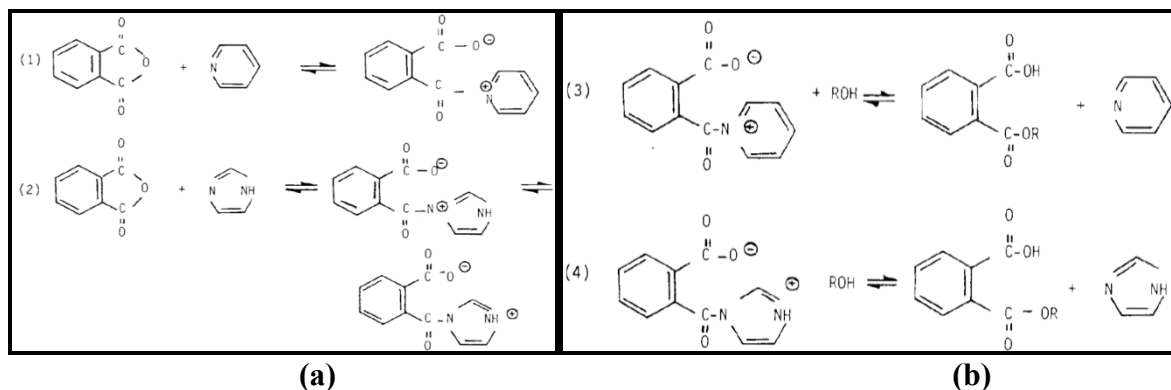
Fig. 2.13. (a) Reaction mechanism of phthalic anhydride with pyridine and imidazole, and **(b)** esterification mechanism of OH group with reagent (Carey et al. 1984).

Phthalic anhydride reacts with pyridine and imidazole and yields to complexes I and II shown in Fig. 2.13a. The OH groups in the bio-oil reacts with the complexes I and II and yield to an ester and one equivalent of titratable acids as shown in Fig. 2.13b. Using phenolphthalein as the indicator, OH groups in the carboxylic acids (-COOH) is titrated with 0.5 N sodium hydroxide (NaOH), and number of OH groups present in the bio-oil is calculated quantitatively. The excess phthalic anhydride may react with the OH groups in the phenolphthalein. Therefore, the excess phthalic anhydride is destroyed by addition of water in prior to addition of indicator.

2.2.3.2.1 Test Procedure and Calculation

Titration reagent for esterification is prepared by dissolving approximately $111 - 116$ gram of phthalic anhydride in 700 mL of pyridine. The reagent should stand overnight before

31

use. Accurately 25 mL of reagent is pipetted into the pressure bottles prepared for sample and blank. Appropriate amount of sample (eq. 1) is introduced into the pressure bottle reserved for sample. Pressure bottles (sample and blank) are placed into boiling water for 15 min. if imidazole is used in the reagent, or 2 hours if imidazole is not used in the reagent system, and then pressure bottles are allowed to cool down to room temperature.

$$Sample\ size\ (g) = \frac{561}{estimated\ OH\ number} \tag{eq.1}$$

After the temperature equilibrium, 50 mL pyridine and 10 mL distilled water is added into pressure bottles respectively, and 0.5 mL of 1.0 percent solution of phenolphthalein in pyridine is added to the pressure bottles. Blank solution is titrated until the pink point with 0.5 N NaOH. pH at the pink point and the volume of NaOH consumed are recorded. Since bio-oil is a black solution, pink point cannot be seen in titrated bio-oil. Therefore, bio-oil solution is titrated with 0.5 NaOH until the recorded pH of the blank solution, and volume of NaOH consumed is recorded. Number of OH group is calculated as follows (eq. 2):

$$OHN\ (mg\ KOH/g\ bio-oil) = \frac{(B-A)\times 56.1}{W} \tag{eq. 2}$$

where, A and B is the volume of NaOH required for titration of the sample (mL) and blank solution (mL), respectively, N is the normality of the NaOH, 56.1 is the equivalent weight of KOH (mg/meq), and W is the weight of sample (g). The important point here is that the volume difference between blank and sample (B-A) should be between 18 – 22 mL. If B-A is not in this range, titration should be repeated by adjusting the sample size accordingly.

References

1. Akhtar, J. and N. A. S. Amin. 2011. A review on process conditions for optimum bio-oil yield in hydrothermal liquefaction of biomass. Renewable and Sustainable Energy Reviews **15**:1615-1624.

2. Auvergne, R., S. Caillol, G. David, B. Boutevin, and J. P. Pascault. 2014. Biobased Thermosetting Epoxy: Present and Future. Chemical Reviews **114**:1082-1115.

3. Ben, H. X. and A. J. Ragauskas. 2011. NMR Characterization of Pyrolysis Oils from Kraft Lignin. Energy & Fuels **25**:2322-2332.

4. Bradley, W., J. Forrest, and O. Stephenson. 1951. 359. The catalysed transfer of hydrogen chloride from chlorohydrins to epoxides. A new method of preparing glycidol and some of its derivatives. Journal of the Chemical Society (Resumed):1589-1598.

5. Budija, F., C. Tavzes, L. Zupancic-Kralj, and M. Petric. 2009. Self-crosslinking and film formation ability of liquefied black poplar. Bioresource Technology **100**:3316-3323.

6. Carey, M. A., S. L. Wellons, and D. K. Elder. 1984. Rapid Method for Measuring the Hydroxyl Content of Polyurethane Polyols. Journal of Cellular Plastics **20**:42-48.

7. Cheng, S., I. D'cruz, M. Wang, M. Leitch, and C. Xu. 2010. Highly Efficient Liquefaction of Woody Biomass in Hot-Compressed Alcohol−Water Co-solvents. Energy & Fuels **24**:4659-4667.

8. Czernik, S., D. K. Johnson, and S. Black. 1994. Stability of Wood Fast Pyrolysis Oil. Biomass & Bioenergy **7**:187-192.

9. D'Souza, J. and N. Yan. 2013. Producing Bark-based Polyols through Liquefaction: Effect of Liquefaction Temperature. Acs Sustainable Chemistry & Engineering **1**:534-540.

10. Demirbaş, A. 2000. Mechanisms of liquefaction and pyrolysis reactions of biomass. Energy Conversion and Management **41**:633-646.

11. Durig, J. D. 2000. Comparisons of Epoxy Technology for Protective Coatings and Linings in Wastewater Facilities in Wastewater Facilities. Journal of protective coatings & linings **17**:49-54.

12. Elliott, D. C., P. Biller, A. B. Ross, A. J. Schmidt, and S. B. Jones. 2015. Hydrothermal liquefaction of biomass: Developments from batch to continuous process. Bioresource Technology **178**:147-156.

13. Ellis, B. 2012. Chemistry and Technology of Epoxy Resins. Springer Netherlands.

14. EU. 2011. The restriction of use of Bisphenol A in plastic infant feeding bottles. http://eur-lex.europa.eu/LexUriServ/LexUriServ.do?uri=OJ:L:2011:026:0011:0014:EN:PDF (accessed September 2016)

15. FDA. 2013. Indirect Food Additives: Adhesives and Components of Coatings. http://eur-lex.europa.eu/LexUriServ/LexUriServ.do?uri=OJ:L:2011:026:0011:0014:EN:PDF (accessed September 2016).

16. Guo, Z.-h., Y.-n. Liu, F.-y. Wang, and X.-y. Xiao. 2014. Liquefaction of metal-contaminated giant reed biomass in acidified ethylene glycol system: Batch experiments. Journal of Central South University **21**:1756-1762.

17. Hu, S., X. Luo, and Y. Li. 2014. Polyols and Polyurethanes from the Liquefaction of Lignocellulosic Biomass. Chemsuschem **7**:66-72.

18. Jasiukaityte, E., M. Kunaver, and C. Crestini. 2010. Lignin behaviour during wood liquefaction-Characterization by quantitative P-31, C-13 NMR and size-exclusion chromatography. Catalysis Today **156**:23-30.

19. Kishi, H., A. Fujita, H. Miyazaki, S. Matsuda, and A. Murakami. 2006. Synthesis of wood-based epoxy resins and their mechanical and adhesive properties. Journal of Applied Polymer Science **102**:2285-2292.

20. Kosinkova, J., J. A. Ramirez, J. Nguyen, Z. Ristovski, R. Brown, C. S. K. Lin, and T. J. Rainey. 2015. Hydrothermal liquefaction of bagasse using ethanol and black liquor as solvents. Biofuels, Bioproducts and Biorefining. DOI: 10.1002/bbb.1578.

21. Krammer, P. and H. Vogel. 2000. Hydrolysis of esters in subcritical and supercritical water. The Journal of Supercritical Fluids **16**:189-206.

22. Kunaver, M., E. Jasiukaityte, N. Cuk, and J. T. Guthrie. 2010. Liquefaction of Wood, Synthesis and Characterization of Liquefied Wood Polyester Derivatives. Journal of Applied Polymer Science **115**:1265-1271.

23. Kuo, P.-Y. 2016. Development and Characterization of an Extractive-based Bio-Epoxy Resin from Beetle-Infested Lodgepole Pine (Pinus contorta var. latifolia) Bark. PhD Dissertation. University of Toronto.

24. Lee, H. and K. Neville. 1957. Epoxy resins: their applications and technology. McGraw-Hill.

25. Li, S., G. Guo, X. Nan, Y. Ma, S. Ren, and S. Han. 2013. Selective Liquefaction of Lignin from Bio-ethanol Production Residue Using Furfuryl Alcohol. Bioresources **8**.

26. Liang, L., Z. Mao, Y. Li, C. Wan, T. Wang, L. Zhang, and L. Zhang. 2007. LIQUEFACTION OF CROP RESIDUES FOR POLYOL PRODUCTION. Bioresources **1**.

27. Lin, L., M. Yoshioka, Y. Yao, and N. Shiraishi. 1994. Liquefaction of wood in the presence of phenol using phosphoric acid as a catalyst and the flow properties of the liquefied wood. Journal of Applied Polymer Science **52**:1629-1636.

28. Liu, Y., X.-z. Yuan, H.-j. Huang, X.-l. Wang, H. Wang, and G.-m. Zeng. 2013. Thermochemical liquefaction of rice husk for bio-oil production in mixed solvent (ethanol–water). Fuel Processing Technology **112**:93-99.

29. Lourdin, D., L. Coignard, H. Bizot, and P. Colonna. 1997. Influence of equilibrium relative humidity and plasticizer concentration on the water content and glass transition of starch materials. Polymer **38**:5401-5406.

30. Mohan, D., C. U. Pittman, and P. H. Steele. 2006. Pyrolysis of Wood/Biomass for Bio-oil: A Critical Review. Energy & Fuels **20**:848-889.

31. Mullen, C. A., G. D. Strahan, and A. A. Boateng. 2009. Characterization of Various Fast-Pyrolysis Bio-Oils by NMR Spectroscopy. Energy & Fuels **23**:2707-2718.

32. Okada, H., T. Tokunaga, X. Liu, S. Takayanagi, A. Matsushima, and Y. Shimohigashi. 2008. Direct Evidence Revealing Structural Elements Essential for the High Binding Ability of Bisphenol A to Human Estrogen-Related Receptor-γ. Environmental Health Perspectives **116**:32-38.

33. Ouyang, X., X. Huang, Y. Zhu, and X. Qiu. 2015. Ethanol-Enhanced Liquefaction of Lignin with Formic Acid as an in Situ Hydrogen Donor. Energy & Fuels **29**:5835-5840.

34. Pham, H. Q. and M. J. Marks. 2000. Epoxy Resins. Ullmann's Encyclopedia of Industrial Chemistry. Wiley-VCH Verlag GmbH & Co. KGaA.

35. Pielichowski, J. and P. Czub. 1997. Application of phase transfer catalysis in the synthesis of low-molecular-weight epoxy resins. Die Angewandte Makromolekulare Chemie **251**:1-12.

36. Pu, Y. Q., S. L. Cao, and A. J. Ragauskas. 2011. Application of quantitative P-31 NMR in biomass lignin and biofuel precursors characterization. Energy & Environmental Science **4**:3154-3166.

37. Reinking, N. H. 1960. Preparation of monomeric glycidyl polyethers of polyhydric phenols. US Patent number: US2943096 A.

38. Research, G. V. 2016. Epoxy Resin Market Analysis By Application (Paints & Coatings, Wind Turbine, Composites, Construction, Electrical & Electronics, Adhesives) And Segment Forecasts To 2024.

39. Rezzoug, S.-A. and R. Capart. 2002. Liquefaction of wood in two successive steps: solvolysis in ethylene-glycol and catalytic hydrotreatment. Applied Energy **72**:631-644.

40. Sjostrom, E. 1993. Chapter 4 - LIGNIN. Pages 71-89 Wood Chemistry (Second Edition). Academic Press, San Diego.

41. Toor, S. S., L. Rosendahl, and A. Rudolf. 2011. Hydrothermal liquefaction of biomass: A review of subcritical water technologies. Energy **36**:2328-2342.

42. Vasilakos, N. P. and D. M. Austgen. 1985. Hydrogen-donor solvents in biomass liquefaction. Industrial & Engineering Chemistry Process Design and Development **24**:304-311.

43. Via, B. K., S. Adhikari, and S. Taylor. 2013. Modeling for proximate analysis and heating value of torrefied biomass with vibration spectroscopy. Bioresource Technology **133**:1-8.

44. vom Saal, F. S. and C. Hughes. 2005. An Extensive New Literature Concerning Low-Dose Effects of Bisphenol A Shows the Need for a New Risk Assessment. Environmental Health Perspectives **113**:926-933.

45. vom Saal, F. S. and J. Myers. 2008. BIsphenol a and risk of metabolic disorders. JAMA **300**:1353-1355.

46. Wei, N., B. K. Via, Y. F. Wang, T. McDonald, and M. L. Auad. 2014. Liquefaction and substitution of switchgrass (Panicum virgatum) based bio-oil into epoxy resins. Industrial Crops and Products **57**:116-123.

47. Wroblewski, A. E., C. Lensink, R. Markuszewski, and J. G. Verkade. 1988. Phosphorus-31 NMR spectroscopic analysis of coal pyrolysis condensates and extracts for heteroatom functionalities possessing labile hydrogen. Energy & Fuels **2**:765-774.

48. Wu, C. C. and W. J. Lee. 2010. Synthesis and Properties of Copolymer Epoxy Resins Prepared from Copolymerization of Bisphenol A, Epichlorohydrin, and Liquefied Dendrocalamus latiflorus. Journal of Applied Polymer Science **116**:2065-2073.

49. Xiao, W. H., W. J. Niu, F. Yi, X. Liu, and L. J. Han. 2013. Influence of Crop Residue Types on Microwave-Assisted Liquefaction Performance and Products. Energy & Fuels **27**:3204-3208.

50. Xie, T. and F. Chen. 2005. Fast liquefaction of bagasse in ethylene carbonate and preparation of epoxy resin from the liquefied product. Journal of Applied Polymer Science **98**:1961-1968.

51. Yamada, T., M. Aratani, S. Kubo, and H. Ono. 2007. Chemical analysis of the product in acid-catalyzed solvolysis of cellulose using polyethylene glycol and ethylene carbonate. Journal of Wood Science **53**:487-493.

52. Yamada, T. and H. Ono. 1999. Rapid liquefaction of lignocellulosic waste by using ethylene carbonate. Bioresource Technology **70**:61-67.

53. Yan, X., B. Wang, and J. Zhang. 2015. Liquefaction of cotton seed in sub-critical water/ethanol with modified medical stone for bio-oil. Bioresource Technology **197**:120-127.

54. Ye, L., J. Zhang, J. Zhao, and S. Tu. 2014. Liquefaction of bamboo shoot shell for the production of polyols. Bioresource Technology **153**:147-153.

55. Ye, Y., J. Fan, and J. Chang. 2012. Effect of reaction conditions on hydrothermal degradation of cornstalk lignin. Journal of Analytical and Applied Pyrolysis **94**:190-195.

56. Yip, J., M. Chen, Y. S. Szeto, and S. Yan. 2009. Comparative study of liquefaction process and liquefied products from bamboo using different organic solvents. Bioresource Technology **100**:6674-6678.

57. Yuan, X. Z., H. Li, G. M. Zeng, J. Y. Tong, and W. Xie. 2007. Sub- and supercritical liquefaction of rice straw in the presence of ethanol–water and 2-propanol–water mixture. Energy **32**:2081-2088.

58. Yuan, Z., S. Cheng, M. Leitch, and C. Xu. 2010. Hydrolytic degradation of alkaline lignin in hot-compressed water and ethanol. Bioresource Technology **101**:9308-9313.

59. Zawadzki, M. and A. Ragauskas. 2001. N-Hydroxy Compounds as New Internal Standards for the 31P-NMR Determination of Lignin Hydroxy Functional Groups. Page 283 Holzforschung.

60. Zhang, H., H. Pang, J. Shi, T. Fu, and B. Liao. 2012. Investigation of liquefied wood residues based on cellulose, hemicellulose, and lignin. Journal of Applied Polymer Science **123**:850-856.

61. Zhang, T., Y. Zhou, D. Liu, and L. Petrus. 2007. Qualitative analysis of products formed during the acid catalyzed liquefaction of bagasse in ethylene glycol. Bioresource Technology **98**:1454-1459.

62. Zhang, Y., A. Ikeda, N. Hori, A. Takemura, H. Ono, and T. Yamada. 2006. Characterization of liquefied product from cellulose with phenol in the presence of sulfuric acid. Bioresource Technology **97**:313-321.

63. Zou, X. W., T. F. Qin, L. H. Huang, X. L. Zhang, Z. Yang, and Y. Wang. 2009. Mechanisms and Main Regularities of Biomass Liquefaction with Alcoholic Solvents. Energy & Fuels **23**:5213-5218.

Chapter 3

Characterization of Residue and Bio-oil Produced by Liquefaction of Loblolly Pine at

Different Reaction Times*

Abstract

The objective of this study was to analyze the effect of liquefaction time on the properties

of residue and bio-oil produced by liquefaction of loblolly pine using ethylene glycol at 150 ºC.

Liquefaction was carried out in a glass reactor for 30, 60, 90, 120, and 150 minutes. The lowest

residue content of 42 wt.% was obtained from 90 minutes of liquefaction. Fourier transform

infrared analysis of residue and bio-oil revealed that as liquefaction time was prolonged, more

hemicellulose underwent degradation, resulting in the formation of compounds containing

carbonyl groups. An inverse correlation between the intensity of peaks at 1,734 cm^{-1} (carbonyl

groups) and 3,293 cm^{-1} (OH stretching) in the infrared spectra of bio-oil was observed. X-Ray

diffraction analysis of residue supported the degradation of hemicellulose in the early stage of

liquefaction as well as cellulose degradation as the liquefaction was prolonged. Finally, the

hydroxyl number of bio-oil was determined by the phthalic anhydride esterification method and

was found to be in the range of 1,230 to 1,427 mg KOH/g, depending on liquefaction time.

3.1. Introduction

Forest biomass is receiving increased attention as an alternative feedstock to petroleum for the production of fuel and chemicals due to environmental concerns, the decrease in petroleum resources, and the instability in the petroleum market. Approximately 1,400 million dry tons of forest biomass per year are being produced in the United States (Perlack et al. 2005); therefore, there is a tremendous amount of research on the utilization of forest biomass as renewable and sustainable feedstock in the field of bioenergy and bioproduct. Moreover, the US Department of Energy and the US Department of Agriculture set a goal to produce 18 percent of the current US chemical commodities from biomass by 2020 and 25% by 2030 to reduce the country's dependency on petroleum (Perlack et al. 2005). This should also lower fossil fuel emissions, which have increased by 3.4% since 2010 (Bergman et al. 2014).

Organic solvent liquefaction, pyrolysis, and hydrothermal liquefaction are thermomechanical conversion techniques to convert forest biomass into a liquid product called "bio-oil." High hydroxyl (OH) functionality of bio-oil makes it a great candidate to be used as a bio-based polyol to synthesize a variety of polymers, including phenolic resins (Alma and Basturk 2006), polyurethane (Hu and Li 2014), epoxy resin (Kuo et al. 2014), polyester (Yu et al. 2006), and melamine formaldehyde and melamine urea-formaldehyde resin precursors, for the forest products industry (Kunaver et al. 2010). Replacement rates of phenol for various adhesives and polymers can often reach 50 percent, offering significant environmental supplementation to an otherwise petroleum-dependent process (Wei et al. 2014, Zhang et al. 2015).

In the organic solvent liquefaction technique, bio-oil is produced by liquefying biomass using an organic solvent in the presence of an acid or base catalyst at moderate temperatures (100ºC to 300ºC). The optimum liquefaction temperature was reported to be around 150ºC to 200ºC in terms of low residue content (RC) and high bio-oil yield when ethylene glycol (EG) was used as the liquefying solvent in the presence of acid catalyst (Celikbag et al. 2014). Different types of solvents have been previously studied. Phenol has been reported as the best liquefying solvent for biomass in terms of bio-oil yield (Zhang et al. 2006); however, owing to the toxicity of phenol, more environmental friendly solvents, such as EG, diethylene glycol (DEG), and glycerol, have gained more attention for liquefaction. Liquefaction of bagasse with EG (Zhang et al. 2007), spruce with DEG-glycerol (Jasiukaityte et al. 2010), pine with EG (Rezzoug and Capart 2002), switchgrass with DEG (Wei et al. 2014), and bamboo with EG (Ye et al. 2014) have been previously reported. These studies focused mainly on the effect of liquefaction time and temperature on bio-oil yield and bio-oil composition; however, information is sparse on residue formation and OH analysis of bio-oil, which are important considerations because they positively impact the financial feasibility for use as bioenergy or bioproducts (Kim et al. 2015).

Characterization of residue and bio-oil is necessary to improve our understanding behind organic solvent liquefaction of forest biomass, which enhances the utilization of bio-oil for the production of bio-based value-added products. Therefore, the objective of this study was to investigate the effect of liquefaction time on residue production and OH content of bio-oil.

3.2. Materials and Methods

3.2.1. Materials

Clean loblolly pine (*Pinus* spp.) wood chips were obtained from a local chipping plant in Opelika, Alabama. Physiochemical properties of loblolly pine were determined by traditional wet-chemistry analysis (Zhou et al. 2015). Extractives, cellulose, hemicellulose, and lignin content were also determined by the near-infrared (NIR) and Fourier transform infrared (FTIR) spectroscopy models generated by Jiang et al. (2014) and Zhou et al. (2015), respectively. Physiochemical properties determined by wet chemistry, NIR, and FTIR models are summarized in Table 3.1. All chemicals were purchased from VWR in reagent grade and used as received.

Table 3.1. Content of extractives, lignin, cellulose, and hemicellulose determined by wet chemistry, near-infrared (NIR), and Fourier transform infrared (FTIR) models.

	Content (wt.%)		
	Wet chemistry	NIR	FTIR
Extractives	4.5	4.6	2.5
Lignin	25.8	28.3	28.3
Cellulose	48.5	43.1	46.1
Hemicellulose	31.3	28.9	26.6

3.2.2. Wood Liquefaction

Loblolly pine was ground to 20-mesh particle size by a hammer mill (New Holland grinder model 358) for particle size reduction. The wood particles were kept in an oven at 105 ºC for 24 hours to remove moisture. Liquefaction was carried out in a three-neck atmospheric glass reactor equipped with a mechanical stirrer and condenser. The reactor was charged with 400 g of EG, 12 g of sulfuric acid (3 wt.% based on EG), and 100 g of pine wood particles. The reactor was then immersed in a preheated silicon oil bath at 150ºC. After the preset time (30, 60, 90, 120, and 150 min), the reaction was stopped, and the glass reactor was immersed in cold water to quench the reaction.

3.2.3. Determination of Residue Content

Liquefied wood was diluted with 1,4-dioxane–water–acetone (4:1:2, vol/vol) mixture and filtered with Whatman no. 1 filter paper under vacuum. The insoluble solid portion was labeled as residue, which was dried in an oven at 105 °C for 24 hours and then cooled to room temperature in a desiccator. The residue content (RC) was calculated as follows (eqn 1):

$$RC(\%) = \frac{\text{Weight of residue (g)}}{\text{Weight of starting pine wood (g)}} \times 100 \qquad (1)$$

The excess 1,4-dioxane–water–acetone was removed from the liquid portion by a rotary evaporator, and resulting liquid was labeled bio-oil. The liquefaction and separation methods are illustrated in Fig. 3.1.
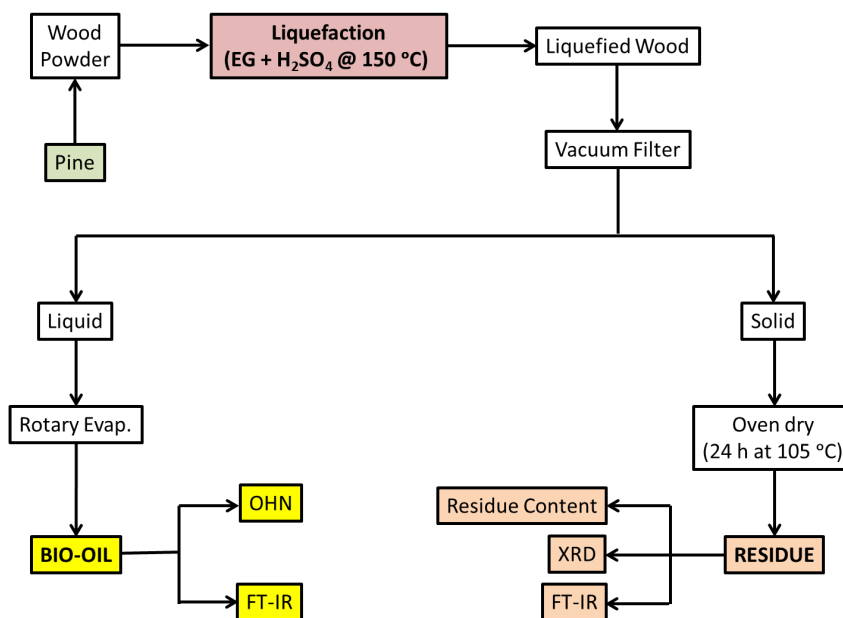
Fig. 3.1. Process scheme of bio-oil and residue production (EG = ethylene glycol; H_2SO_4 = sulfuric acid; Evap. = evaporator; OHN = total hydroxyl number; FT-IR = Fourier transform infrared; XRD = X-ray diffraction).

3.2.4. Degree of crystallinity index of residue

X-Ray diffractograms were collected by X-ray diffraction (Bruker D-8 Advanced, with a lynx eye detector) in the range of 0° to 40° at a scanning speed of 1°/s. The crystallinity index (CrI) was then calculated according to Eqn 2 (Segal et al. 1959) as follows:

$$\text{CrI}\left(\%\right) = \frac{I_{002} - I_{am}}{I_{002}} \tag{2}$$

where I_{002} is the maximum intensity of the (002) plane at $2\theta = 22.6°$ and I_{am} is the intensity diffraction of the amorphous band at $2\theta = 18°$.

3.2.5. Attenuated total reflection FTIR

Attenuated total reflection FTIR (ATR-FTIR) spectra of residue and bio-oil were acquired between 4,000 and 650 cm^{-1} with an ATR-FTIR spectrometer (Model Spectrum400, Perkin Elmer Co.) to identify functional groups. A small amount of residue (1 to 2 g) was put on the diamond crystal, and spectra were collected at room temperature (22°C ± 1 °C).

3.2.6. Determination of hydroxyl number of bio-oil

Total hydroxyl number (OHN) of bio-oil was determined using the phthalic esterification technique as described by Carey et al. (1984). In this technique, the phthalation reagent was prepared by dissolving phthalic anhydride (113.5 ± 2.5 g) and imidazole (17 ± 1 g) in 700 mL of pyridine. An appropriate amount of bio-oil was esterified with 25 mL of phthalation reagent in a pressure bottle at 100ºC for 20 minutes. After cooling to room temperature, 50 mL of pyridine and 10 mL of distilled water were added to the pressure bottles, and OHN was then quantitatively determined by titrating the esterified bio-oil with 0.5 N NaOH. OHN was defined

as milligrams of potassium hydroxide (KOH) per gram of sample and calculated as follows (eqn 3):

$$\text{OHN (mg KOH/g)} = \frac{(V_B - V_S) \times 56.1 \times 0.5}{W} \tag{3}$$

where V_B and V_S are the volume of NaOH consumed by blank (phthalation reagent only) and sample (bio-oil), respectively; W is the weight of sample (g); 56.1 is the equivalent weight of KOH (mg/meq); and 0.5 is the normality of NaOH.

3.3. Results and Discussion

3.3.1. RC analysis

RC was calculated in the range of 42 to 48 wt.%, depending on liquefaction time. As can be seen in Fig. 3.2, the RC decreased from 47 to 42 wt.% at 90 minutes of liquefaction and then increased again to 48 wt.% as the liquefaction was prolonged to 120 minutes. Other researchers have observed the RC decrease followed by an increase as well (Celikbag et al. 2014, Wei et al. 2014). Two reactions take place during liquefaction: alcoholysis and recondensation (Zhang et al. 2006, Zou et al. 2009). In alcoholysis reactions, wood polymers are degraded by solvent to low-molecular-weight components. As the liquefaction time is prolonged, highly reactive degraded wood components react with each other, and nonsoluble high-molecular-weight components are produced as the result of recondensation reactions. Therefore, a decrease and then an increase in RC are attributable to the alcoholysis reaction and the recondensation reaction, respectively.

Our laboratory has previously studied the liquefaction of loblolly pine using a sealed Parr reactor where the RC was found to be 25 wt.% when liquefaction was carried out at 150 ºC for

60 minutes under 70 to 80 psi of pressure (Celikbag et al. 2014). However, in this study, an atmospheric glass reactor was used for liquefaction, and the RC was calculated to be 47 wt.% (Fig. 3.2) at 150 °C for 60 minutes. Although liquefaction in both a sealed Parr and a glass reactor was carried out at the same biomass-to-solvent ratio (1:4, wt/wt) and acid catalyst concentration (3 wt.%, based on EG) as a similar study (Celikbag et al. 2014), the glass reactor was determined to be less efficient and lower in RC. Similar trends have also been reported by other researchers who studied wood liquefaction using different reactors (Pan et al. 2007). In their study, the RC was found to be 70 wt.% and 50 wt.% when an atmospheric glass reactor and a sealed Parr reactor were used for liquefaction, respectively. Less RC when using a Parr reactor could be attributable to the pressurized effect, which facilitates the penetration of liquefying solvent through biomass so that more biomass undergoes decomposition, resulting in less residue (Vasilakos and Austgen 1985, Toor et al. 2013).
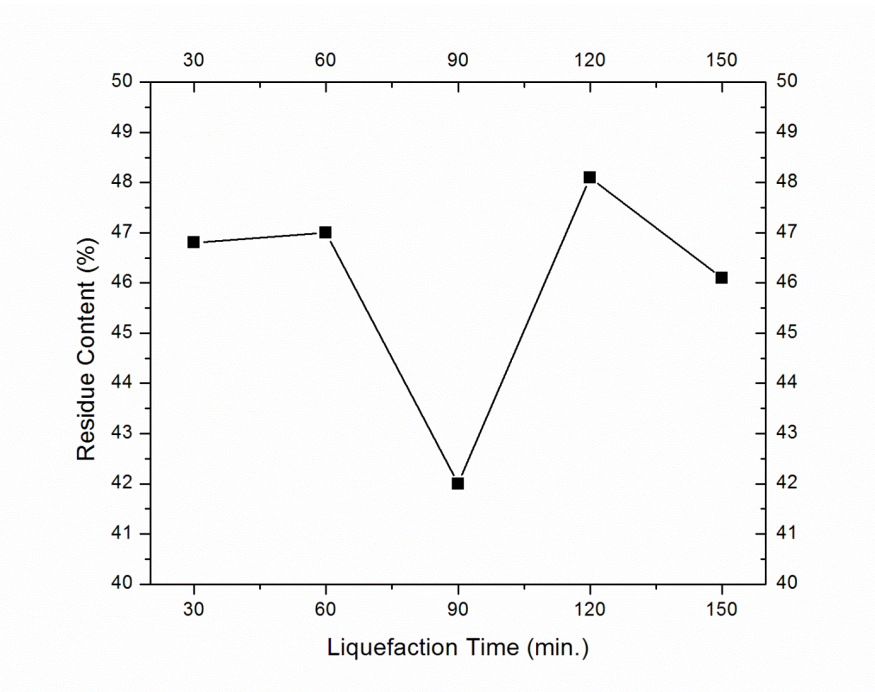
Fig. 3.2. Residue content obtained from liquefaction of loblolly pine with ethylene glycol at 150 °C for 30, 60, 90, 120 and 150 minutes.

3.3.2. FTIR analysis of residues

Because woody biomass is a highly complex composite material composed of cellulose, hemicellulose, and lignin, as shown in Table 3.1, it has various functional groups in its structure. Therefore, many peaks exist in the IR spectra of pine and residues, as shown in Fig. 3.3, and their respective peak assignments are presented in Table 3.2.
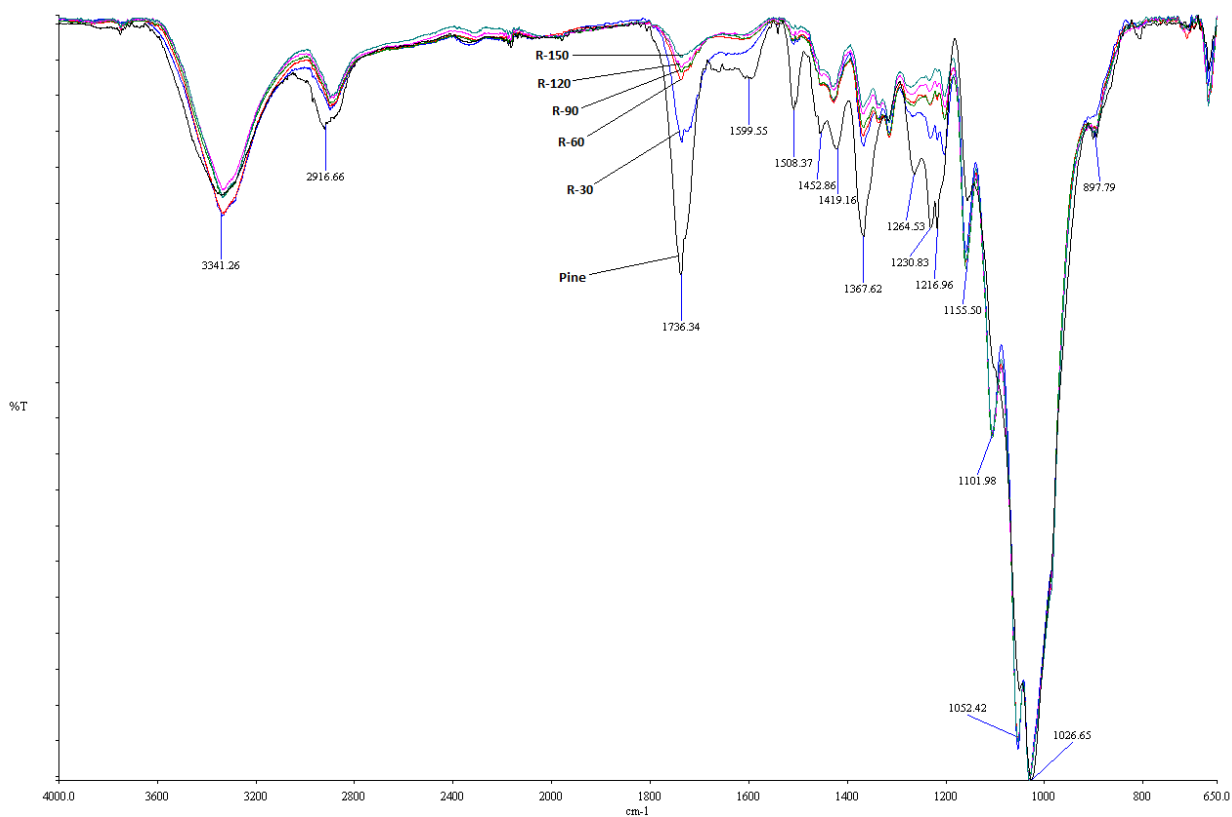
Fig. 3.3. Infrared spectra of loblolly pine and liquefaction residues obtained from different liquefaction times (R-30, R-60, R-90, R-120, and R-150 are the residues obtained from 30, 60, 90, 120, and 150 min of liquefaction, respectively).

There was a significant difference between pine and residues in the intensity of spectral peaks at 1,736 cm^{-1} owing to the carbonyl (C=O) stretching of acetyl or carboxylic acid. Acetyl ester groups in xylan, the major carbohydrate in hemicellulose, is the main source of C=O

47

stretching (Pérez et al. 2002, Pan et al. 2007); therefore, the peak at 1,736 cm^{-1} is considered the characteristic peak of hemicellulose (Pan et al. 2007, Rana et al. 2010, Huang et al. 2012, Casas et al. 2013). As the liquefaction time was prolonged, it was observed that the intensity of peak at 1,736 cm^{-1} decreased. Intensity reductions were most pronounced after 30 minutes and then continued to decrease significantly after 90 minutes of exposure time. This finding suggests that the longer liquefaction time yields more hemicellulose degradation products. This agrees with the literature where hemicellulose was reported as the wood polymer most subject to degradation under acidic conditions (Xiao et al. 2013). Lee et al. (2010) also reported that hemicellulose degraded faster than lignin and cellulose, as observed in our study. Longer residence times yielded additional decomposition but at much slower rates. Other studies that characterized residues from liquefaction of cypress biomass in hot-compressed water found a complete disappearance of the peak at 1,722 cm^{-1} as liquefaction time and temperature increased. Their study likewise witnessed the disappearance of hemicellulose before lignin and cellulose when the residues were analyzed with FTIR (Liu et al. 2013).

Another significant change in the IR spectra was observed at the peaks at 1,508 cm^{-1}, which was because of the C=C stretching in the aromatic ring. The peak at 1,508 cm^{-1} was considered the characteristic peak of lignin (Colom et al. 2003, Rana et al. 2010, Huang et al. 2012, Casas et al. 2013, Salehian et al. 2013). Lignin is also responsible for the peak at 1,367 cm^{-1}, which was attributed to phenolic OH groups (Gonzalez Alriols et al. 2009, Zhao et al. 2013). It was observed that the intensity of these two characteristic peaks of lignin at 1,508 and 1,367 cm^{-1} decreased as the reaction was prolonged, indicating that the degradation of lignin

increased during liquefaction. But the degradation rates observed for lignin appeared less pronounced than hemicellulose based on the spectrum in this analysis.

The peaks at 1,155, 1,101, 1,052, and 897 cm^{-1} are assigned to cellulose (Table 3.2). As opposed to hemicellulose and lignin, the intensity of the peaks associated with cellulose was increased with liquefaction time. Most of the hemicellulose and lignin were decomposed during liquefaction, while the relative content of cellulose within the residues increased. The increase in cellulose content was indicative of higher resistance to degradation than hemicellulose and lignin in EG solvolysis because of (i) its highly crystalline structure and (ii) the structure of the cell wall, where lignin and hemicellulose shield cellulose. Therefore, the peaks attributed to cellulose became more visible (sharper) in the IR spectra. Zheng et al. (2012) also reported that cross-linking of cellulose caused an increase in intensity at 1,156 cm^{-1}.

Table 3.2. Characteristic FT-IR bands of pine and residues obtained from different liquefaction times

Wavenumber (cm^{-1})	Functional group	Assignment	References
3,341	–OH stretch	Cellulose, hemicellulose, lignin (alcohols, phenols)	Pan et al. (2007), Huang et al. (2012)
2,916	–C–H, –CH2– stretching in methyl and methylene group, hydrocarbon chains	Cellulose, extractives	Huang et al. (2012), Salehian et al. (2013)
1,736	C=O stretching of acetyl or carboxylic acid (frequently carbohydrate origin)	Hemicellulose	Pan et al. (2007), Rana et al. (2010), Huang et al. (2012), Casas et al. (2013), Salehian et al. (2013)
1,599, 1,508	C=C stretching in aromatic ring	Lignin	Colom et al. (2003), Rana et al. (2010), Huang et al. (2012), Casas et al. (2013), Salehian et al. (2013), Shibata et al. (2013)
1,452	C–H bending	Lignin	Bakirtzis et al. (2012)
1,419	C–H$_2$ symmetric bending	Cellulose	Colom et al. (2003), Salehian et al. (2013)
1,367	–OH (phenolic)	Lignin	Gonzalez Alriols et al. (2009), Zhao et al. (2013)
1,264, 1,230, 1,216	Vibration of guaiacyl ring	Lignin	Li et al. (2010), Casas et al. (2013)
1,155	C–O–C asymmetric stretching	Cellulose	Colom et al. (2003), Salehian et al. (2013)
1,101, 1,052	C–O stretching	Cellulose, hemicellulose	Chen et al. (2011)
1,026	C–O–C stretching	Cellulose	Pholosi et al. (2013)
897	Out-of-phase ring stretching	Cellulose	Colom et al. (2003), Salehian et al. (2013)

3.3.3. Degree of crystallinity index of residue

Degree of crystallinity of residue, which is defined as the weight fraction of crystalline material (crystalline cellulose) in residue (Jiang et al. 2007), was calculated by X-ray diffraction (XRD) analysis. The XRD patterns and the crystallinity index of residues are shown in Fig. 3.4. There are typically three diffraction peaks of cellulose at 2θ of 15°, 16.5°, and 23° due to 101, 10Ī, and 002 reflections, respectively (Popescu et al. 2008); however, owing to the complex structure of wood, peaks of 101 and 10Ī diffractions overlapped and generated a broad peak at around 2θ of 14° to 16°.
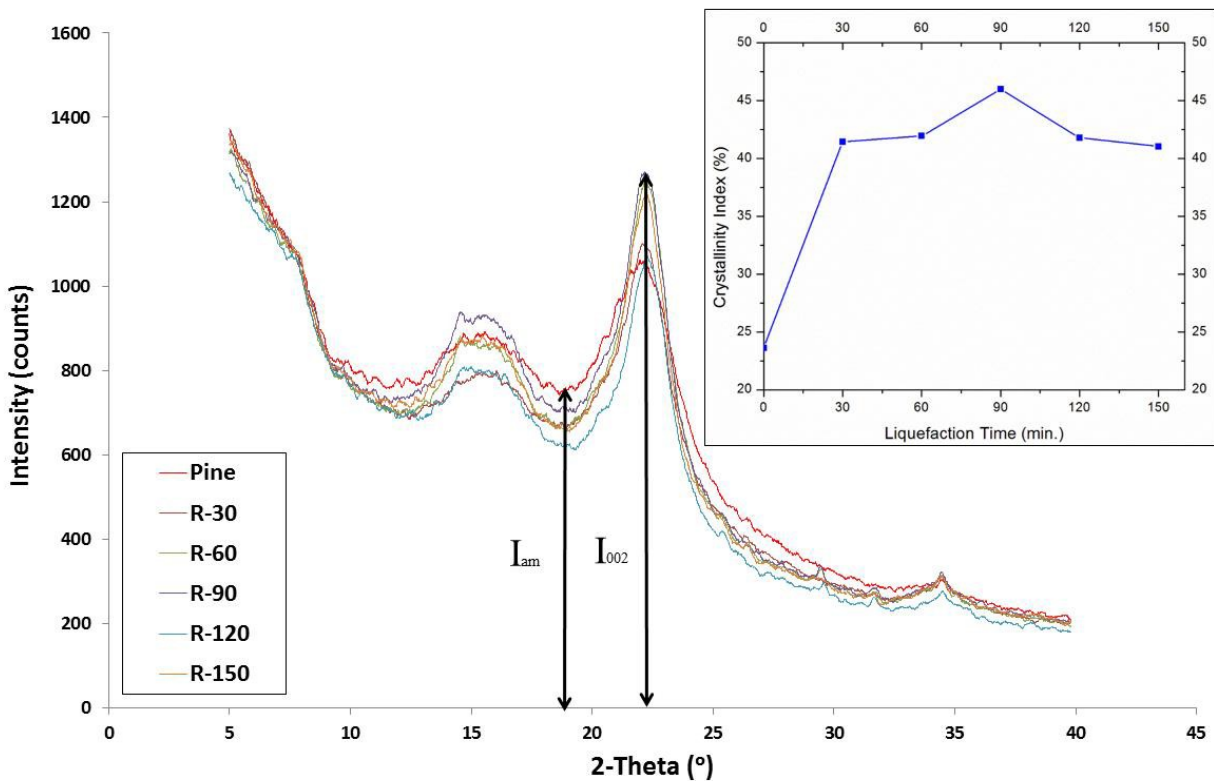
Fig. 3.4. XRD diffractogram of the residues obtained from liquefaction of loblolly pine with ethylene glycol at 150 °C for 30 (R-30), 60 (R-60), 90 (R-90), 120 (R-120) and 150 (R-150) min. I_{002} is the maximum intensity of the (002) plane at 2θ = 22.6°, and I_{am} is the intensity diffraction of the amorphous band at 2θ = 18°. Inset: Crystallinity index of residues.

The crystallinity index of loblolly pine before liquefaction was calculated to be 23%, as shown in Figure 4. After liquefaction, the crystallinity indices of residues were found to be 41, 42, 46, 42, and 41% for 30, 60, 90, 120, and 150 minutes of liquefaction, respectively. This dramatic increase in crystallinity index from 23 to 41% for just 30 minutes of liquefaction time may be attributable to hemicellulose degradation, which is an amorphous polymer and very sensitive to temperature. Via et al. (2013) reported that hemicellulose was the first depolymerized wood component under thermal treatment. Thus, hemicellulose degradation in the early stage of liquefaction resulted in an increase in relative crystallinity. As the liquefaction was carried out for 90 minutes, the highest crystallinity index of 45% was obtained. As discussed in the FTIR analysis of residues, an increase in the degradation of lignin was observed as liquefaction was prolonged, using the decrease in intensity of characteristic peaks of lignin (1,508 and 1,367 cm^{-1}) as an indicator. An increase in crystallinity index as a result of decomposition of amorphous components in wood has been observed by other researchers as well (Pan et al. 2007, Liu et al. 2013). Therefore, lignin and hemicellulose degradation likely contributed to the increase in the crystallinity index at 90 minutes of liquefaction because more amorphous components of wood were decomposed. It was observed that the crystallinity index of residues obtained from 120 and 150 minutes of liquefaction started decreasing. By definition, the crystallinity index is the weight fraction of crystalline material in residue; thus, a decrease in the crystallinity index could be interpreted as the indication of decomposition of the crystalline portion of the wood, which is mostly cellulose.

3.3.4. OHN of bio-oil

Bio-oil is used to produce a variety of polymers, including phenolic resin, polyurethane, epoxy, and polyester, and OH groups in bio-oil are utilized to synthesize these polymers (Pan 2011). The reaction behavior of bio-oil based polymers is assumed to depend on the interaction between OH groups from the bio-oil and the formaldehyde (CH_2O) for phenol-formaldehyde resin, isocyanate ($R–N=C=O$) for the polyurethane, the epoxide (C_2H_4O) group for epoxy resin, and ester (–COOH) groups for polyester production. Therefore, characterization of the OH groups plays a crucial role in process optimization of bio-oil–based polymer synthesis.

The total OHN of bio-oils was quantitatively calculated by the esterification method. The OHN of pure EG was also calculated by the esterification method in order to confirm the accuracy of the method. OHN of EG was calculated to be $1,830 \pm 10$ mg KOH/g, which was quite close to the theoretical OHN value of EG, 1,808 mg KOH/g.

The total OHN of bio-oil from the liquefaction time treatments ranged from 1,230 to 1,427 mg KOH/g, as shown in Fig. 3.5. Analysis of variance (single factor, 95% confidence interval, and three replications) was performed, and it was found that liquefaction time had a significant effect on OHN ($p < 0.0001$). The high OHN across the entire range was consistent with other studies (Budija et al. 2009, Kunaver et al. 2010, Wei et al. 2014). However, relatively lower OHN, such as 212 to 450 mg KOH/g, has also been reported by other researchers (Zou et al. 2012, D'Souza and Yan 2013, Xiao et al. 2013). Considerable differences in OHN may be attributable to solvent type, solvent-to-biomass ratio, heating source (microwave, heat bath, and autoclave), and liquefaction time and temperature. Celikbag et al. (2014) reported that unreacted

liquefying solvent retained in the bio-oil was the major source for OH groups and accounted for 70 to 94 percent of the OHN, depending on liquefaction conditions. Therefore, the high OHN in this study could be attributable to the unreacted EG retained in bio-oil after liquefaction.
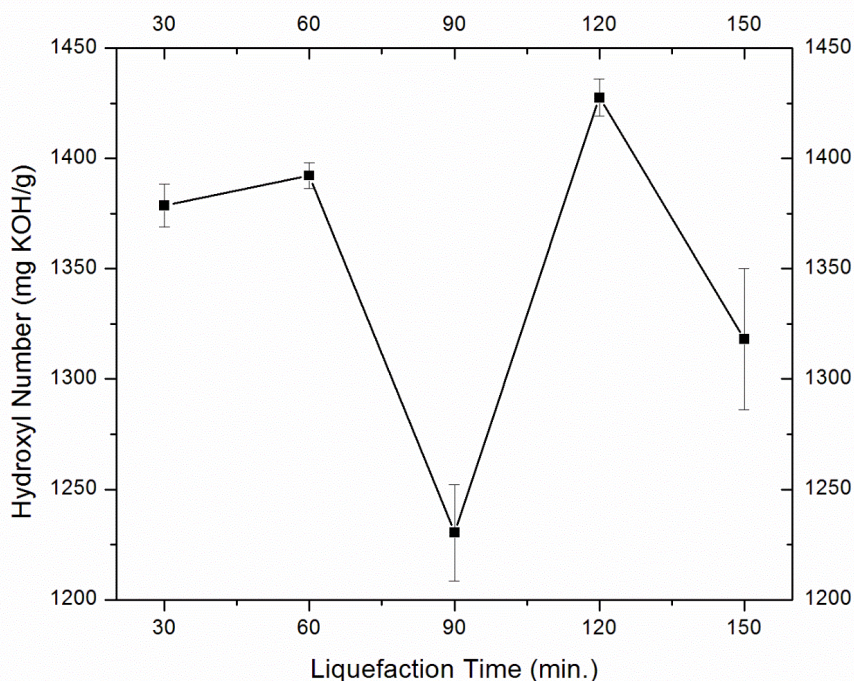
Fig. 3.5. Hydroxyl number (OHN) of the liquefaction oil of loblolly pine produced at 150 °C for 30, 60, 120 and 150 min.

The first decrease in OHN was observed at 90 minutes of liquefaction (Fig. 3.5) and could be attributable to the biomass decomposition by EG (alcoholysis reaction). It was expected that a decreasing trend in the OHN as the liquefaction time was prolonged would be seen because of the alcoholysis reaction; however, this was not the case. We observed that OHN increased again at 120 minutes of liquefaction. An increase in OHN at prolonged liquefaction times was also reported by other researchers who conjectured that condensation reactions during liquefaction resulted in increased OHN (Sun et al. 2011, Wei et al. 2014).

3.3.5. FTIR analysis of bio-oil

The IR spectra of pure EG and bio-oils were obtained from different reaction times and are shown in Fig. 3.6. The IR spectra of bio-oils and EG were quite similar, indicating that EG was the dominant factor driving the distribution of reaction products of bio-oil (Fig. 3.6). The unreacted residual EG in the bio-oil could also cause similar IR spectra (Celikbag et al. 2014) as observed for bio-oil. Bio-oils are labeled BO-30, BO-60, BO-90, BO-120, and BO-150 for 30, 60, 90, 120, and 150 minutes of liquefaction, respectively, for this discussion. All bio-oils exhibited a broad peak at 3,293 cm^{-1}, which is because of the OH groups, indicating that all liquefaction oils contain a significant amount of OH groups, as evidenced by phthalic anhydride esterification. The peak at 1,736 cm^{-1} was owing to the carbonyl (C=O) stretching groups. Oxidation of EG is the main reason for the generation of carbonyl groups containing compounds such as aldehydes, ketones, and carboxylic acids (Xiao et al. 2011). Levulinic acid, a compound that contains carbonyl and carboxyl group in its structure, was reported as the main component that contributed to intensity of the peak at 1,736 cm^{-1} (Budija et al. 2009).

Compounds containing carbonyl groups are formed by the reaction of six carbon sugars (degradation products of cellulose or hemicellulose) with OH groups of the EG. Formation of carbonyls, therefore, is related to the consumption of OH groups. This phenomenon explains the inverse correlation between the intensity of peaks at 1,736 and 3,293 cm^{-1} (attributed to OH stretching) that was observed in the IR spectra (Fig. 3.6). For example, BO-90 exhibited the lowest peak intensity at 3,293 cm^{-1} and the highest peak intensity at 1,736 cm^{-1}. Because more OH groups underwent oxidation reactions, a lower intensity was observed at the peak at 3,293 cm^{-1}. Conversely, more OH consumption yielded more carbonyls, resulting in higher peak

intensity at 1,736 cm^{-1} for BO-90. Peak intensity of bio-oils at 1,736 cm^{-1} shows the following

order (Fig. 6): BO-30 < BO-60 < BO150 ≈ BO-120 < BO-90. This sequence was perhaps the

consequence of condensation reactions. After 90 minutes of liquefaction, the intensity at 1,736

cm^{-1} decreased, suggesting the presence of condensation reactions. One study showed that

insoluble residues could be generated from hydroxymethyl furfural derivatives in the presence of

water (Yamada et al. 2007). In fact, we observed an increase in RC after 90 minutes of
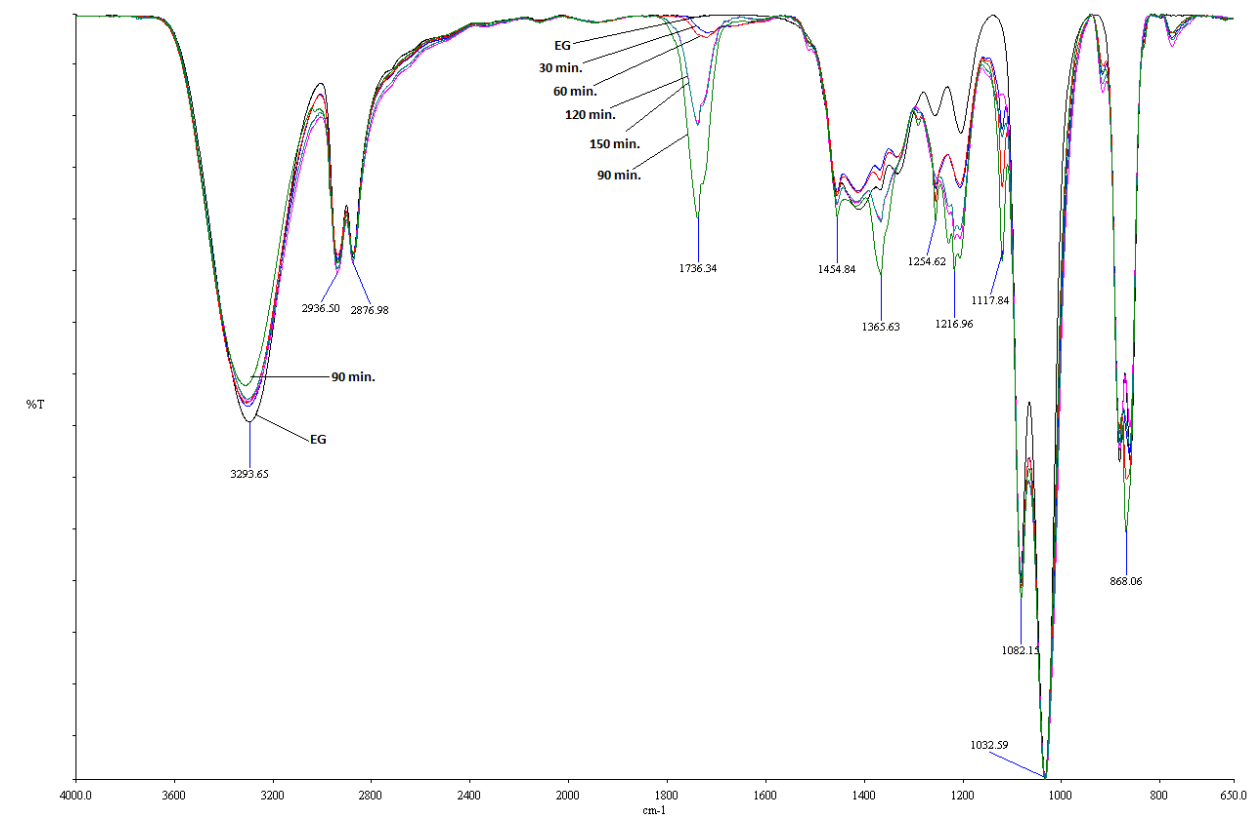
liquefaction.

Fig. 3.6. FT-IR spectra of liquefaction oils produced at 150 °C for various liquefaction times (EG = Ethylene glycol).

3.4. Summary of Results

Loblolly pine was liquefied in a glass reactor using EG at 150 ºC in the presence of acid

catalyst for five different reaction times: 30, 60, 90, 120, and 150 minutes. RC was found to be in

the range of 42 to 48 wt.%, depending on liquefaction time. The lowest RC was obtained from 90 minutes of liquefaction. The intensity of the hemicellulose peak (1,736 cm^{-1}) in the IR spectra of residues was observed to be decreasing as the liquefaction time was prolonged, indicating significant hemicellulose degradation. XRD analysis of residues also supported the hemicellulose degradation in the early stages of liquefaction. The crystallinity index of residues was found to be 41, 42, 46, 42, and 41% for 30, 60, 90, 120, and 150 minutes of liquefaction, respectively. All bio-oils were found to be rich in OH groups attributable to the excess EG, which generated broad peaks at 3,293 cm^{-1} in the IR spectra. OHN of bio-oil were calculated to be 1,230 to 1,427 mg KOH/g, depending on the liquefaction time.

3.5. Conclusion

This study shows that loblolly pine could be successfully converted to a liquid product called bio-oil using EG at 150 ºC. Bio-oil has the potential to be used as a bio-based polyol because of the high OHN. With continuous research, this field can provide a profitable and renewable resource that will reduce the US dependence on petrochemical polyols. Continued research must explore the source and variation of OHN found within the bio-oil as well as the effect of liquefaction parameters, such as temperature, pressure, and the biomass-to-solvent ratio, on OHN.

References

1. Alma, M. H. and M. A. Basturk. 2006. Liquefaction of grapevine cane (*Vitis vinisera* L.) waste and its application to phenol-formaldehyde type adhesive. *Ind. Crops Prod.* 24:171–176.

2. Bakirtzis, D., V. Tsapara, S. Liodakis, and M. A. Delichatsios. 2012. ATR investigation of the mass residue from the pyrolysis of fire retarded lignocellulosic materials. *Thermochim Acta* 550:48–52.

3. Bergman, R., Puettmann, M., Taylor, A., and Skog, K. 2014. The carbon impacts of wood products. *Forest Prod. J.,* 641(7/8): 220-231.

4. Budija, F., C. Tavzes, L. Zupancic-Kralj, and M. Petric. 2009. Self-crosslinking and film formation ability of liquefied black poplar. *Bioresour. Technol.* 100:3316–3323.

5. Carey, M. A., S. L. Wellons, and D. K. Elder. 1984. Rapid method for measuring the hydroxyl content of polyurethane polyols. *J. Cell. Plast.* 20:42–48.

6. Casas, A., M. Oliet, M. V. Alonso, T. M. Santos, and F. Rodriguez. 2013. Dissolution of *Pinus radiata* and *Eucalyptus globulus* woods in 1-allyl-3-methylimidazolium chloride for cellulose or lignin regeneration. *Ind. Eng. Chem. Res.* 52:3628–3636.

7. Celikbag, Y., B. K. Via, S. Adhikari, and Y. Wu. 2014. Effect of liquefaction temperature on hydroxyl groups of bio-oil from loblolly pine (*Pinus taeda*). *Bioresour. Technol.* 169:808–811.

8. Chen, B. L., M. X. Yuan, and H. Liu. 2011. Removal of polycyclic aromatic hydrocarbons from aqueous solution using plant residue materials as a biosorbent. *J. Hazard. Mater.* 188:436–442.

9. Colom, X., F. Carrillo, F. Nogues, and P. Garriga. 2003. Structural analysis of photodegraded wood by means of FTIR spectroscopy. *Polym. Degrad. Stabil.* 80:543–549.

10. D'Souza, J. and N. Yan. 2013. Producing bark-based polyols through liquefaction: Effect of liquefaction temperature. *ACS Sustain. Chem. Eng.* 1:534–540.

11. Gonzalez Alriols, M., A. Tejado, M. Blanco, I. Mondragon, and J. Labidi. 2009. Agricultural palm oil tree residues as raw material for cellulose, lignin and hemicelluloses production by ethylene glycol pulping process. *Chem. Eng. J.* 148:106–114.

12. Hu, S. J. and Y. B. Li. 2014. Two-step sequential liquefaction of lignocellulosic biomass by crude glycerol for the production of polyols and polyurethane foams. *Bioresour. Technol.* 161:410–415.

13. Huang, X. A., D. Kocaefe, Y. Kocaefe, Y. Boluk, and A. Pichette. 2012. Changes in wettability of heat-treated wood due to artificial weathering. *Wood Sci. Technol.* 46:1215–1237.

14. Jasiukaityte, E., M. Kunaver, and C. Crestini. 2010. Lignin behaviour during wood liquefaction—Characterization by quantitative P-31, C-13 NMR and size-exclusion chromatography. *Catal. Today* 156:23–30.

15. Jiang, W., G. Han, B. Via, M. Tu, W. Liu, and O. Fasina. 2014. Rapid assessment of coniferous biomass lignin–carbohydrates with near-infrared spectroscopy. *Wood Sci. Technol.* 48:109–122.

16. Jiang, Z.-H., Z. Yang, C.-L. So, and C.-Y. Hse. 2007. Rapid prediction of wood crystallinity in *Pinus elliotii* plantation wood by near-infrared spectroscopy. *J. Wood Sci.* 53:449–453.

17. Kim, D., N. M. Anderson, and W. Chung. 2015. Financial performance of a mobile pyrolysis system used to produce biochar from sawmill residues. *Forest Prod. J.* 65(5/6):189–197.

18. Kunaver, M., S. Medved, N. Cuk, E. Jasiukaityte, I. Poljansek, and T. Strnad. 2010. Application of liquefied wood as a new particle board adhesive system. *Bioresour. Technol.* 101:1361–1368.

19. Kuo, P. Y., M. Sain, and N. Yan. 2014. Synthesis and characterization of an extractive-based bio-epoxy resin from beetle infested *Pinus contorta* bark. *Green Chem.* 16:3483–3493.

20. Lee, D. H., E. Y. Cho, C. J. Kim, and S. B. Kim. 2010. Pretreatment of waste newspaper using ethylene glycol for bioethanol production. *Biotechnol. Bioprocess Eng.* 15:1094–1101.

21. Li, G. Y., A. M. Huang, T. F. Qin, and L. H. Huang. 2010. FTIR studies of Masson pine wood decayed by brown-rot fungi. *Spectrosc. Spectral Anal.* 30:2133–2136.

22. Liu, H.-M., M.-F. Li, S. Yang, and R.-C. Sun. 2013. Understanding the mechanism of cypress liquefaction in hot-compressed water through characterization of solid residues. *Energies* 6:1590–1603.

23. Pan, H. 2011. Synthesis of polymers from organic solvent liquefied biomass: A review. *Renew. Sustain. Energy Rev.* 15:3454–3463.

24. Pan, H., T. F. Shupe, and C.-Y. Hse. 2007. Characterization of liquefied wood residues from different liquefaction conditions. *J. Appl. Polym. Sci.* 105:3740–3746.

25. Pérez, J., J. Muñoz-Dorado, T. D. L. Rubia, and J. Martínez. 2002. Biodegradation and biological treatments of cellulose, hemicellulose and lignin: An overview. *Int. Microbiol.* 5:53–63.

26. Perlack, R. D., L. L. Wright, A. F. Turhollow, R. L. Graham, B. J. Stokes, and D. C. Erbach. 2005. Biomass as feedstock for a bioenergy and bioproducts industry: The technical feasibility of a billion-ton annual supply. Defense Technical Information Center, Washington, D.C.

27. Pholosi, A., A. E. Ofomaja, and E. B. Naidoo. 2013. Effect of chemical extractants on the biosorptive properties of pine cone powder: Influence on lead(II) removal mechanism. *J.Saudi Chem. Soc.* 17:77–86.

28. Popescu, C. M., C. M. Tibirna, I. E. Raschip, M. C. Popescu, P. Ander, and C. Vasile. 2008. Bulk and surface characterization of unbleached and bleached softwood kraft pulp fibres. *Cellulose Chem. Technol.* 42:525–547.

29. Rana, R., R. Langenfeld-Heyser, R. Finkeldey, and A. Polle. 2010. FTIR spectroscopy, chemical and histochemical characterisation of wood and lignin of five tropical timber wood species of the family of Dipterocarpaceae. *Wood Sci. Technol.* 44:225–242.

30. Rezzoug, S. A. and R. Capart. 2002. Liquefaction of wood in two successive steps: Solvolysis in ethylene-glycol and catalytic hydrotreatment. *Appl. Energy* 72:631–644.

31. Salehian, P., K. Karimi, H. Zilouei, and A. Jeihanipour. 2013. Improvement of biogas production from pine wood by alkali pretreatment. *Fuel* 106:484–489.

32. Segal, L., J. J. Creely, A. E. Martin, and C. M. Conrad. 1959. An empirical method for estimating the degree of crystallinity of native cellulose using the X-ray diffractometer. *Text. Res. J.* 29:786–794.

33. Shibata, M., N. Teramoto, T. Nakamura, and Y. Saitoh. 2013. All-cellulose and all-wood composites by partial dissolution of cotton fabric and wood in ionic liquid. *Carbohydr. Polym.* 98:1532–1539.

34. Sun, P. Q., M. X. Heng, S. H. Sun, and J. W. Chen. 2011. Analysis of liquid and solid products from liquefaction of paulownia in hot-compressed water. *Energy Convers. Manag.* 52:924–933.

35. Toor, S. S., H. Reddy, S. Deng, J. Hoffmann, D. Spangsmark, L. B. Madsen, J. B. Holm-Nielsen, and L. A. Rosendahl. 2013. Hydrothermal liquefaction of *Spirulina* and *Nannochloropsis salina* under subcritical and supercritical water conditions. *Bioresour. Technol.* 131:413–419.

36. Vasilakos, N. P. and D. M. Austgen. 1985. Hydrogen-donor solvents in biomass liquefaction. *Ind. Eng. Chem. Process Des. Dev.* 24:304–311.

37. Via, B. K., S. Adhikari, and S. Taylor. 2013. Modeling for proximate analysis and heating value of torrefied biomass with vibration spectroscopy. *Bioresour. Technol.* 133:1–8.

38. Wei, N., B. K. Via, Y. F. Wang, T. McDonald, and M. L. Auad. 2014. Liquefaction and substitution of switchgrass (*Panicum virgatum*) based bio-oil into epoxy resins. *Ind. Crops Prod.* 57:116–123.

39. Xiao, W. H., L. J. Han, and Y. Y. Zhao. 2011. Comparative study of conventional and microwave-assisted liquefaction of corn stover in ethylene glycol. *Ind. Crops Prod.* 34:1602–1606.

40. Xiao, W. H., W. J. Niu, F. Yi, X. Liu, and L. J. Han. 2013. Influence of crop residue types on microwave-assisted liquefaction performance and products. *Energy Fuels* 27:3204–3208.

41. Yamada, T., M. Aratani, S. Kubo, and H. Ono. 2007. Chemical analysis of the product in acid-catalyzed solvolysis of cellulose using polyethylene glycol and ethylene carbonate. *J. Wood Sci.* 53:487–493.

42. Ye, L. Y., J. M. Zhang, J. Zhao, and S. Tu. 2014. Liquefaction of bamboo shoot shell for the production of polyols. *Bioresour. Technol.* 153:147–153.

43. Yu, F., Y. H. Liu, X. J. Pan, X. Y. Lin, C. M. Liu, P. Chen, and R. Ruan. 2006. Liquefaction of corn stover and preparation of polyester from the liquefied polyol. *Appl. Biochem. Biotechnol.* 130:574–585.

44. Zhang, T., Y. J. Zhou, D. H. Liu, and L. Petrus. 2007. Qualitative analysis of products formed during the acid catalyzed liquefaction of bagasse in ethylene glycol. *Bioresour. Technol.* 98:1454–1459.

45. Zhang, Y., D.-Q. Yang, X.-M. Wang, M. Feng, and G. He. 2015. Fungus-modified lignin and its use in wood adhesive for manufacturing wood composites. *Forest Prod. J.* 65:43–47.

46. Zhang, Y. C., A. Ikeda, N. Hori, A. Takemura, H. Ono, and T. Yamada. 2006. Characterization of liquefied product from cellulose with phenol in the presence of sulfuric acid. *Bioresour. Technol.* 97:313–321.

47. Zhao, Y., N. Yan, and M. W. Feng. 2013. Effects of reaction conditions on phenol liquefaction of beetle-infested lodgepole pine barks. *Curr. Org. Chem.* 17:1604–1616.

48. Zheng, A. Q., Z. L. Zhao, S. Chang, Z. Huang, F. He, and H. B. Li. 2012. Effect of torrefaction temperature on product distribution from two-staged pyrolysis of biomass. *Energy Fuels* 26:2968–2974.

49. Zhou, C., W. Jiang, B. K. Via, O. Fasina, and G. Han. 2015. Prediction of mixed hardwood lignin and carbohydrate content using ATR-FTIR and FT-NIR. *Carbohydr. Polym.* 121:336–341.

50. Zou, X. W., T. F. Qin, L. H. Huang, X. L. Zhang, Z. Yang, and Y. Wang. 2009. Mechanisms and main regularities of biomass liquefaction with alcoholic solvents. *Energy Fuels* 23:5213–5218.

51. Zou, X. W., T. F. Qin, Y. Wang, L. H. Huang, Y. M. Han, and Y. Li. 2012. Synthesis and properties of polyurethane foams prepared from heavy oil modified by polyols with 4,4'-methylene-diphenylene isocyanate (MDI). *Bioresour. Technol.* 114:654–657.

Chapter 4

Effect of Liquefaction Temperature on Hydroxyl Groups of Bio-oil from Loblolly Pine

(Pinus taeda)*

Abstract

The goal of this study was to analyze the effect of liquefaction temperature on hydroxyl (OH) groups of bio-oil, and to establish a comprehensive OH characterization to determine the source and variation of OH groups. Loblolly pine was liquefied with ethylene glycol (EG) at 100, 150, 200 and 250 °C. Hydroxyl number (OHN) of the bio-oil was ranged from 632 to 1430 mg KOH/g. GC-MS analysis showed that 70 – 90 % of OHN was generated from unreacted EG. ^{31}P-NMR analysis showed that the majority of OH groups were aliphatic, and none of the bio-oil exhibited any detectable OH groups from phenolic sources. A condensation reaction model was provided to explain how lignin fragments reacted with EG to remove available phenolic OH groups. Carbonyl formation was confirmed by ATR-FT-IR analysis. Finally, it was found that all bio-oils were stable in terms of OHN for two months when stored at -10 °C.

4.1. Introduction

Polyol is a compound that has multiple hydroxyl groups in its structure and is essential for the synthesis of a variety of polymers such as epoxy, polyurethane, polyester, polycarbonate, and phenolic resin. However, today the major source for polyols is petroleum. Research has thus shifted to bio-based polyols in the face of depleting petroleum reserves, increased greenhouse effect, as well as increase in demand by the consumers for bio-based products.

Lignocellulosic biomass is being used as an alternative feedstock for the production of bio-based polyols in order to reduce our dependency on petroleum. Lignocellulosic biomass is considered the most abundant natural resource with annual production of around 1.3 billion dry tons in the U.S.A. (Perlack et. al., 2005). There is a tremendous amount of research on utilization of lignocellulosic biomass to produce bio-based materials. The U.S. Department of Energy (DOE) and the U.S. Department of Agriculture (USDA) have prioritized the development of bioenergy and bioproducts, and they have a goal to produce 18% of the current U.S. chemical commodities from biomass by 2020, and 25% by 2030 (Perlack et. al., 2005). Organic solvent liquefaction is one thermomechanical conversion technique to convert lignocellulosic biomass to bio-oil in which biomass is liquefied with an organic solvent under acid or base catalyzed conditions at moderate temperatures (100 – 300 °C). The percentage of conversion from biomass to bio-oil depends on the liquefaction time and temperature, and the solvent type used (Durak and Aysu, 2014). Phenol based solvents showed the highest bio-oil yield (Zhang et al., 2006); however, because of the toxicity of phenol and the environmental concerns, more environmental and human friendly alcoholic solvents such as ethylene glycol (EG), diethylene glycol (DEG) and glycerol are preferable.

Gas chromatography–mass spectrometry (GC-MS) studies have shown that bio-oil is a highly complex mixture of carbohydrates, furans, phenols, and organic acids as a result of the depolymerization of biomass polymers which are primarily cellulose, hemicellulose and lignin (Yip et al., 2009). Degradation products of lignocellulosic biomass and the liquefying solvent provide a great amount of hydroxyl (OH) groups; therefore, bio-oil has attracted interest to be used as a bio-based polyol. Recently variety of polymers including epoxy resin (Wei et al., 2014), melamine-formaldehyde and melamine-urea-formaldehyde resin precursors (Kunaver et al., 2010) and polyurethane (Hu and Li., 2014; Zou et al., 2012) have been synthesized using bio-oil as a polyol, and these studies showed that OH groups of bio-oil play important role on determining the properties of resulting polymer. For example, Wei et al. (2014) used bio-oil to modify an epoxy resin, and they found that the OHN of the bio-oil had significant effect on glass transition temperature (Tg) of the modified epoxy resin. In that study, plasticizer effect of the unreacted liquefying solvent on the modified epoxy was reported. In another study, bio-oil was used to synthesize a new adhesive system to be used in the particle board industry and it was found that OH groups of the liquefying solvent contributed to the condensation reactions with melamine-formaldehyde and melamine-urea-formaldehyde resin precursors and this ultimately affected the properties of the resulting resin system (Kunaver et al., 2010). Zou et al. (2012) synthesized a polyurethane foam using bio-oil, and they reported a high number of primary OH groups from the bio-oil was necessary to increase the mechanical and thermal properties of PU.

It could be hypothesized that the reaction behavior and the mechanical and thermal properties of resulting bio-based polymer depend on the reactivity, accessibility and source of hydroxyl groups within the bio-oil. Characterization of bio-oil hydroxyl groups plays an

important role in the improvement of bio-oil for the utilization as a polyol. Therefore, a comprehensive hydroxyl group analysis is necessary to understand the source and variation of bio-oil hydroxyl groups which will make it possible to engineer the properties of bio-based polymers synthesized by bio-oil in future studies. However, literature for the organic solvent liquefaction of biomass lacks specific information regarding the source and variation of OH groups. Thus, the objectives of this study were to (i) investigate the effect of liquefaction temperature on hydroxyl groups, and (ii) analyze the variation and source of hydroxyl groups in bio-oil.

4.2. Materials and Methods

4.2.1. Materials

Clean loblolly pine (*Pinus taeda*) was obtained from West Fraser Sawmill, Opelika, AL USA. All chemicals were purchased from VWR; except phosphorylating agent, 2–chloro–4,4,5,5–tetramethyl–1,3,2–dioxaphospholane (TMDP), which was purchased from Sigma Aldrich. All chemicals were reagent grade and used as received.

4.2.2. Biomass Liquefaction

Twenty mesh sieve size was used for particle size reduction. Loblolly pine (LP) passed through 20 mesh was dried at 105 °C overnight before use. Liquefaction was carried out in a Parr® reactor (Model 4567 Mini bench top reactor, and 4843 temperature controller, Parr Instrument, Moline, IL) equipped with a stirrer using ethylene glycol (LP/EG = 1/4, w/w) along with sulfuric acid (EG/H$_2$SO$_4$ = 100/3, w/w) for 1 hour at 100, 150, 200 and 250 °C. Liquefaction start time was considered to occur when the preset temperature was reached. After

1 hour, the reaction vessel was immersed in ice water to quench the reaction, and let it cool down quickly to room temperature. After cooling, liquefied wood was diluted with 500 mL acetone, and then vacuum filtered through a Whatman No. 2 filter paper. The solid residue was dried at 105 °C overnight before weighing. Residue content (RC) was calculated as given in Eqn. 1:

$$RC\ (\%) = \frac{weight\ of\ dried\ solid\ residue\ (g)}{weight\ of\ starting\ LP\ (g)} \times 100 \qquad (1)$$

After vacuum filtering, the excess acetone in the liquid part was removed using a rotary evaporator. In order to completely remove the acetone, samples were kept in a vacuum oven (Thermo electron, VT 6060 M, Germany) at 40 °C for 12 hours under 100 m bar vacuum pressure, and then the resulting liquid was labeled as bio-oil.

4.2.3. GC/MS

The amount of unreacted EG in the bio-oil was determined by GC-MS. Before GC-MS analysis, all bio-oils were silylated with N,O-bis(trimethylsilyl)trifluoroacetamide (BSTFA) in order to increase the volatility of OH groups according to silylation method reported by Rojas-Escudero et al. (2004). In this method, BSTFA reacts with the OH groups of the bio-oil, and silylated bio-oil is produced. Approximately 17.5 ± 2.5 mg bio-oil was silylated with BSTFA, and then diluted with methanol (silylated bio-oil/methanol = 1/20, v/v) before injecting into the GC column (ZB-5MS, 30mx0.25mmx0.25µm, Phenomemex). Each sample was silylated and analyzed in three independent experiments, and the amount of unreacted EG was reported as an average of three samples. An external standard method where seven data points were generated to form calibration curve was used for calculations.

The GC-MS analysis utilized a Waters 6890N GC with a ZB-5MS column coupled to a Time of Flight Mass Analyzer (GCT Premier, Waters). Mass was scanned from 50 to 500 m/z starting at 4.5 min to 60 min in DRE mode with 0.9 sec scan time with 0.1 sec inter-scan delay, Centroid data was acquired. The temperature program used 35 °C for 4 min, ramp up at 3 °C/min to 140 °C and 10 °C/min to 280 °C and hold at 280 °C for 7 min, in a total 60 min run. Component identification was done by comparing the electron impact fragmentation pattern (70eV) with those in the compound library (NIST 2003). Compounds with Match and Reverse Match scores above 700 and probabilities above 90% were selected as matches. The identification was confirmed by elemental composition analysis using accurate mass measurement with an internal calibrant (lockmass 218.9856 m/z, heptacosafluorotributylamine, Sigma) with an acceptable error of less than 5 ppm and by isotope modeling comparing the experimental and theoretical isotope distribution. The component identifications from the GC-MS were also confirmed by retention time of standard compounds by the same method.

4.2.4. Hydroxyl Group Analysis

The total OHN of bio-oil was determined using esterification technique (titration) as described by Carey et al. (1984) and defined as *mg KOH/g sample*. The type of OH groups (aliphatic, phenolic and acidic) were determined and quantitatively calculated using ^{31}P NMR. Prior to ^{31}P NMR analysis, bio-oils were phosphitylated with 150 mL of TMDP and then spectra were acquired with a Bruker Avance II 250 MHz according to the method reported by David et al. (2010).

4.2.5. ATR-FT-IR

Attenuated total reflection Fourier Transform Infrared (ATR-FT-IR) spectra of the bio-oils were acquired between 4000 and 650 cm^{-1} with an ATR-FT-IR spectrometer (Model Spectrum400, Perkin Elmer Co., Waltham, MA) to determine the functional groups present in the bio-oil. All ATR-FT-IR spectra were collected at room temperature (22 ± 1 °C).

4.3. Results and Discussion

4.3.1. GC-MS Analysis of Bio-oils and Residue Content Analysis

Fig. 4.1 shows the GC-MS chromatograms of all the silylated bio-oils. The peak at 13.63 − 13.73 min. was observed for each bio-oil, indicating the existence of EG (molecule I). Formation of diethylene glycol (DEG, molecule II) at 150, 200 and 250 °C, and triethylene glycol (TEG, molecule III) at 200 and 250 °C was also found. These results support a condensation reaction between EG molecules in the presence of sulfuric acid as the liquefaction temperature increased. Ether formation as a result of the condensation reaction of alcohols in the presence of acid catalyst is well-established, and this may explain the formation of DEG and TEG in this study. In summary, the oxygen atom of the EG is protonated by sulfuric acid. The protonated EG is then attacked by another EG molecule and undergoes S_N2 displacement (Wade, 2003). Bigger molecules (DEG and TEG) are produced as more EG is attached to protonated EG.

At lower temperatures (100 and 150 °C), some sugar derivatives (molecules IV and V in Fig. 1) were observed at 46 and 47 min. Via et al. (2013) reported that hemicellulose was very sensitive to temperature, and was the first depolymerized wood component. Therefore, sugar

derivatives at lower temperature may be attributable to hemicellulose degradation. However, these molecules disappeared as the temperature increased. A recombination of degraded fragments has been previously reported by other researchers (Zhang et al., 2006; Zou et al., 2009). It is conjectured that sugar derivatives reacted with each other and/or EG at a higher temperature because of the highly reactive functional groups i.e. hydroxyl and carbonyl groups; therefore, no sugar derivatives were observed at 200 and 250 °C in the GC-MS chromatogram.
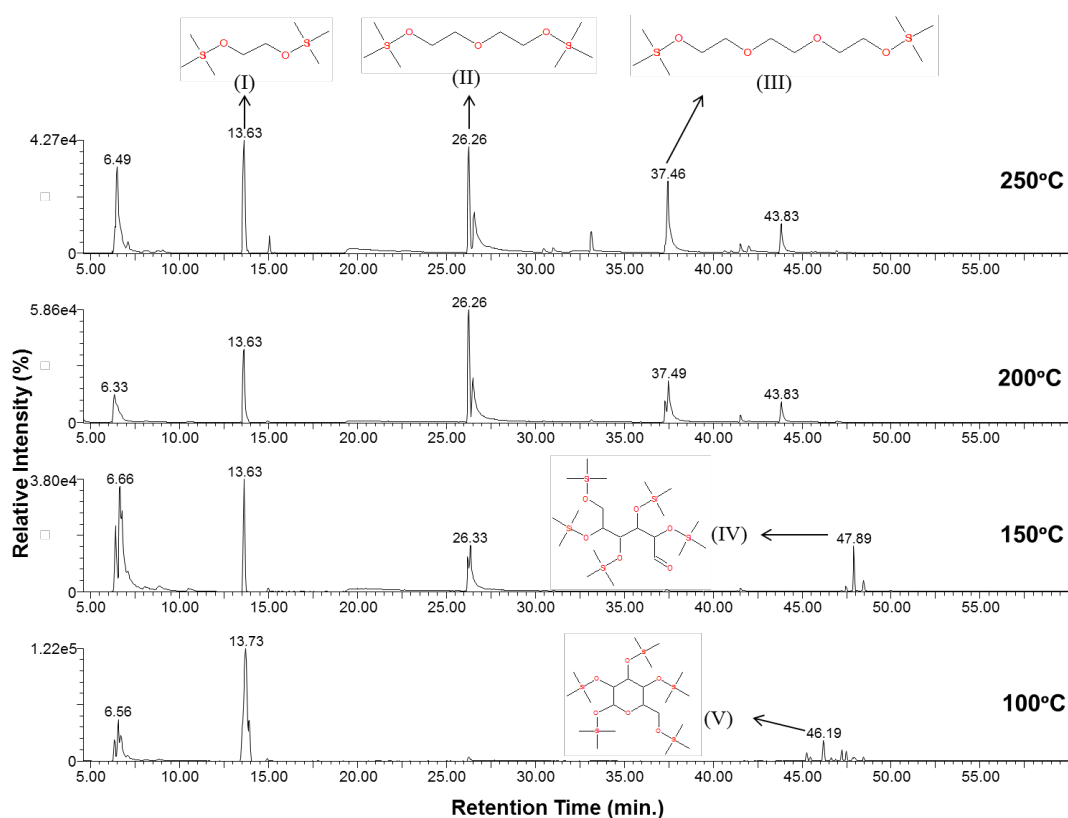
Fig. 4.1. GC-MS results of silylated bio-oils using selected ion chromatogram displaying 73.05 (m/z), the base peak from the fragmentation of 1,2-Bis(trimethylsiloxy) ethane from total ion chromatogram (TIC) in EI+ mode. Molecule I, molecule II and III are ethylene glycol, diethylene glycol and triethylene glycol, respectively. Molecule IV and V are the sugar derivatives obtained at 150 and 100 °C, respectively.

Fig. 4.2 shows the percentage of unreacted EG (EG/bio-oil, w/w) retained in the bio-oil and the residue content (RC) after liquefaction. As can be seen in Fig. 4.2, unreacted EG was calculated as 75, 48, 28 and 24 % of the bio-oil weight produced at 100, 150, 200 and 250 °C, respectively. Similar results were also reported by Budija et al. (2009). In that study, sawdust was liquefied with DEG at 150 °C for 95 min, and unreacted DEG was isolated by a distillation method under a vacuum. They reported that unreacted DEG represented 62% of the bio-oil. Fig. 2 demonstrates an almost linear decrease ($R^2 = 0.92$) in the amount of unreacted EG with an increase in liquefaction temperature. This trend may be explained by the (i) formation of DEG and TEG which clearly indicates the consumption of EG, as explained above, and (ii) decomposition of biomass by EG (alcoholysis reaction).
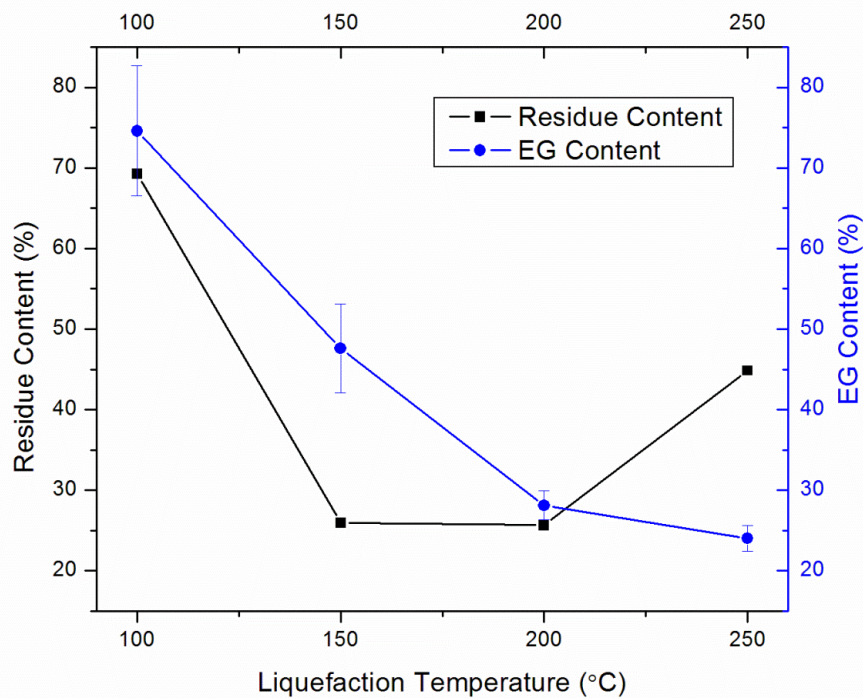
Fig. 4.2. Percentage of unreacted EG (EG/bio-oil, w/w) retained in the bio-oil and the residue content (RC) after liquefaction.

The highest RC (70 wt.%) and EG content (75 wt.%) was obtained at 100 °C liquefaction

as illustrated in Fig. 4.2. A high EG content suggests that the majority of EG was not consumed,

and 70% of RC clearly indicates that biomass did not undergo complete decomposition reaction

with EG. Poor liquefaction at 100 °C may be explained by Zou et al. (2009) who studied the

biomass liquefaction with EG. They found that there are three stages during biomass

liquefaction: (i) biomass dehydration, (ii) solvent volatilization and (iii) biomass alcoholysis, and

volatilization temperature of EG was reported to be 156 °C. Liquefaction temperature should be

higher than the volatilization temperature of the solvent for a successful biomass alcoholysis.

Therefore, a high EG content and RC at 100 °C in our study may be attributable to the low

liquefaction temperature at which EG did not reach a good level of permeability and fluidity.

Moreover, there was no DEG or TEG formation at 100 °C, yet some five-carbon sugar

derivatives were detected by GC – MS. This result suggests that consumption of EG at 100 °C

was due to some degree of hemicellulose degradation. The extracted 30% from biomass could be

attributable to hemicellulose, organic impurities and extractives.

A dramatic decrease from 70% to 25% in RC was observed as the temperature reached to

150 °C. A similar trend was reported by D'Souza et al. (2013). In that study, 77.5 % and 20.4 %

RC was reported at 90 °C and 160 °C, respectively. Formation of diethylene glycol and sugar

derivatives at 150 °C indicates that both of the reactions, condensation reaction between EG

molecules and alcoholysis between EG and biomass, took place.

EG content decreased from 48 to 28 % at 200 °C; however, only a 1 % decrease in RC

was observed. The mechanism of liquefaction has been previously explained by others (Xiao et

al., 2013; Zhang et al., 2006; Zou et al., 2009). During liquefaction, there are two main reactions that take place; (i) decomposition of biomass (alcoholysis), and (ii) condensation of degraded biomass. Biomass (cellulose, hemicellulose and lignin) is degraded to its monomers by H_2SO_4 and EG, then a recombination of degraded fragments takes place. In the presence of excess EG, these fragments could create high molecular weight components via condensation reaction with EG. Therefore, no change in RC while decrease in EG content may be attributable to the rate of alcoholysis reactions between biomass and EG is being close to the rate of condensation reactions between degraded fragments. On the other hand, the formation of DEG at 200 °C may also be another reason for decrease in EG content.

The RC increased from 26 to 45 % as the temperature reached to 250 °C while EG content decreased from 28 to 24 %. The increase in RC is most likely due to the condensation reaction between degraded fragments of biomass with EG. It could also be conjectured that increasing the liquefaction temperature further than 250 °C could increase the possibility of condensation reaction between degraded fragments (Rackemann et al., 2012). Therefore, liquefaction at 300 °C and further temperatures were not performed in this study. Additionally, polymerization of EG into DEG and TEG also played a role in the overall decrease in EG.

Since the amount of EG retained in the bio-oil was known, OHN arisen from the EG was also calculated in order to determine the contribution of EG to the total OHN of bio-oil. As can be seen in Table 4.1, it was found that the unreacted EG retained after liquefaction accounted for 70 - 95 % of the total OHN of bio-oil depending on liquefaction temperature. This agreed with Kunaver et al. (2010) who pursued the wood liquefaction with glycerol/DEG mixture at 180 °C.

In that study, OH group contribution from liquefying solvent was calculated to be around 70% at 180 °C for 60 min. liquefaction. In another study, it was reported that unreacted DEG left in the bio-oil (liquefaction of sawdust with DEG at 150 °C for 95 min) was accounted for 40 % of the total OHN (Budija et al., 2009). This is considerably lower than our finding because they isolated the unreacted DEG by a distillation method and then calculated the OHN of distilled DEG. Therefore, the DEG which was not successfully distillated from bio-oil might be the reason for their lower contribution.

Table 4.1. OHN numbers (mg KOH/g) of bio-oils produced at different liquefaction temperatures calculated by quantitative ^{31}P-NMR after derivatization with TMDP, and phthalic anhydride esterification method (titration). OHN from EG was calculated by GC-MS analysis. OHN contribution of EG is the ratio of OHN from EG to total OHN.

| Sample | ^{31}P-NMR | | | | Titration | OH from EG | OHN Contribution of EG (%) |
	Aliphatic OH[a]	Phenolic OH[b]	Acidic OH[c]	Total OH[d]	Total OH		
100 °C	1479	-	-	1479	1430	1348	94
150 °C	1083	-	2	1085	1100	860	78
200 °C	737	-	6	743	725	508	70
250 °C	640	-	26	666	632	434	69

[a] Integration region=150 – 145.5 ppm, [b] Integration region=144.7 – 137.3 ppm, [c] Integration region=136.6 – 133.6 ppm, [d] Calculated by sum of aliphatic, phenolic and acidic OH.

It was found that EG provided two important functions during biomass liquefaction, (i) EG acted as a solvent for biomass decomposition and (ii) EG was a major source for the hydroxyl groups (Wei et al., 2014). The high OHN number, therefore, may be attributable to the high volume of EG used. Future work around reducing the EG while staying above the threshold for complete solvent capacity would be useful. Our GC-MS findings suggest that the overall OHN of bio-oil can be controlled by EG volume coupled with temperature; however, biomass/solvent ratio should be taken into account since it is an important consideration for the economic viability of the process. Biomass liquefaction with EG at different ratios has been

previously studied, and 1/3 – 1/5 (biomass/solvent, w/w) was reported as the optimum ratio (Guo et al., 2014; Yip at al., 2009).

It could be concluded that 100 and 250 °C are not optimum liquefaction temperatures because of high amount of residue content. Bio-oil produced at 150 and 200 °C had 47 and 28 % EG content, respectively, as well as 25 % of residue content. This finding suggests that bio-oils produced at 150 and 200 °C could be used as a polyol for polymer production. Since EG has a plasticizer effect in polymer synthesis (Wei et al., 2014), bio-oils could be used as a polyol to synthesize rigid or soft polymer by adjusting the OH number.

4.3.2. Hydroxyl Group Analysis

The total OHN determined by titration method ranged from 632 to 1430 mg KOH/g sample as shown in Table 4.1, with a decrease in OHN as liquefaction temperature increased. ANOVA analysis with 95% confidence interval was performed, and found that liquefaction temperature had significant effect on OHN (p-value<0.0001). Majority of hydroxyl groups was found to be aliphatic from ^{31}P-NMR analysis (Fig. 4.3). As discussed in GC-MS analysis, it was found that EG was the major source for hydroxyl groups in bio-oil. Therefore, having the majority of peaks in the aliphatic OH region was expected because of the excess solvent at even higher temperatures. Since loblolly pine from the southeastern U.S. ranges between 24 to 30 % by weight lignin (Jiang et al., 2014), some phenolic hydroxyl was also expected; however, no peak was observed in the phenolic OH region. An explanation for this was found in D'Souza and Yan (2013) and Zou et al. (2009). They suggest that lignin fragments may undergo a condensation reaction with EG during liquefaction which results in a decrease in overall phenolic

OH content. Therefore, a lack of phenolic OH groups in the ^{31}P-NMR spectra was most likely

due to the condensation reaction (Fig. 4.4) of phenolics in the presence of EG and sulfuric acid.
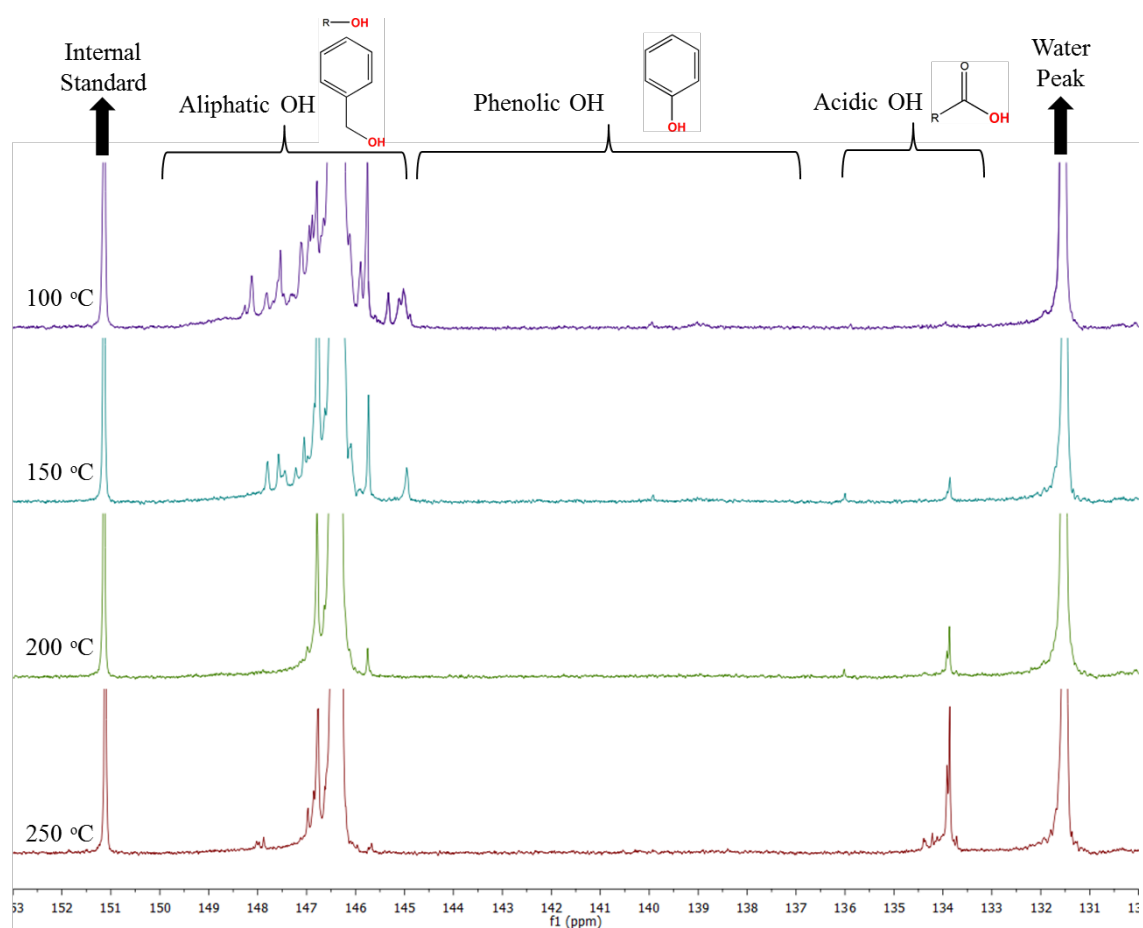
Fig. 4.3. ^{31}P-NMR spectra for the bio-oils phosphitylated with TMDP (150 – 145 ppm is aliphatic region, 145 – 135 ppm is phenolic region, and 135 – 133 ppm is acidic region).

Highest amount of acidic OH (26 mg KOH/g) was observed at 250 °C liquefaction (Table

1). Formation of acidic OH groups may be attributable to alcoholysis reaction of wood by EG.

Yamada and Ono (2001) studied the cellulose degradation by EG, and confirmed the formation

of levulinic acid from glucose at high temperature. Therefore, formation of acidic OH groups is

conjectured to alcoholysis reaction of wood and by EG.
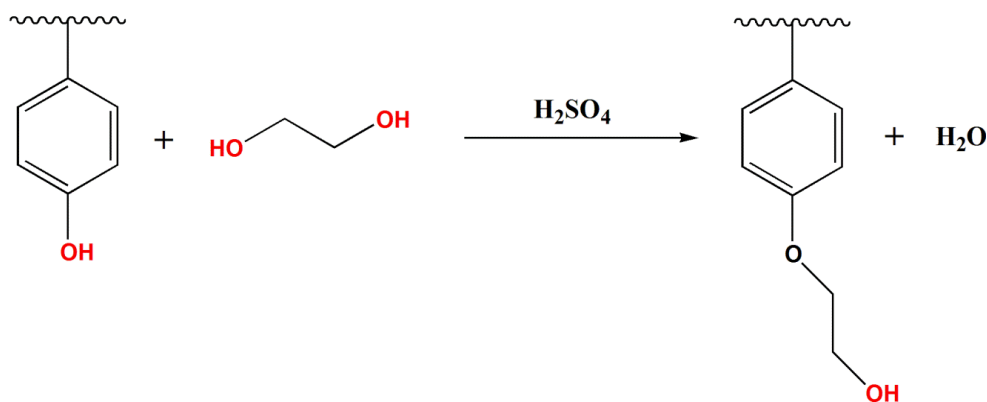
Fig. 4.4. Proposed mechanism of condensation reaction between lignin fragments and EG in the presence of sulfuric acid during the liquefaction.

4.3.3. ATR-FT-IR

Four peaks (3337, 1724, 1123 and 1082 cm^{-1}) were identified from IR spectra (Fig. 4.5a). An inverse correlation between the intensity of peaks at 1724 cm^{-1} and 3337 cm^{-1} that was observed (Fig. 4.5b) which are due to the carbonyl (C=O stretching) and OH groups, respectively. As discussed in ^{31}P-NMR analysis, oxidation of EG and alcoholysis of wood are the main reasons for the generation of carbonyl groups containing compounds such as aldehydes, ketones, and carboxylic acids. Compounds containing carbonyl groups are formed by reaction of sugar fragments (degradation products of cellulose or hemicellulose) with hydroxyl groups of the EG (Xiao et al., 2011). Formation of carbonyls, therefore, is related to the consumption of EG. This phenomenon explains the inverse correlation between the intensity of peaks at 1724 cm^{-1} and 3337 cm^{-1}. For example, 250 °C exhibited the lowest peak intensity at 3337 cm^{-1} and the highest peak intensity at 1724 cm^{-1}. Since more OH groups underwent oxidation reactions, a lower intensity was observed at the peak at 3337 cm^{-1}. Conversely, more OH consumption yielded more carbonyls, resulting in higher peak intensity at 1724 cm^{-1} for 250 °C liquefaction. Peak intensity of bio-oils at 1724 cm^{-1} showed following order: 100 °C < 150 °C < 200 °C < 250 °C. Polymerization of EG to diethylene glycol (DEG) and triethylene glycol (TEG) was also

76

confirmed by ATR-FT-IR. The characteristic ether peak of DEG and TEG at 1123 cm^{-1} due to

C–O–C asymmetry stretching was observed at 150, 200 and 250 °C (Fig. 4.5c). Moreover, the

peak at 1082 cm^{-1} is mainly due to the C – O stretching in EG which disappeared as the

temperature increased to 200 and 250 °C. This clearly shows the polymerization of EG to DEG

and TEG at higher temperatures.
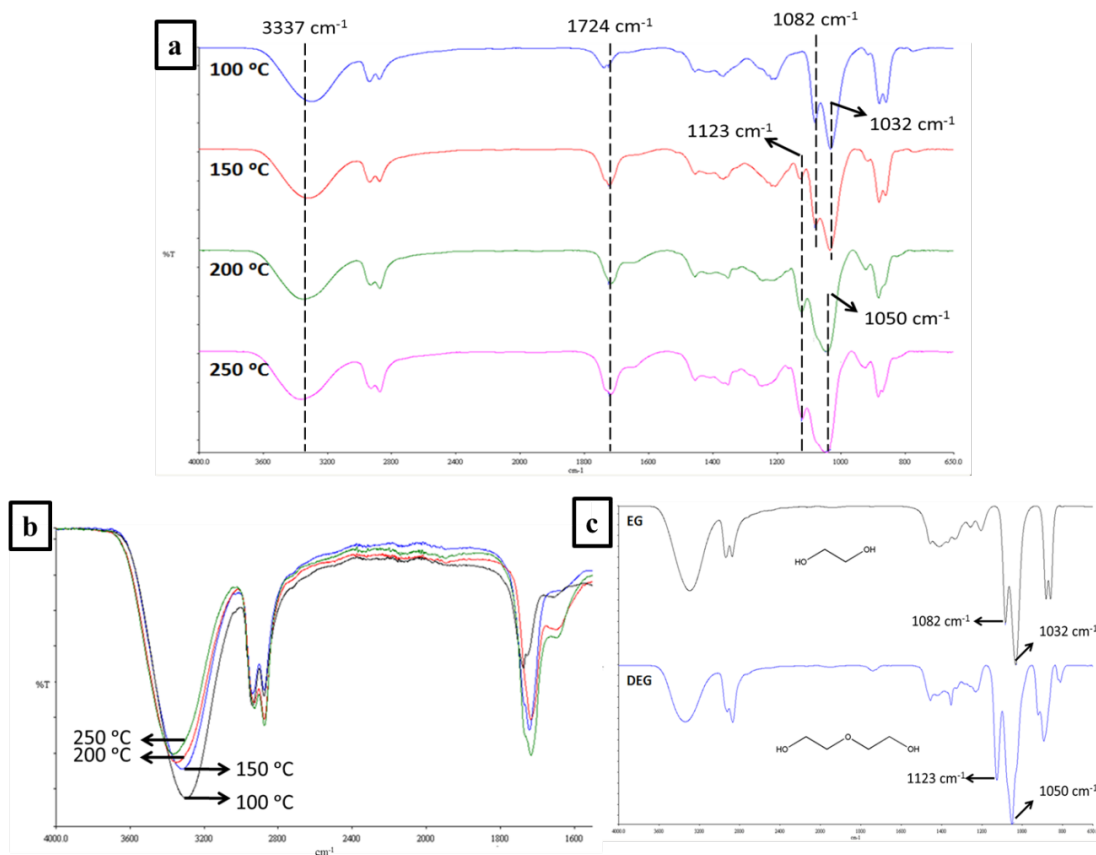
Fig. 4.5. (a) FT-IR spectra of all bio-oils, **(b)** FT-IR spectra of all bio-oils displaying the peaks at 1724 cm^{-1} and 3337 cm^{-1}, **(c)** FT-IR spectra of ethylene glycol (EG) and diethylene glycol (DEG).

4.3.4. Stability of Hydroxyl Groups

Bio-oil aging is one problem that occurs during storage. Reactions between aldehydes

and hydroxyl components in the bio-oil have been reported one reason for bio-oil aging resulting

in the polymerization and consequent viscosity (Czernik et al. 1994). A change in the OHN is

therefore expected during storage resulting in a dynamic feedstock and increased variance during polymer or bioenergy processes. However, in this study, we found that all bio-oil could be stabilized when stored at -10 °C as can be seen in Fig. 4.6. OHN stability may be attributable to (i) lower storage temperature which reduces the aging rate, and (ii) stabilizing effect of EG present in the bio-oil. Alcohol addition to pyrolysis oil was one of the methods to slow the aging effect. Low molecular weight alcohols such as methanol and ethanol reduce the reactivity of aldehydes and prevent the formation of oligomers and polymers during storage (Diebold, 2002). As discussed in the GC-MS results, it was found that EG accounted for 75 % of the bio-oil composition. Therefore, the OHN stability observed in this study may be attributable to the excess amount of EG in the bio-oil which acts as stabilizing alcohol.
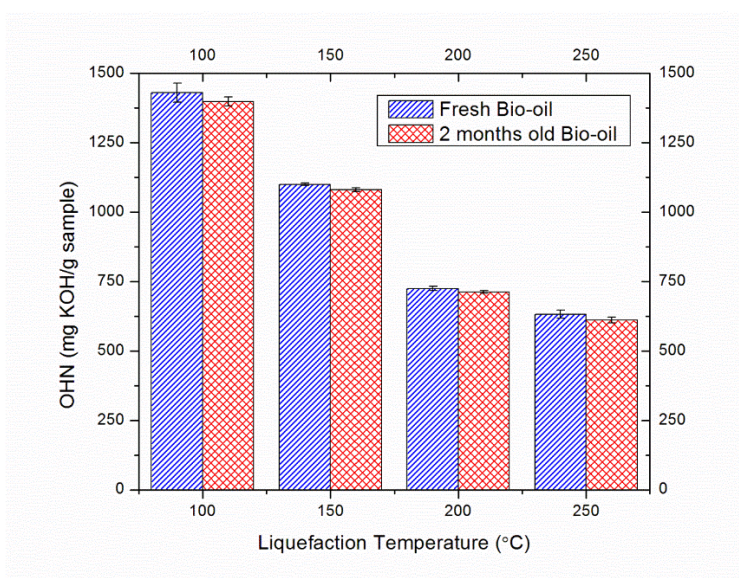
Fig. 4.6. OHN of fresh and 2 months old bio-oil calculated by phthalic anhydride esterification (titration) method.

4.4. Conclusion

The effect of liquefaction temperature on OHN was studied. It was found that unreacted EG was the major source for OH groups, and accounted for 70 – 95 % of the OHN depending on

78

liquefaction temperature. Aliphatic OHs accounted for the majority of hydroxyl groups as evidenced by ^{31}P-NMR analysis. GC-MS and ATR-FT-IR analysis proved the formation of DEG and TEG as a result of condensation polymerization of EG. It was also found that OHN number was stable over 2 months when stored in a freezer. Analysis showed that high OHN could enable researchers to use bio-oil as a polyol.

Acknowledgements

References

1. Budija, F., Tavzes, C., Zupancic-Kralj, L., Petric, M. 2009. Self-crosslinking and film formation ability of liquefied black poplar. *Bioresource Technol.* 100(13): 3316-3323.

2. Carey, M. A., Wellons, S. L., Elder, D. K. 1984. Rapid Method for Measuring the Hydroxyl Content of Polyurethane Polyols. *J Cell Plast.* 20(1), 42-48.

3. Czernik, S., Johnson, D. K., Black, S. 1994. Stability of Wood Fast Pyrolysis Oil. *Biomass Bioenerg.* 7(1-6): 187-192.

4. David, K., Kosa, M., Williams, A., Mayor, R., Realff, M., Muzzy, J., Ragauskas, A. 2010. 31P-NMR analysis of bio-oils obtained from the pyrolysis of biomass. Biofuels, 1(6): 839 – 845.

5. Diebold, J. P. 2002. A review of the chemical and physical mechanisms of the storage stability of fast pyrolysis bio-oils, in: Bridgwater, A. V., (Ed.), Fast Pyrolysis of Biomass: A Handbook, Vol. 2, CPL Press: Newbury, U.K.

6. D'Souza, J., Yan, N. 2013. Producing Bark-based Polyols through Liquefaction: Effect of Liquefaction Temperature. *Acs Sustain Chem Eng.* 1(5): 534-540.

7. Durak, H., Aysu, T. 2014. Effects of catalysts and solvents on liquefaction of Onopordum heteracanthum for production of bio-oils. *Bioresource Technol.* doi: http://dx.doi.org/10.1016/j.biortech.2014.05.051

8. Guo, Z.-h.; Liu, Y.-n.; Wang, F.-y.; Xiao, X.-y. 2014. Liquefaction of metal-contaminated giant reed biomass in acidified ethylene glycol system: Batch experiments. *J. Cent. South Univ.*, 21(5), 1756-1762.

9. Hu, S., Li, Y. 2014. Two-step sequential liquefaction of lignocellulosic biomass by crude glycerol for the production of polyols and polyurethane foams. *Bioresource Technol.* 161: 410-415.

10. Jiang, W., Han, G. T., Via, B. K., Tu, M. B., Liu, W., Fasina, O. 2014. Rapid assessment of coniferous biomass lignin-carbohydrates with near-infrared spectroscopy. *Wood Sci Technol.* 48(1): 109-122.

11. Kunaver, M., Medved, S., Cuk, N., Jasiukaityte, E., Poljansek, I., Strnad, T. 2010. Application of liquefied wood as a new particle board adhesive system. *Bioresource Technol.* 101(4): 1361-1368.

12. Perlack, R.D., Wright, L.L., Turhollow, A.F., Graham, R.L., Stokes, B.J., Erbach, D.C. 2005. Biomass as a Feedstock for a Bioenergy and Bioproducts Industry: The Technical Feasibility of a Billion-ton Annual Supply. USDA/DOE, DOE/GO-102005-2135, ORNL/TM-2005/66.

13. Rackemann, D.W., Moghaddam, L., Rainey, T.J., Fellows, C.F., Hobson, P.A., Doherty, W.O.S. 2012. Hydrothermal Technologies for the Production of Fuels and Chemicals from Biomass, in: Sanghi, R., Singh, V. (Eds.), Green Chemistry for Environmental Remediation. Scrivener Publishing LLC., Salem, Massachusetts, pp. 291 – 342.

14. Rojas-Escudero, E., Alarcón-Jiménez, A. L., Elizalde-Galván, P., Rojo-Callejas, F. 2004. Optimization of carbohydrate silylation for gas chromatography. *Journal of Chromatography A*. 1027(1–2): 117-120.

15. Via, B. K., Adhikari, S., Taylor, S. 2013. Modeling for proximate analysis and heating value of torrefied biomass with vibration spectroscopy. *Bioresource Technol.,* 133: 1-8.

16. Wade, L. G. 2003. Organic Chemistry, 5th ed., Pearson Education: Upper Saddle River, NJ. U.S.A.

17. Wei, N., Via, B. K., Wang, Y., McDonald, T., Auad, M. L. 2014. Liquefaction and substitution of switchgrass (Panicum virgatum) based bio-oil into epoxy resins. *Ind Crop Prod,* 57(0): 116-123.

18. Xiao, W. H., Han, L. J., Zhao, Y. Y. 2011. Comparative study of conventional and microwave-assisted liquefaction of corn stover in ethylene glycol. *Ind Crop Prod.* 34(3): 1602-1606.

19. Xiao, W. H., Niu, W. J., Yi, F., Liu, X., Han, L. J. 2013. Influence of Crop Residue Types on Microwave-Assisted Liquefaction Performance and Products. *Energ Fuel.* 27(6): 3204-3208.

20. Yamada, T., Ono, H. 2001. Characterization of the products resulting from ethylene glycol liquefaction of cellulose. *J Wood Sci.* 47(6): 458-464.

21. Yip, J., Chen, M. J., Szeto, Y. S., Yan, S. C. 2009. Comparative study of liquefaction process and liquefied products from bamboo using different organic solvents. *Bioresource Technol.* 100(24), 6674-6678.

22. Zhang, Y. C., Ikeda, A., Hori, N., Takemura, A., Ono, H., Yamada, T. 2006. Characterization of liquefied product from cellulose with phenol in the presence of sulfuric acid. *Bioresource Technol.* 97(2): 313-321.

23. Zou, X. W., Qin, T. F., Huang, L. H., Zhang, X. L., Yang, Z., Wang, Y. 2009. Mechanisms and Main Regularities of Biomass Liquefaction with Alcoholic Solvents. *Energ Fuel.* 23: 5213-5218.

24. Zou, X. W., Qin, T. F., Wang, Y., Huang, L. H., Han, Y. M., Li, Y. 2012. Synthesis and properties of polyurethane foams prepared from heavy oil modified by polyols with 4,4 '-methylene-diphenylene isocyanate (MDI). *Bioresource Technol.* 114: 654-657.

Chapter 5

The Effect of Ethanol on Hydroxyl and Carbonyl Groups in Biopolyol Produced by Hydrothermal Liquefaction of Loblolly Pine: ^{31}P-NMR and ^{19}F-NMR Analysis*

Abstract

The goal of this study was to investigate the role of ethanol and temperature on the hydroxyl and carbonyl groups in biopolyol produced from hydrothermal liquefaction of loblolly pine (*Pinus spp*) carried out at 250, 300, 350 and 390 °C for 30 min. Water and water/ethanol mixture (1/1, wt/wt) were used as liquefying solvent in the HTL experiments. HTL in water and water/ethanol is donated as W-HTL and W/E-HTL, respectively. It was found that 300 °C and water/ethanol solvent was the optimum liquefaction temperature and solvent, yielding up to 68.1 wt.% bio-oil and 2.4 wt.% solid residue. ^{31}P-NMR analysis showed that biopolyol produced by W-HTL was rich in phenolic OH while W/E- HTL produced more aliphatic OH rich biopolyols. Moreover, biopolyols with higher hydroxyl concentration were produced by W/E-HTL. Carbonyl groups were analyzed by ^{19}F-NMR, which showed that ethanol reduced the concentration of carbonyl groups.

5.1. Introduction

Lignocellulosic biomass is being used as an alternative feedstock for the production of bio-based polyols (biopolyols) in order to reduce our dependency on petroleum. Polyol is a compound that has multiple hydroxyl groups in its structure and is essential for the synthesis of a variety of polymers such as epoxy, polyurethane, polyester, polycarbonate, and phenolic resin. However, today the major source for polyols is petroleum. Researchers have thus focused on biopolyol in the face of depleting petroleum reserves, increased greenhouse effect, as well as an increasing demand by the consumers for bio-based products. Moreover, the U.S. Department of Energy (DOE) and the U.S. Department of Agriculture (USDA) have prioritized the development of bioenergy and bioproducts with the goal to produce 18% of the current U.S. chemical commodities from lignocellulosic biomass by 2020, and 25% by 2030 (Perlack et al. 2005).

Bio-oil, the black liquid produced by degradation of lignocellulosic biomass through thermomechanical processes, has attracted interest to be used as a biopolyol because of its high hydroxyl concentration. Gas chromatography–mass spectrometry (GC-MS) analysis of bio-oil showed that bio-oil is a highly complex mixture, mainly composed of carbohydrates, furans, phenols, guaiacols, syringols type of compounds (Thangalazhy-Gopakumar et al. 2010). Hydrothermal liquefaction (HTL), also known as direct liquefaction, is a thermomechanical conversion technique to produce bio-oil where lignocellulosic biomass is converted into liquid (bio-oil), gas and solid products using subcritical or supercritical water at elevated temperature (250 – 370 °C) and pressure (2 – 24 MPa). Bio-oil produced by the HTL process has a significant potential for commercialization in terms of price and life cycle assessment (Elliott et al. 2015).

83

The effect of process parameters such as temperature, pressure, reaction time and feedstock type on the bio-oil yield in HTL process has been intensively studied and valuable literature reviews can be found elsewhere (Akhtar and Amin 2011, Toor et al. 2011). Approximately 30 – 40 wt.% bio-oil (based on dry mass of biomass) is obtained from the hydrothermal liquefaction of lignocellulosic biomass (Akhtar and Amin 2011). Recently, ethanol has received attention to be used as a co-solvent in the HTL process due to its high hydrogen solvent capability. Yuan et al. (2007) proposed that the highly reactive free radicals generated from the HTL of biomass were stabilized by the ethanol which acts as a hydrogen-donor solvent, and Cheng et al. (2010) reported that bio-oil yield could be increased from 40 to 65 wt.% when ethanol was used along with water in a sub-critical condition. In another study, alkaline lignin was liquefied in hot compressed water/ethanol medium, and found that addition of ethanol increased the degradation of lignin which resulted in a lower amount of solid residue (Yuan et al. 2010). This improvement may be due to the low dielectric constant of ethanol which facilitates dissolving of high molecular weight lignin at supercritical temperatures (Krammer and Vogel 2000). The synergistic effect of water/ethanol mixture in the liquefaction of rice husk for bio-oil production via the HTL process was also observed by Liu et al. (2013). Besides the high bio-oil yield, the addition of ethanol to water also affects the distribution of phenolics such as phenol, ethylphenol and guaiacols, ethylguaiacol and syringol in the bio-oil as well (Ye et al. 2012, Ouyang et al. 2015). Recently, Kosinkova et al. (2015) reported that aqueous ethanol improved the higher heating value (HHV) of bio-oil to be used in the field of biodiesel applications. Moreover, the addition of medical stone as a catalyst into aqueous ethanol could further increase the yield of bio-oil produced by HTL of cotton seed (Yan et al. 2015).

Compounds containing hydroxyl and carbonyl groups in bio-oil play a major role in its utilization as a biopolyol. There are a variety of polymers synthesized using bio-oil including phenolic resin (Choi et al. 2015), polyurethane (Hu and Li 2014), epoxy (Kuo et al. 2014) and polyester (Yu et al. 2006), and the hydroxyl groups in bio-oil are utilized to synthesize these polymers. Wei et al. (2014) used bio-oil to modify an epoxy resin, and found that hydroxyl number (OHN) of the bio-oil had a significant effect on the glass transition temperature (Tg) of the modified epoxy resin. In another study, bio-oil was used to synthesize a new adhesive system for application in particle boards. Here, the hydroxyl groups in bio-oil contributed to the condensation reactions with melamine-formaldehyde and melamine-urea-formaldehyde resin precursors which ultimately affected the properties of the resulting resin system (Kunaver et al. 2010). Zou et al. (2012) synthesized a polyurethane foam using bio-oil, and reported that a high number of primary hydroxyl groups from the bio-oil was necessary to increase the mechanical and thermal properties of polyurethane foam. Thus, it could be hypothesized that the reaction behavior and the mechanical/thermal properties of the resulting polymer depend on the interaction between hydroxyl groups in bio-oil and the formaldehyde for phenol formaldehyde resin, isocyanate for the polyurethane, epoxide groups for epoxy resin, and ester groups for polyester production.

Compounds containing carbonyl groups in the bio-oil such as aldehydes, ketones and quinones are found to play a major role in the aging of bio-oil during storage (Czernik et al. 1994). Reactions between compounds containing carbonyl and hydroxyl groups in the bio-oil have been reported to be a reason for bio-oil aging which results in the polymerization and consequently a change in viscosity (Czernik et al. 1994). The production of carboxylic acid as a

result of oxidation of carbonyl groups is another problem which may cause equipment corrosion. Most recently, our group has studied the curing reaction of a commercial epoxy resin (EPON828) with a bio-oil, and found that carbonyl groups in the bio-oil contributed the curing of epoxy resin along with the hydroxyl groups as well (Celikbag et al. 2015). Therefore, the characterization and quantification of hydroxyl and carbonyl groups in the bio-oil is crucial to determine its quality as well as optimization for bio-oil based polymer synthesis.

The literature on liquefaction of lignocellulosic biomass in water/ethanol mixture via HTL process lacks specific information regarding the source and variation of hydroxyl and carbonyl groups in the bio-oil. Characterization of these functional groups plays an important role in the improvement of bio-oil for its effective utilization as a biopolyol. Therefore, a comprehensive hydroxyl and carbonyl group analysis is necessary to understand the source and variation of bio-oil hydroxyl and carbonyl group content which will make it possible to engineer the properties of bio-based polymers and their synthesis in future studies. To the best of our knowledge, this is the first study that has used the ^{31}P-NMR and ^{19}F-NMR analytical tools to partition out the hydroxyl and carbonyl groups to understand the role of ethanol in the HTL process of lignocellulosic biomass. Thus, the objectives of this study were to (i) investigate the effect of ethanol and liquefaction temperature and on hydroxyl and carbonyl groups, and (ii) analyze the variation and source of these functional groups in the bio-oil using ^{31}P-NMR and ^{19}F-NMR.

5.2. Materials and Methods

5.2.1. Materials

Loblolly pine wood chips that are free from bark and leaf were obtained from a local chipping plant in Opelika, AL, USA. Loblolly pine composition (48.5% cellulose, 31.3% hemicellulose, 25.8% lignin and 4.5% extractives) was determined using standard wet chemistry analysis protocol. All chemicals were purchased from VWR; except the phosphorylating agent for ^{31}P-NMR analysis, 2–chloro–4,4,5,5–tetramethyl–1,3,2–dioxaphospholane (TMDP), purchased from Sigma Aldrich. All chemicals were reagent grade and used as received.

5.2.2. Hydrothermal Liquefaction (HTL) of Loblolly Pine

Loblolly pine was ground by a hammer mill (New Holland grinder model 358, New Holland, PA.) using 40 mesh sieve size for particle size reduction, and the pine passed through 40 mesh were used. HTL was carried out in 1 L high pressure/high temperature Parr® Reactor (Parr Instrument Company, Model 4577 HP/HT pressure reactor, Moline, IL., USA) equipped with mechanical stirrer and reactor controller (Parr Instrument Company, Model 4848, Moline, IL., USA). The reactor was charged with 25 g of 40 mesh loblolly pine and 250 g of solvent (biomass/solvent=1/10, wt/wt) which consisted of either DI water or DI water/ethanol mixture (1/1, wt/wt). The HTL process with water and water/ethanol is denoted as W-HTL and W/E-HTL, respectively. Before heating up the reactor, high purity nitrogen was purged into the reactor to remove the air, and then reactor was pressurized to 2 MPa with nitrogen to force all the reactive materials into the liquid phase. Hydrothermal liquefaction was carried out at 300 rpm for 30 min. at four different conditions: 250 °C (far-critical), 300 °C (sub-critical), 350 °C (near-critical), and 390 °C (super-critical). HTL time was started once the set temperature was reached. For the 390 °C super-critical condition, the reactor was not initially pressurized to 2 MPa with nitrogen due to the safety limit of the reactor. The final pressure in the reactor at each

87

temperature was read from the reactor controller and is shown in Table 4.1. A typical temperature-pressure profile during HTL experiment is illustrated in Fig. 5.1. After 30 min. reaction, the reactor is immersed in iced water to quench the reaction.
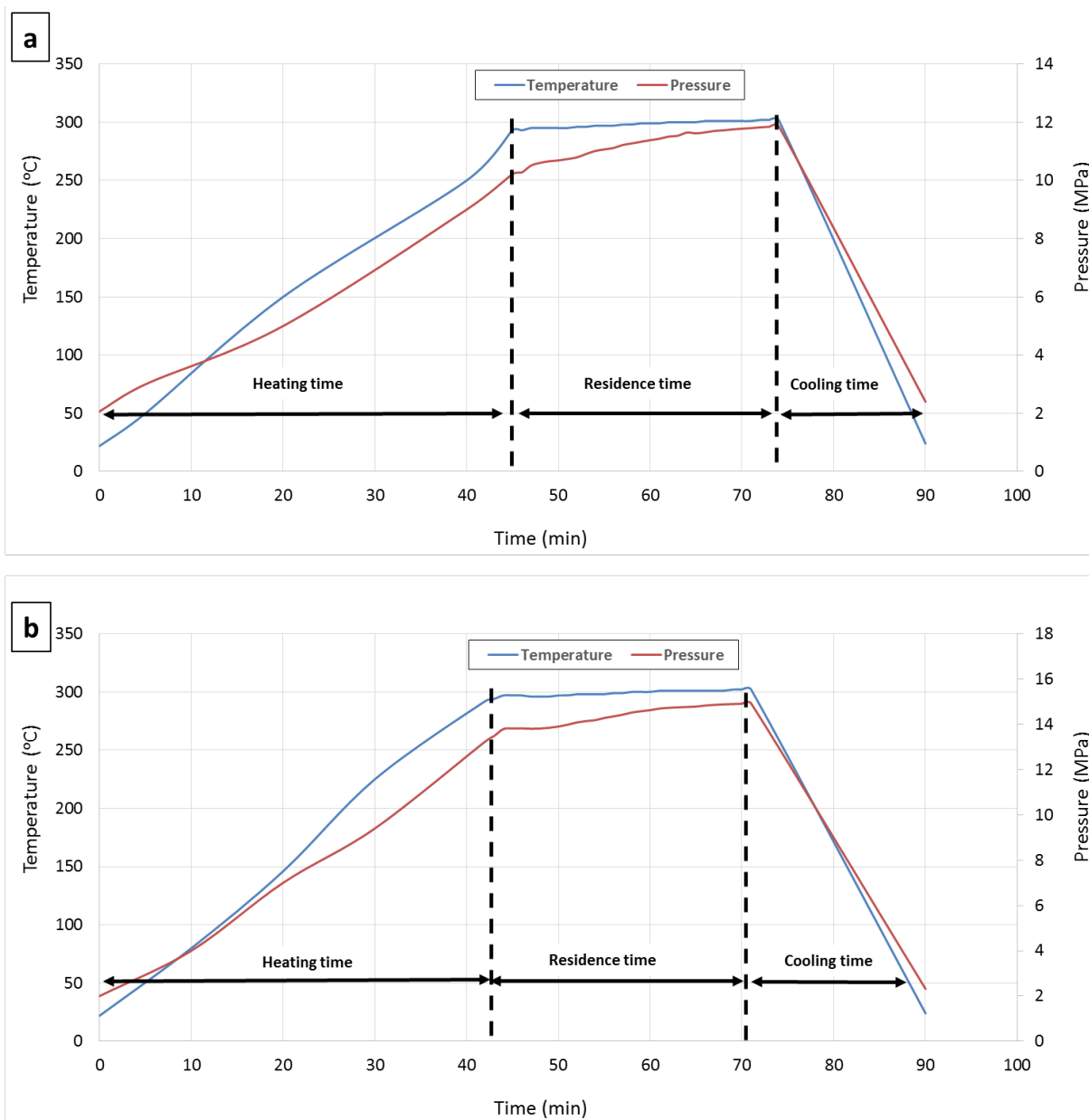
Fig. 5.1. Graphical representation of temperature – pressure profile of W-HTL **(a)** and W/E-HTL **(b)** at 300 ℃.

Table 5.1. The initial and final pressure in the reactor at each temperature in HTL process.

Temperature (°C)	Initial N_2 Pressure (MPa)		Final Pressure (MPa)	
	H_2O	H_2O/EtOH	H_2O	H_2O/EtOH
250	2	2	7	9
300	2	2	11	14
350	2	2	19	22
390	0	0	24	24

5.2.3. Product Separation and Calculation of the Product Yields

The procedure of product separation is illustrated in Fig. 5.2. Once the reactor was cooled

down to 24 °C, the gas fraction was released, and the reactor was opened. The composition of the

gas fraction was not analyzed in this study. The amount of gas produced was calculated by the

weight difference of the reactor after venting the gas (Eqn. 1), where W1 is the weight of the

reactor before HTL containing biomass and solvent; and W2 is the weight of the reactor

(containing liquefied biomass) after HTL and venting the gas. The slurry (liquefied wood) was

poured into a flask, and the reactor was rinsed with dichloromethane (DCM) to collect all the

contents in the reactor. The slurry was then diluted with 400 mL DCM. The solid and the liquid

part in the slurry was vacuum filtered using preweighed Whatmann#5 filter paper. The solid part,

accumulated on the filter paper, was oven dried at 105 °C for overnight, and assigned as

"residue". The yield of residue was calculated using Eqn. 2. The liquid part was poured into a 1

L separatory funnel to isolate the organic and the aqueous phases. Since water is not miscible in

DCM, organic and aqueous products separated naturally in the separatory funnel. The organic

products were carefully transferred to a rotary evaporator. The DCM and the solvent (water

and/or ethanol) retained in the organic phase was removed by rotary evaporation at 65 °C. The

DCM soluble compounds, a viscous-black liquid, were collected in the flask, which was donated

as "bio-oil", and the yield of bio-oil was calculated using Eqn. 3. The aqueous products (water and water soluble products) accumulated in the top layer, and assigned as "light oil". Since the major interest of this study was the bio-oil, the light oil was not further analyzed in this study. Quantification of light-oil is one challenge in HTL studies due to the high boiling point of water (Cheng et al. 2010). Therefore, the yield of the light oil was calculated by difference using Eqn. 4 for simplicity. However, it should be noted that calculating the yield of light-oil by difference results experimental errors. All experiments were carried out in duplicates and ANOVA was performed at 95% confidence interval to find out whether the results were statistically significant.

$$Gas\ yield\ (wt.\%) = \frac{W1 - W2}{wt. of\ the\ loblolly\ pine\ (dry\ basis)} \times 100 \qquad \text{(Eqn. 1)}$$

$$Residue\ yield\ (wt.\%) = \frac{wt. of\ the\ solid\ products}{wt. of\ the\ loblolly\ pine\ (dry\ basis)} \times 100 \qquad \text{(Eqn. 2)}$$

$$Bio - oil\ yield\ (wt.\%) = \frac{wt. of\ the\ bio-oil\ after\ rotary\ evaporator}{wt. of\ the\ loblolly\ pine\ (dry\ basis)} \times 100 \qquad \text{(Eqn. 3)}$$

$$Light\ oil\ yield\ (wt.\%) = 100 - Yield_{Gas+residue+bio-oil} \qquad \text{(Eqn. 4)}$$
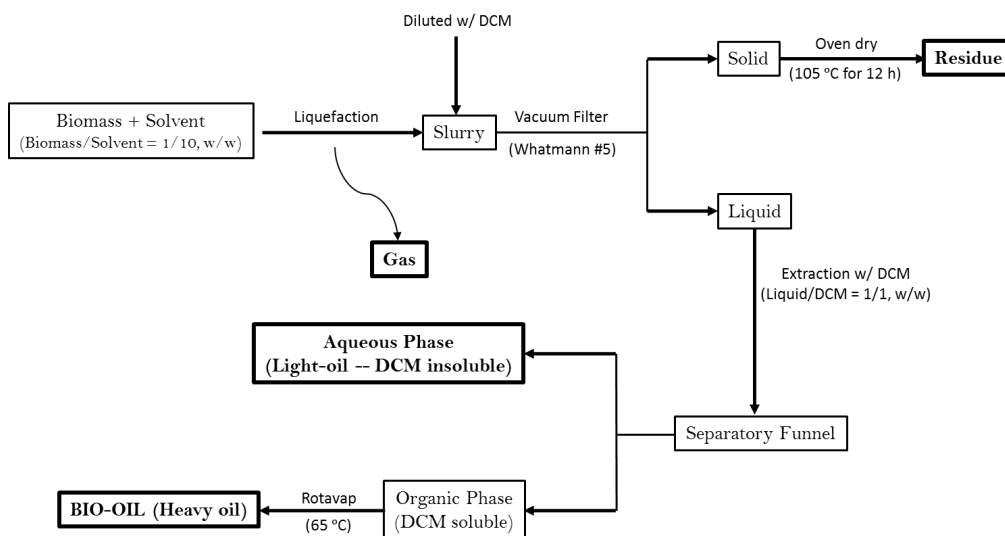
Fig. 5.2. Product separation procedure of HTL of loblolly pine.

90

5.2.4. Hydroxyl (OH) Group Analysis of Bio-oil: ^{31}P-NMR

^{31}P-NMR provides great deal of information to determine the content of OH groups present in the bio-oil. In this technique, OH groups belonging to aliphatic, phenolic, carboxylic units were phosphitylated by TMDP followed by quantitative ^{31}P-NMR. In the phosphitylation reaction, TMDP reacted with the free OH groups in the bio-oil, and yielded the derivatized compound and hydrochloric acid (HCl). Phosphitylation of bio-oil was performed according to Celikbag et al. (2015), and ^{31}P-NMR spectra were acquired with a Bruker Avance II 250 MHz spectrometer using inverse gated decoupling pulse sequence, 90° pulse angle, 25 s pulse delay and 128 scans following the methods of Ben and Ragauskas (2011). All experiments were performed in duplicates with ANOVA at 95% confidence interval.

5.2.5. Carbonyl Groups Analysis of Bio-oil: ^{19}F-NMR

The carbonyl groups in bio-oil was quantitatively determined by ^{19}F-NMR according to the method reported by Huang et al. (2014). In this technique, the carbonyl groups (aldehydes, ketones and quinones) in the bio-oil were derivatized with 4-(tri-fluoromethyl)phenylhydrazine. For quantitative analysis, 3-trifluoromethoxybenzoic was used as the internal standard. ^{19}F-NMR spectra were acquired with a Bruker Avance II 250 MHz spectrometer using 90° pulse angle without proton decoupling, 10 s pulse delay and 400 scans. All experiments were performed in triplicates and ANOVA was performed at 95% confidence interval.

5.3. Results and Discussion

5.3.1. Product Yields

5.3.1.1. Effect of Temperature on Product Yields

Product yields obtained under different HTL conditions are illustrated in Fig. 5.3. It was

found that temperature had a significant effect on bio-oil yield (p-value=0.0007 and <0.0001 for

W-HTL and W/E-HTL, respectively), and residue yield (p-value=0.0001 and <0.0001 for W-

HTL and W/E-HTL, respectively). The maximum bio-oil yield of 68 wt.% and minimum residue

yield of 2 wt.% was obtained at W/E-HTL at 300 °C. The bio-oil yield first increased when the

temperature increased from 250 °C to 300 °C, and then decreased as the temperature further

increased to 390 °C. The first increase in the bio-oil yield could be attributable to enhanced

degradation of lignocellulosic biomass into bio-oil due to the elevated temperature. The

minimum temperature for hemicellulose decomposition in water was reported to be 180 °C

(Changi et al. 2015), and higher temperatures (>260 °C) are required to overcome the activation

energy for lignin degradation (Yuan et al. 2010); therefore, it is reasonable that HTL at 300 °C

resulted in higher degradation of biomass than at 250 °C, and consequently led to increased bio-

oil yield. However, bio-oil yield decreased while residue and gas yield increased as the HTL

temperature increased to 390 °C as can be seen in Fig. 5.3. Many of the HTL studies reported

similar trends regarding a critical temperature for HTL of lignocellulosic biomass at which bio-

oil yield begins to drop and more solid residue and gaseous products are produced at above the

critical temperature (Akhtar and Amin 2011). In this study, 300 °C was found to be the best

temperature in terms of bio-oil and residue yield for both W-HTL and W/E-HTL. A kinetic study

also showed that gaseous products and solid residue are formed by the secondary reactions of

bio-oil at higher temperatures as a result of cracking and recondensation of bio-oil (Valdez and

Savage 2013). Thus, it is possible that the decrease in bio-oil yield at higher temperatures is

attributable to the enhanced cracking and condensation reactions. The decrease in the dielectric

constant (ε) of water at higher temperature and pressure could be another reason for the decrease

in bio-oil yield. Since the dielectric constant of water measures the polarity, it could be defined as the rough measurement of water's ability to dissolve polar compounds, and it decreases from 27.1 at subcritical conditions (150 °C<T<350 °C, 0.4 MPa<p<20 MPa) to 5.9 at supercritical condition (T>370 °C, p=25 MPa) (Krammer and Vogel 2000). Moreover, water at subcritical conditions acts like an acid/base catalyst precursor which is desirable for biomass liquefaction while water at supercritical conditions exhibits more like a non-polar solvent properties (Kruse and Dinjus 2007). Therefore, it could also be conjectured that the lower dielectric constant of water at higher temperatures could have contributed to lower bio-oil yield observed in this study.
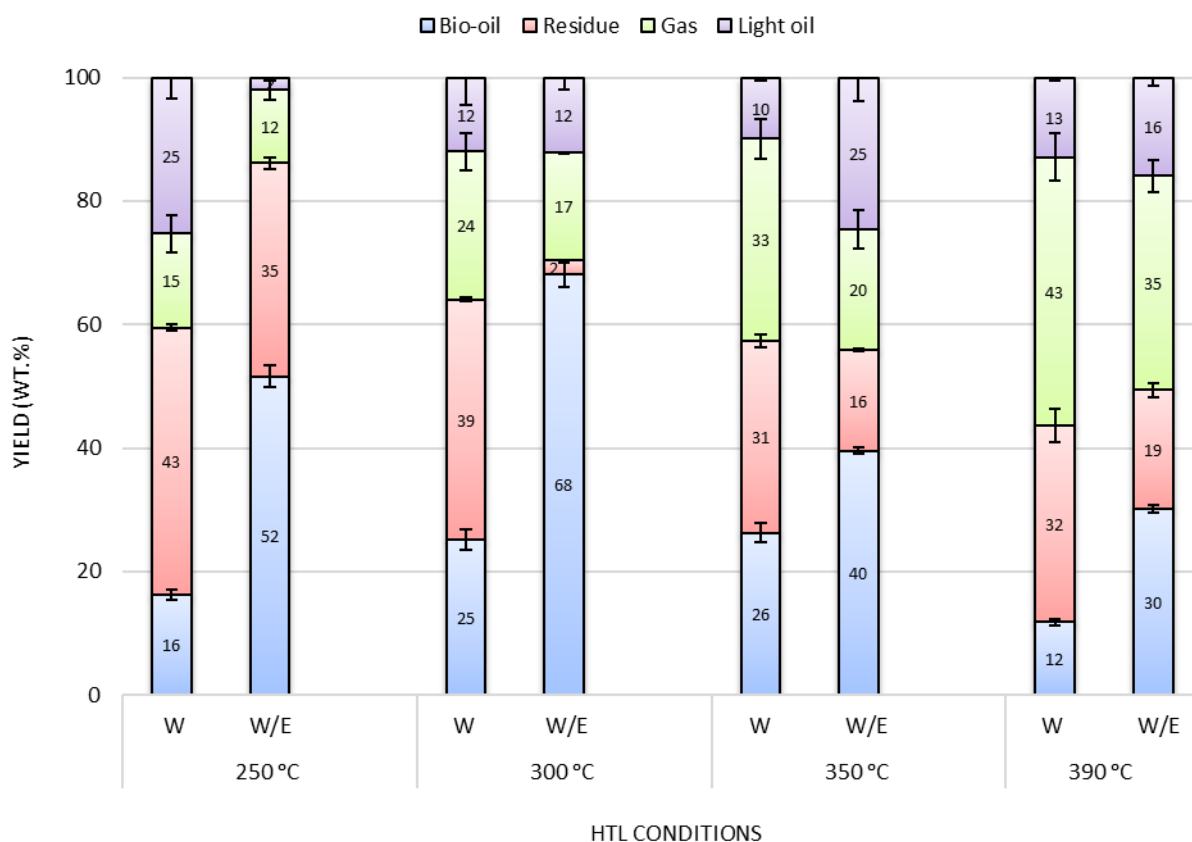
Fig. 5.3. Product yields at different HTL conditions (W=water, W/E=water/ethanol solvent).

5.3.1.2. Effect of Ethanol on Product Yields

ANOVA analysis with 95% confidence interval showed that addition of ethanol significantly increased the bio-oil yield obtained at each HTL temperature (p-value=0.0016, 0.0017, 0.0076 and 0.0014 for 250, 300, 350 and 390 °C, respectively), and decreased the amount of residue generated during the HTL (p-value=0.0063, <0.0001, 0.0027 and 0.0003 for 250, 300, 350 and 390 °C, respectively). All the W/E-HTL experiments exhibited higher bio-oil yield and lower residue yield than the W-HTL experiments; in fact, the lowest bio-oil yield (30 ± 0.5 wt.%) obtained from W/E- HTL was even higher than the maximum bio-oil yield (26 ± 1.6 wt.%) obtained from the W-HTL suggesting that water/ethanol shows great synergy effect for HTL of the lignocellulosic biomass. Moreover, much lower solid residue (2 wt.%) was produced by W/E- HTL at 300 °C while W-HTL produced 39 wt.% solid residue at 300 °C which indicates that addition of ethanol effectively inhibited the re-condensation of degradation products of lignocellulosic biomass. During the HTL, biomass is degraded to fragments and free radicals are generated. When there is no hydrogen donor solvent, these reactive free radicals recombine and forms high molecular weight products called solid residue or char. In case a sufficiently high amount of a hydrogen donor solvent such as ethanol is introduced to the HTL, free radicals can be stabilized and the formation of solid residue is decreased (Vasilakos and Austgen 1985). Thus, lower residue content at W/E-HTL is attributable to the hydrogen donor capability of ethanol. As Liu et al. (2013) summarized the synergetic effect of water/ethanol, the high bio-oil and low residue yield from W/E-HTL experiments could be attributed to (i) enhanced hydrogen donor capability of ethanol at subcritical and supercritical conditions and acting as a reaction substrate, (ii) high ability of ethanol to dissolve oily products, (iii) ability of ethanol to stabilize the free radicals resulting in lower residue content, and (iv) the increased solubility of high

molecular weight products in water/ethanol mixture at subcritical conditions. In addition to the synergistic effects mentioned above, conversion of highly reactive carbonyl groups in the bio-oil to more stable acetal groups by ethanol could be another reason for the low residue content in W/E- HTL. Compounds containing carbonyl groups such as aldehydes and ketones are primarily responsible for the repolymerization of bio-oil due to their high reactivity and consequently result in the generation of solid residue as well as an increase in the viscosity of bio-oil (Czernik et al. 1994). In this study, it was found that bio-oil produced from W/E- HTL had a lower carbonyl concentration (see below, section 5.3.3. Carbonyl (C=O) Group Analysis of Bio-oil: 19F-NMR) suggesting that ethanol stabilized the carbonyl groups, and as a result, a lower amount of solid residue was generated.

5.3.2. Hydroxyl (OH) Group Analysis of Bio-oil: ^{31}P-NMR

The OHNs of all bio-oils produced at different HTL conditions are illustrated in Fig. 5.4. A typical ^{31}P-NMR spectrum of a bio-oil is shown in Fig. 5.5. The type of OH groups including aliphatic, phenolic (guaiacyl, catechol, C_5 substituted condensed phenolic types) and acidic type of OH were identified according to ^{31}P-NMR chemical shifts reported by Ben and Ragauskas (2011). High OHN (5.35–10.70 mmol/g) is required for a bio-oil to be considered as a high quality biopolyol (Zou et al. 2012). All the bio-oils, except the bio-oils produced from W-HTL at 300 °C and 350 °C, exhibited higher OHN than 5.35 mmol/g; therefore, could thus be considered as a good candidate as biopolyols.
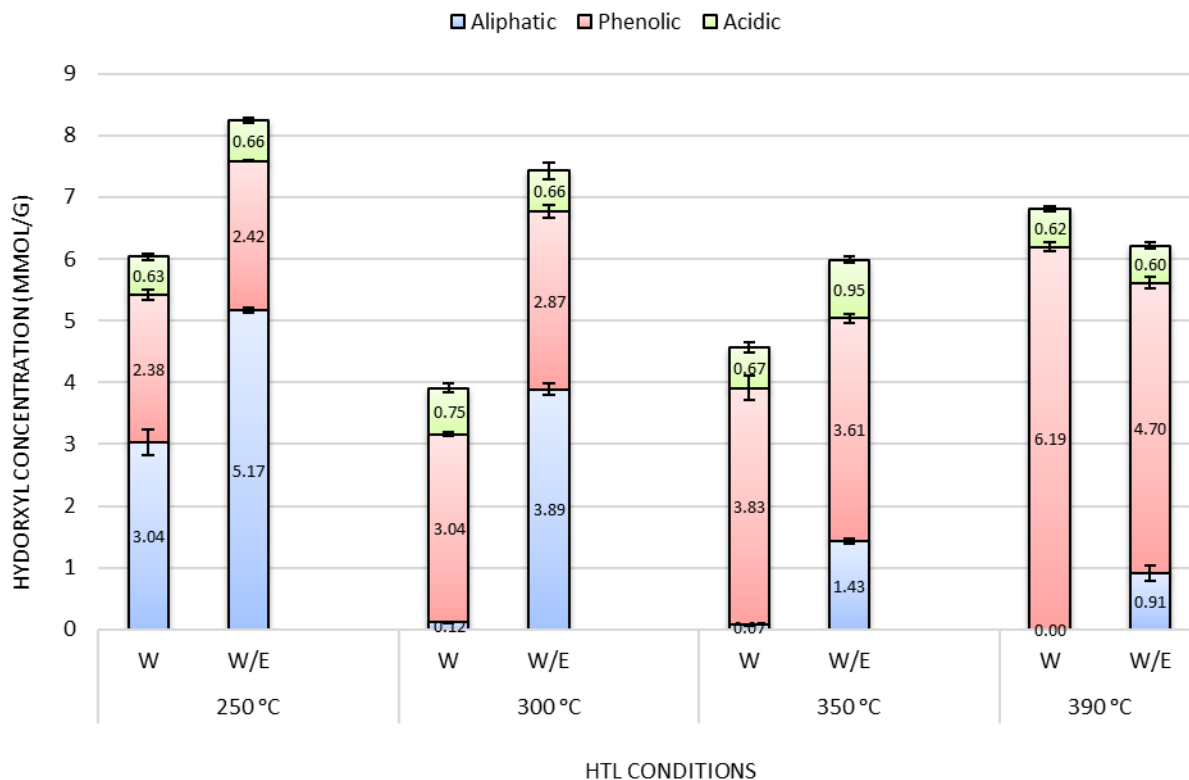
Fig. 5.4. OHN of bio-oils produced by HTL of loblolly pine at different conditions derivatized with TMDP.

5.3.2.1. Effect of Temperature on Hydroxyl Groups

ANOVA analysis showed that temperature had a significant effect on the total OHN of bio-oils produced by both W-HTL (p-value=0.0007) and W/E-HTL (p-value=0.0015). In the case of W-HTL, the total OHN first decreased (p-value=0.0142) as the temperature was increased from 250 to 300 °C, and then increased (p-value=0.0873 and 0.0088 for 300-350 °C and 350-390 °C, respectively) with the increasing temperature to 390 °C. On the other hand, the total OHN of bio-oils from W/E-HTL experiments decreased steadily (p-value=0.0782 and 0.0285 for 250-300 °C and 300-350 °C, respectively) till 350 °C, and then started to increase (p-value=0.3759) as the temperature reached to 390 °C. A similar trend in the OHN with temperature was observed for the bio-oils produced by organic solvent liquefaction of biomass

where authors attributed this trend to condensation reactions that occurred between degradation fragments of biomass (Wei et al. 2014). It is noteworthy to mention that for the both W-HTL and W/E-HTL experiments, aliphatic OH decreased while phenolic OH increased with increasing HTL temperature from 250 to 390 °C. Aliphatic OH was the dominant hydroxyl type at the lower temperature; however, at higher temperature, phenolic type OH was observed to be the major hydroxyl type. For instance, at 250 °C HTL, the aliphatic OH accounted for 50.3% and 62.7% of the total OHN of W-HTL and W/E-HTL, respectively. On the other hand, when the HTL temperature reached to 390 °C, phenolic OH accounted for 91% and 75.6% of the total OHN of W-HTL and W/E-HTL, respectively. Statistical analysis also showed that HTL temperature had significant effect on aliphatic and phenolic OH (p-value<0.0001 for both aliphatic and phenolic OH at W-HTL and W/E-HTL). This trend (decrease in the aliphatic OH and increase in the phenolic OH with increasing HTL temperature) could be due to the thermal stabilities of wood polymers (cellulose, hemicellulose and lignin). The higher concentration of aliphatic OH at lower temperature may be attributable to mainly hemicellulose degradation since (i) hemicellulose is the first depolymerized wood polymer under heat (Via et al. 2013), and (ii) the degradation route of hemicellulose in water yields sugar derivatives containing aliphatic OH groups (Changi et al. 2015). Lignin is the main source of the phenolic compounds in a bio-oil (Cheng et al. 2010), and degradation of lignin occurs at temperature above 260 °C (Yuan et al. 2010). Thus, the increase in the amount of phenolic OH with increasing HTL temperature could mostly be due to the lignin degradation. The acidic OH did not significantly change with temperature (p-value=0.2980 and 0.0462 for W-HTL and W/E-HTL, respectively), and stayed at a concentration of 0.66±0.06 and 0.72±0.16 mmol/g for W-HTL and W/E-HTL, respectively. Changi et al. (2015) reviewed the degradation of cellulose and hemicellulose in water at sub- and

super-critical conditions. Authors reported that at sub-critical conditions, hemicellulose degradation occurs much faster than cellulose while cellulose degradation increases when the HTL conditions are at the near- or super-critical conditions. It was also reported that their degradation products contain acidic components such as formic, acetic and lactic acid. Therefore, degradation products of hemicellulose and cellulose could be attributable to the source of acidic OH at subcritical (250 – 350 °C) and super-critical (390 °C) conditions, respectively.
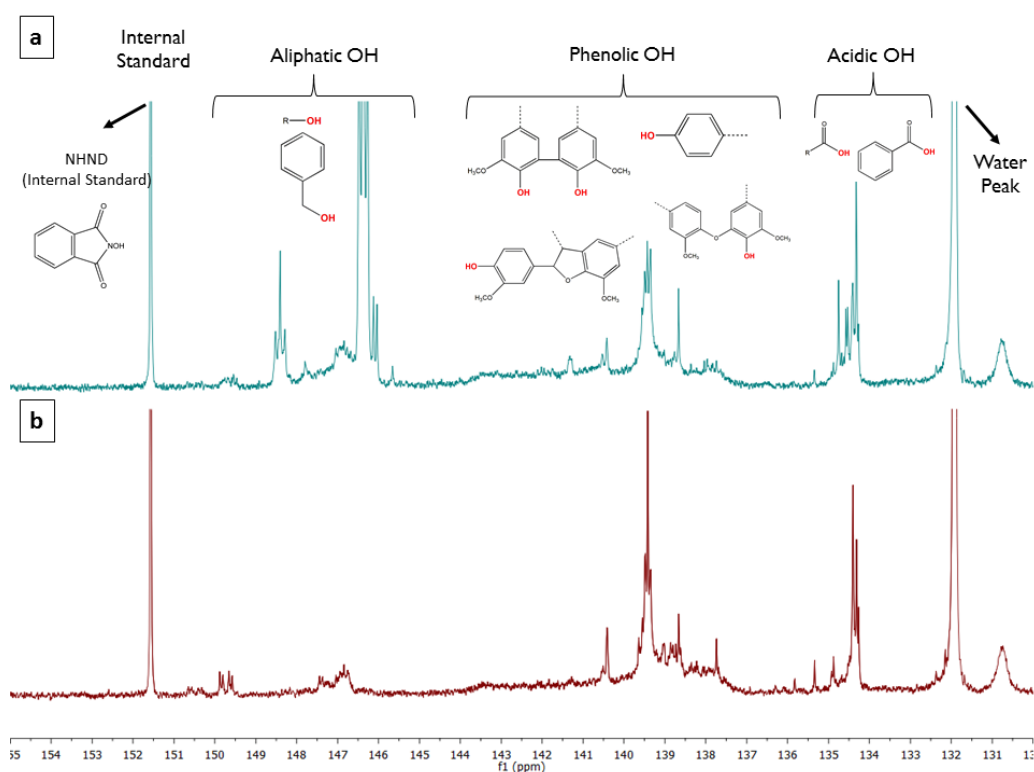
Fig. 5.5. ^{31}P-NMR spectra for the bio-oil produced by HTL of loblolly pine at different conditions derivatized with TMDP (Solvent type: water/ethanol=**a**, water=**b**).

5.3.2.2. Effect of Ethanol on Hydroxyl Groups

All of the bio-oils obtained from W/E-HTL experiments at each temperature exhibited higher total OHN than W-HTL except at 390 °C. Ethanol was found to have a significant effect on the total OHN of the bio-oils produced at 250, 300 and 350 °C (p-value=0.0123, 0.0052 and 0.0193, respectively); however, no significant effect was observed for the experiment at 390 °C (p-value=0.1082). The high OHN at W/E-HTL experiments could be attributed to the synergy effect of water and ethanol as discussed in the section 5.3.1.2. Since ethanol is a good hydrogen donor solvent and effectively inhibits the re-condensation of biomass degradation products, the bio-oil obtained from W/E-HTL had a lower molecular weight and a higher polydispersity index (Cheng et al. 2010) suggesting that the bio-oil mainly contains monomers and oligomers from decomposition of biomass. Therefore, it is conjectured that the higher amount of monomers and oligomers provided more side groups such as hydroxyls in the bio-oil.

One major result found in this study was that the bio-oils produced by W/E-HTL at each temperature contain more aliphatic and less phenolic OH than the bio-oils obtained from W-HTL. This finding suggests that ethanol significantly contributed the aliphatic type OH in the bio-oils (p-value=0.0050, 0.0003, 0.0005 and 0.0107 for 250, 300, 350 and 390 °C, respectively). Our lab has previously studied the source and variation of hydroxyl groups of the bio-oil produced by liquefaction of loblolly pine with ethylene glycol (EG), and found that lignin fragments undergo condensation reaction with EG which results in less phenolic and more aliphatic type of hydroxyl groups (Celikbag et al. 2014). The same rational can be applied to the W/E-HTL in which ethanol may undergo condensation reactions with the phenolic OH groups of the lignin fragments. This finding is also in agreement with previous GC/MS studies of cornstalk

lignin in W/E-HTL where the yields of phenolic compounds (phenol, ethylphenol, guaiacol) were reported to be lower when the ethanol concentration in the water/ethanol mixture was increased (Ye et al. 2012). ANOVA analysis of phenolic OH showed that ethanol had significant effect at 390 °C only (p-value=0.0033). For below supercritical conditions, no significant effect of ethanol was observed on phenolic OH (p-value=0.5963, 0.1555 and 0.2712 for 250, 300 and 350 °C, respectively).

These findings suggest that OHN of a bio-oil could be adjusted by HTL temperature and ethanol. For example, W/E-HTL at lower temperature seems to constitute optimum HTL conditions for the production of biopolyol with high concentration of aliphatic OH. Such biopolyols could be utilized in polyester production. On the other hand, bio-oil produced from high temperature W-HTL offers high concentration of phenolic OH which could be used as a biopolyol for the production of rigid polymers such as epoxy. However, the bio-oil yield should be taken into account as well because it is an important consideration for the economic viability of the process.

5.3.3. Carbonyl (C=O) Group Analysis of Bio-oil: ^{19}F-NMR

5.3.3.1. Effect of Temperature on Carbonyl (C=O) Groups

The carbonyl group concentration of bio-oil derivatized with 4-(tri-fluoromethyl)phenylhydrazine was calculated by quantitative ^{19}F-NMR and results are illustrated in Fig. 5.6, and a typical ^{19}F-NMR spectra is shown in Fig. 5.7.

Fig. 5.6. Carbonyl group concentration of bio-oils produced by HTL of loblolly pine at different conditions derivatized with 4-(tri-fluoromethyl)phenylhydrazine (W=water, W/E=water/ethanol solvent).

ANOVA analysis showed that temperature had no statistically significant effect on the carbonyl concentration in the bio-oil produced from W-HTL (p-value=0.2985); however, a significant temperature effect was found in the bio-oil produced from W/E-HTL (p-value=0.0001). The carbonyl concentration of bio-oils produced from W-HTL and W/E-HTL followed the same pattern under the temperature treatment: first increased (p-value=0.1326 and 0.0002 for W-HTL and W/E-HTL, respectively) as the HTL temperature was increased from 250 °C to 300 °C, and then decreased (p-value= 0.0022 and 0.0099 for W-HTL and W/E-HTL, respectively) with increasing temperature from 300 to 350 °C. A slight increase in the carbonyl concentration (p-value=0.6216 and 0.5658 for W-HTL and W/E-HTL, respectively) was

observed when the HTL temperature had reached to 390 °C. The first increase in the carbonyl

concentration could indicate the enhanced degradation of hemicellulose at 300 °C since the

major degradation product of hemicellulose is xylose which is a 5-carbon sugar aldehyde

(Changi et al. 2015). Moreover, cleavage of ester bonds in lignin could result in the increase of

carbonyl concentration (Huang et al. 2014) as lignin degradation mostly occurs at temperature

above 260 °C (Yuan et al. 2010). Decrease in the carbonyl concertation with increasingly severe

HTL conditions is more likely due to the dehydration (Changi et al. 2015) and re-condensation of

carbonyl groups with other degradation products.

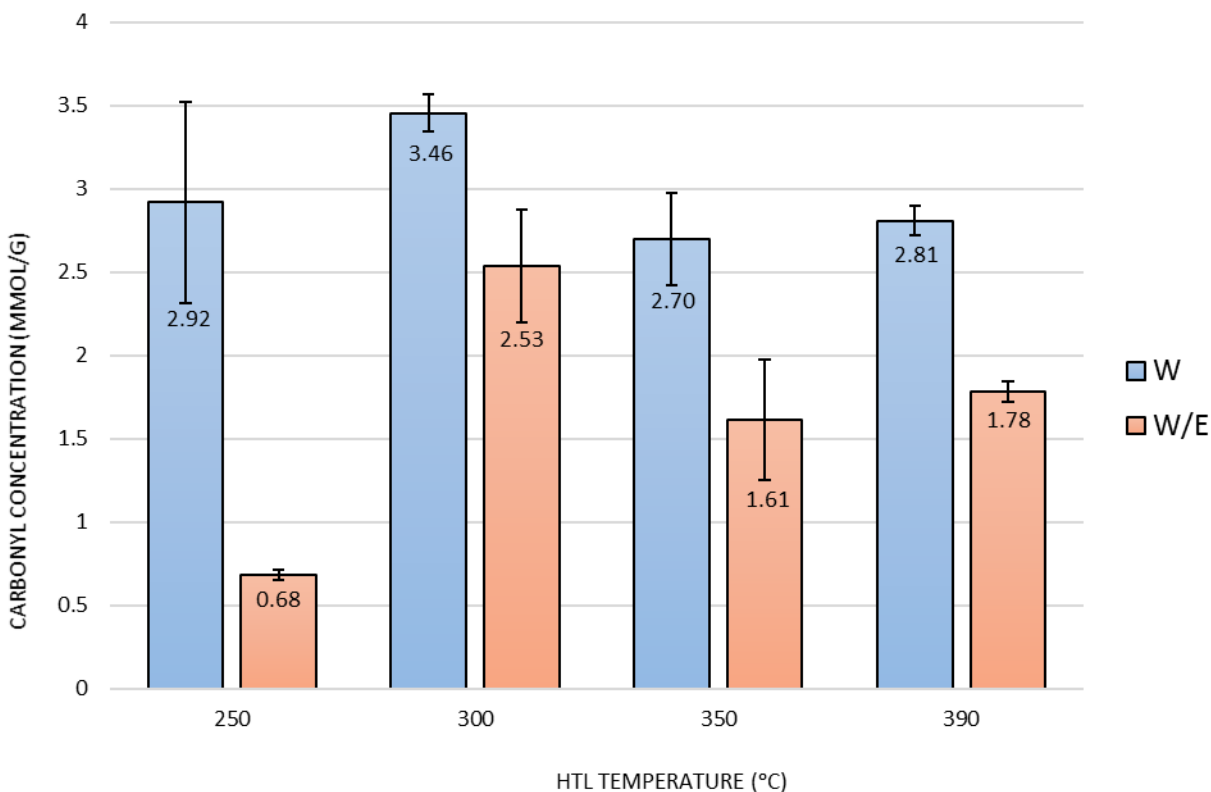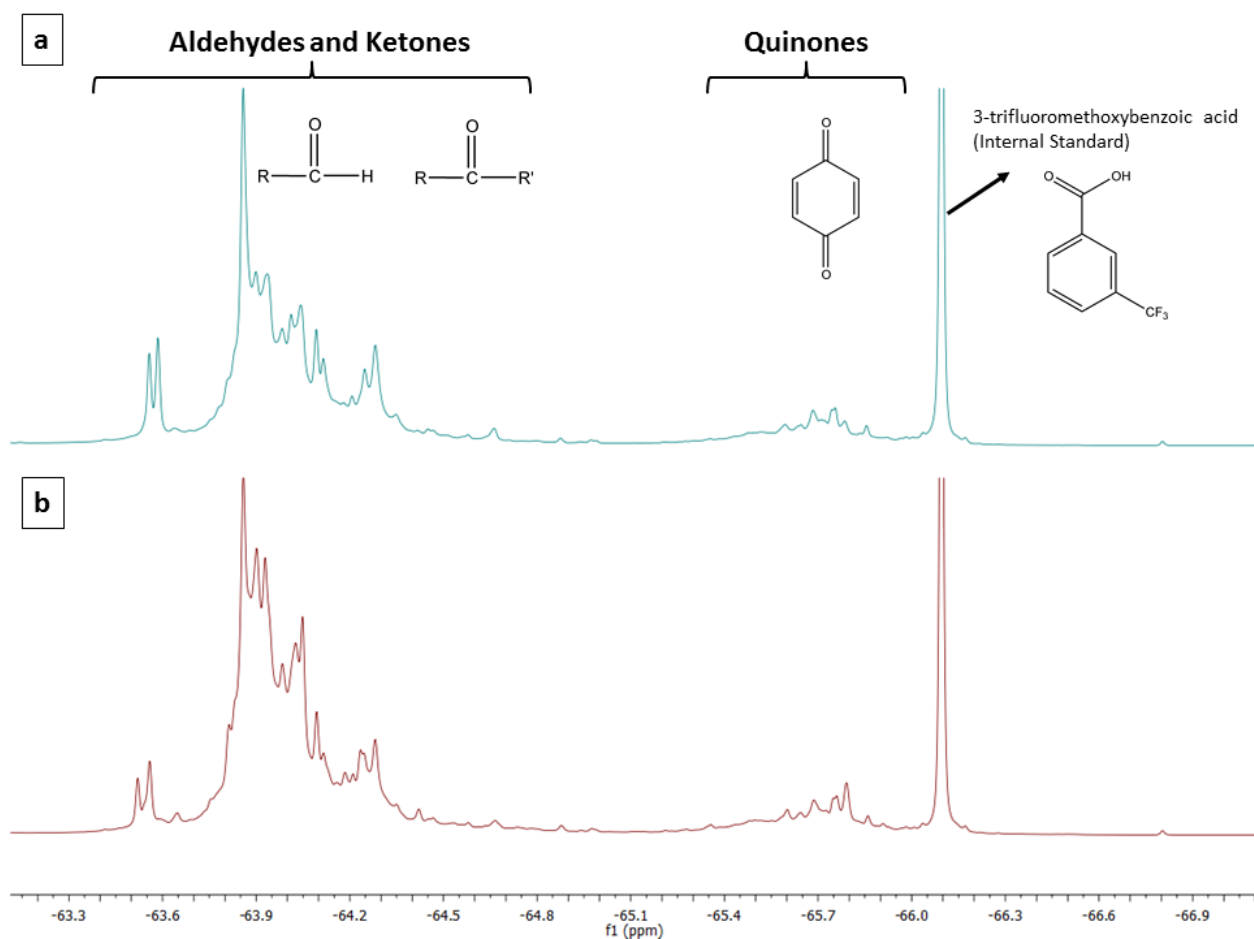**Fig. 5.7.** ^{19}F-NMR spectra for bio-oils produced by HTL of loblolly pine at different conditions derivatized with 4-(tri-fluoromethyl)phenylhydrazine (Solvent type: water/ethanol=**a**, water=**b**).

5.3.3.2. Effect of Ethanol on Carbonyl (C=O) Groups

ANOVA analysis showed that addition of ethanol had significant effect on carbonyl concentration at each HTL temperature (*p*-value=0.0030, 0.0020, 0.0031 and 0.0055 for 250, 300, 350 and 390 °C, respectively). Compared to W-HTL, a lower carbonyl concentration was found in the W/E-HTL bio-oils at each temperature (Fig. 5.6). This is in agreement with research by Kosinkova et al. (2015) who pursued the HTL of bagasse using water/ethanol solvent. In that study, the GC/MS analysis of bio-oil showed that the amount of ketones in the bio-oil decreased as the amount of ethanol was increased in the water/ethanol mixture. Acetalisation studies of bio-oil also showed that highly reactive carbonyl groups could be converted into more stable acetal and hemiacetal groups by low molecular weight alcohols such as methanol and ethanol (Li et al. 2011, Ye et al. 2014). Eckert and Chandler (1998) investigated the tautomeric equilibrium of Schiff base 4-(methoxy)-1-(N-phenylforminidoyl)-2-naphthol in the supercritical ethane in the presence of ethanol as the co-solvent, and reported that ethanol could shift the keto-enol equilibrium toward the enol form with increasing density which suggests that ethanol played a role in the conversion of ketone carbonyls to hydroxyl groups. Similar transformation of ketones to enols was also observed by Nazari et al. (2015) where birchwood sawdust was liquefied in the presence of KOH in a HTL process. Taking the reported observations into account, it is concluded that the lower carbonyl and higher hydroxyl concentration in bio-oil produced via W/E- HTL in this study could be attributed to (i) the stabilization of carbonyl groups to acetal groups by ethanol, and (ii) the shift of keto-enol tautomerism toward the enol form.

Compounds containing carbonyl groups are considered undesirable for the utilization of bio-oil due to their high reactivity which leads to unstable, highly acidic bio-oil (Huang et al.

2014). The results of this study suggest that, especially at lower temperatures, carbonyl concentration could be significantly reduced by addition of ethanol to the HTL process. Such bio-oil with improved properties may open venues to increased utilization.

5.4. Conclusion

The effect of ethanol on hydroxyl and carbonyl groups in bio-oil was studied. The highest bio-oil yield was obtained from W/E-HTL at 300 °C. ^{31}P-NMR and ^{19}F-NMR showed that addition of ethanol had a significant effect on the total hydroxyl and carbonyl concentration of the bio-oils. It was found that addition of ethanol increased the total OHN and aliphatic type OH; however, decreased the phenolic OH concentration. Moreover, lower carbonyl concentration was observed when ethanol was introduced to the HTL process. With optimization of the HTL reaction conditions the properties of bio-oils might be tailored towards their area of application.

References

1. Akhtar, J. and N. A. S. Amin. 2011. A review on process conditions for optimum bio-oil yield in hydrothermal liquefaction of biomass. Renewable and Sustainable Energy Reviews **15**:1615-1624.

2. Ben, H. X. and A. J. Ragauskas. 2011. NMR Characterization of Pyrolysis Oils from Kraft Lignin. Energy & Fuels **25**:2322-2332.

3. Celikbag, Y., T. J. Robinson, B. K. Via, S. Adhikari, and M. L. Auad. 2015. Pyrolysis oil substituted epoxy resin: Improved ratio optimization and crosslinking efficiency. Journal of Applied Polymer Science **132.** DOI: 10.1002/app.42239

4. Celikbag, Y., B. K. Via, S. Adhikari, and Y. Wu. 2014. Effect of liquefaction temperature on hydroxyl groups of bio-oil from loblolly pine (Pinus taeda). Bioresource Technology **169**:808-811.

5. Changi, S. M., J. L. Faeth, N. Mo, and P. E. Savage. 2015. Hydrothermal Reactions of Biomolecules Relevant for Microalgae Liquefaction. Industrial & Engineering Chemistry Research. **54**:11733-11758.

6. Cheng, S., I. D'cruz, M. Wang, M. Leitch, and C. Xu. 2010. Highly Efficient Liquefaction of Woody Biomass in Hot-Compressed Alcohol−Water Co-solvents. Energy & Fuels **24**:4659-4667.

7. Choi, G.-G., S.-J. Oh, S.-J. Lee, and J.-S. Kim. 2015. Production of bio-based phenolic resin and activated carbon from bio-oil and biochar derived from fast pyrolysis of palm kernel shells. Bioresource Technology **178**:99-107.

8. Czernik, S., D. K. Johnson, and S. Black. 1994. Stability of Wood Fast Pyrolysis Oil. Biomass & Bioenergy **7**:187-192.

9. Eckert, C. A. and K. Chandler. 1998. Tuning fluid solvents for chemical reactions. The Journal of Supercritical Fluids **13**:187-195.

10. Elliott, D. C., P. Biller, A. B. Ross, A. J. Schmidt, and S. B. Jones. 2015. Hydrothermal liquefaction of biomass: Developments from batch to continuous process. Bioresource Technology **178**:147-156.

11. Hu, S. J. and Y. B. Li. 2014. Two-step sequential liquefaction of lignocellulosic biomass by crude glycerol for the production of polyols and polyurethane foams. Bioresource Technology **161**:410-415.

12. Huang, F., S. Pan, Y. Pu, H. Ben, and A. J. Ragauskas. 2014. 19F NMR spectroscopy for the quantitative analysis of carbonyl groups in bio-oils. Rsc Advances **4**:17743-17747.

13. Kosinkova, J., J. A. Ramirez, J. Nguyen, Z. Ristovski, R. Brown, C. S. K. Lin, and T. J. Rainey. 2015. Hydrothermal liquefaction of bagasse using ethanol and black liquor as solvents. Biofuels, Bioproducts and Biorefining. DOI: 10.1002/bbb.1578

14. Krammer, P. and H. Vogel. 2000. Hydrolysis of esters in subcritical and supercritical water. The Journal of Supercritical Fluids **16**:189-206.

15. Kruse, A. and E. Dinjus. 2007. Hot compressed water as reaction medium and reactant: Properties and synthesis reactions. The Journal of Supercritical Fluids **39**:362-380.

16. Kunaver, M., S. Medved, N. Cuk, E. Jasiukaityte, I. Poljansek, and T. Strnad. 2010. Application of liquefied wood as a new particle board adhesive system. Bioresource Technology. **101**:1361-1368.

17. Kuo, P.-Y., M. Sain, and N. Yan. 2014. Synthesis and characterization of an extractive-based bio-epoxy resin from beetle infested Pinus contorta bark. Green Chemistry **16**:3483-3493.

18. Li, X., R. Gunawan, C. Lievens, Y. Wang, D. Mourant, S. Wang, H. Wu, M. Garcia-Perez, and C.-Z. Li. 2011. Simultaneous catalytic esterification of carboxylic acids and acetalisation of aldehydes in a fast pyrolysis bio-oil from mallee biomass. Fuel **90**:2530-2537.

19. Liu, Y., X.-z. Yuan, H.-j. Huang, X.-l. Wang, H. Wang, and G.-m. Zeng. 2013. Thermochemical liquefaction of rice husk for bio-oil production in mixed solvent (ethanol–water). Fuel Processing Technology **112**:93-99.

20. Nazari, L., Z. Yuan, S. Souzanchi, M. B. Ray, and C. Xu. 2015. Hydrothermal liquefaction of woody biomass in hot-compressed water: Catalyst screening and comprehensive characterization of bio-crude oils. Fuel **162**:74-83.

21. Ouyang, X., X. Huang, Y. Zhu, and X. Qiu. 2015. Ethanol-Enhanced Liquefaction of Lignin with Formic Acid as an in Situ Hydrogen Donor. Energy & Fuels **29**:5835-5840.

22. Perlack, R. D., L. L. Wright, A. F. Turhollow, R. L. Graham, B. J. Stokes, and D. C. Erbach. 2005. Biomass as feedstock for a bioenergy and bioproducts industry: the technical feasibility of a billion-ton annual supply. DTIC Document.

23. Thangalazhy-Gopakumar, S., S. Adhikari, H. Ravindran, R. B. Gupta, O. Fasina, M. Tu, and S. D. Fernando. 2010. Physiochemical properties of bio-oil produced at various temperatures from pine wood using an auger reactor. Bioresource Technology **101**:8389-8395.

24. Toor, S. S., L. Rosendahl, and A. Rudolf. 2011. Hydrothermal liquefaction of biomass: A review of subcritical water technologies. Energy **36**:2328-2342.

25. Valdez, P. J. and P. E. Savage. 2013. A reaction network for the hydrothermal liquefaction of Nannochloropsis sp. Algal Research **2**:416-425.

26. Vasilakos, N. P. and D. M. Austgen. 1985. Hydrogen-donor solvents in biomass liquefaction. Industrial & Engineering Chemistry Process Design and Development **24**:304-311.

27. Via, B. K., S. Adhikari, and S. Taylor. 2013. Modeling for proximate analysis and heating value of torrefied biomass with vibration spectroscopy. Bioresource Technology **133**:1-8.

28. Wei, N., B. K. Via, Y. F. Wang, T. McDonald, and M. L. Auad. 2014. Liquefaction and substitution of switchgrass (Panicum virgatum) based bio-oil into epoxy resins. Industrial Crops and Products **57**:116-123.

29. Yan, X., B. Wang, and J. Zhang. 2015. Liquefaction of cotton seed in sub-critical water/ethanol with modified medical stone for bio-oil. Bioresource Technology **197**:120-127.

30. Ye, J., C. Liu, Y. Fu, S. Peng, and J. Chang. 2014. Upgrading Bio-oil: Simultaneous Catalytic Esterification of Acetic Acid and Alkylation of Acetaldehyde. Energy & Fuels **28**:4267-4272.

31. Ye, Y., J. Fan, and J. Chang. 2012. Effect of reaction conditions on hydrothermal degradation of cornstalk lignin. Journal of Analytical and Applied Pyrolysis **94**:190-195.

32. Yu, F., Y. H. Liu, X. J. Pan, X. Y. Lin, C. M. Liu, P. Chen, and R. Ruan. 2006. Liquefaction of corn stover and preparation of polyester from the liquefied polyol. Applied Biochemistry and Biotechnology **130**:574-585.

33. Yuan, X. Z., H. Li, G. M. Zeng, J. Y. Tong, and W. Xie. 2007. Sub- and supercritical liquefaction of rice straw in the presence of ethanol–water and 2-propanol–water mixture. Energy **32**:2081-2088.

34. Yuan, Z., S. Cheng, M. Leitch, and C. Xu. 2010. Hydrolytic degradation of alkaline lignin in hot-compressed water and ethanol. Bioresource Technology **101**:9308-9313.

35. Zou, X. W., T. F. Qin, Y. Wang, L. H. Huang, Y. M. Han, and Y. Li. 2012. Synthesis and properties of polyurethane foams prepared from heavy oil modified by polyols with 4,4 '-methylene-diphenylene isocyanate (MDI). Bioresource Technology **114**:654-657.

Chapter 6

Pyrolysis Oil Substituted Epoxy Resin: Improved Ratio Optimization and Crosslinking Efficiency*

Abstract

The objective of this study was to determine the compatibility of whole pyrolysis oil of pine as a substitute for the phenolic component of epoxy resins. Pyrolysis oil-based epoxy resin (POBER) was synthesized by modification of EPON828 epoxy resin with pyrolysis oil at various mixing ratios (1:3 – 1:8, pyrolysis oil:EPON828, w/w). Acetone extraction determined that a ratio of 1:7 – 1:8 resulted in a fully reacted thermoset, leaving neither pyrolysis oil nor EPON828 in a significantly unreacted state. DMA analysis revealed that a ratio of 1:8 produced the highest storage modulus (E'); in addition, it was determined that this ratio provided a superior glass transition temperature of 120 °C and crosslinking density of 1891 mol/m^3. FTIR spectra concluded that the reaction between the EPON828 and pyrolysis oil was complete at the 1:8 ratio, citing the removal of hydroxyl and epoxide peaks within the cured product.

6.1. Introduction

Epoxy resins (ER) are an important class of thermosets which are widely used in the field of automotive, aerospace, insulation and electronics due to their superior properties such as low density, high toughness, excellent thermal and mechanical properties, and flame and chemical resistance (Liu 2001, Manfredi et al. 2005, Auad et al. 2007, Sunitha et al. 2015). ERs owe their excellent properties to epoxide functionality and aromatic/phenolic backbone. When ER is cured, epoxide groups provide a highly crosslinked matrix which enhances thermal and mechanical properties. The phenolic backbone, on the other hand, provides flame resistance and stiffness (Hofmann and Glasser 1993, Auad et al. 2007). The global epoxy production is predicted to be 3 million tons by 2017(Auvergne et al. 2014) with a market size of US$21.5 billion.(Auvergne et al. 2014) Today epoxy and other plastic production processes rely on petroleum resources to assist in the reaction. Current petroleum use is large and creates significant problems such as air pollution, promotion of the greenhouse effect, and depletion of petroleum reserves (Naik et al. 2010). Therefore, environmental concerns, as well as instability in the petrochemical market, have recently increased in using more sustainable and renewable chemical resources.

Lignocellulosic biomass is considered the most abundant natural resource with an annual production of 1.3 billion dry tons in the U.S.A (Perlack et al. 2005). The U.S. Department of Energy (DOE) and the U.S. Department of Agriculture (USDA) have prioritized the development of bioenergy and bioproducts, and they have a goal to produce 18% of the current U.S. chemical commodities from biomass by 2020, and 25% by 2030 (Perlack et al. 2005). Increased research on the utilization of lignocellulosic biomass to produce bio-based epoxy resins has also occurred recently. Valuable reviews on bio-based epoxy systems to date can be

found in the literature (Raquez et al. 2010, Pan 2011, Koike 2012, Auvergne et al. 2014, Islam et al. 2014). Among lignocellulosic biomass, bark (Kuo et al. 2014), woody biomass (Kishi et al. 2011), bamboo (Wu and Lee 2010) and switchgrass (Wei et al. 2014) have been previously studied in the bio-based epoxy systems. These studies mainly focused on the production of difunctional or polyfunctional alcohol (polyol) from biomass as a substitution of bisphenol A (BPA) for epoxy synthesis. Researchers reported promising results, for instance, a high degree of substitution (up to 50%) (Wei et al. 2014) and a low curing activation energy (Kuo et al. 2014); however, thermal and mechanical properties still needed to be improved. Most recently, Tiimob et al. (2014) has reinforced a bio-based epoxy resin with sustainable β-CaSiO$_3$ nanoparticles prepared from egg shell to improve resin properties. During the past decade, lignin has also attracted interests in the bio-based epoxy systems as hardeners (Ismail et al. 2010, Qin et al. 2013) and polyols (Engelmann and Ganster 2014, Ferdosian et al. 2014) because of its natural aromatic structure. However, a complex and variable chemical structure and high polydispersity index (Laurichesse et al. 2014) of lignin restrain its feasibility.

Pyrolysis oil (PO) is a product of the controlled heating of lignocellulosic biomass within a controlled atmosphere in which a rapid quenching of the vapors and aerosols result in PO. In the pyrolysis process, biomass is converted to vapors, aerosols and chars in the absence of oxygen at elevated temperatures (400 – 600°C). Vapors and aerosols are then rapidly condensed, and bio-oil is produced. Bio-oil yield is around 60 – 75% depending on process parameters (temperature, residence time, etc.) (Mohan et al. 2006). The rapid cooling of these vapors produces a highly reactive, two-phase chemical, comprised of an aqueous, hydrophilic phase and a tarry, hydrophobic phase. This hydrophobic phase is rich in pyrolytic lignin, which has been

demonstrated as a viable partial replacement (up to 50%) for phenol during the production of phenol formaldehyde (PF) resin (Czernik and Bridgwater 2004). Therefore, pyrolysis oil of lignocellulosic biomass could be considered as a promising natural phenolic resource (Amen-Chen et al. 2001, Effendi et al. 2008, Fele Žilnik and Jazbinšek 2012, Fu et al. 2014).

Epoxy resins can utilize pyrolysis oil as a phenolic source due to the high concentration of phenolic hydroxyl groups found within the pyrolysis oil (Effendi et al. 2008). Epoxy resins have been used sparingly in the wood products industry, primarily due to the increased cost associated with these types of adhesive systems (Pizzi 2006). However, with the increase in the production of pyrolysis oil, the cost of this product is expected to be less than the traditional petroleum-based phenol used in epoxy-phenolic production (Pizzi 2006). In addition, these adhesives are formulated without the use of formaldehyde, circumventing the current problems associated with off-gassing. After adjustment for inflation, it is anticipated that the significantly cheaper cost of bio-oil ($0.20 - 0.35 / lb) than epoxy ($1.50 / lb) will result in an opportunity to make epoxies that are more cost effective and competitive to other adhesive systems (Czernik and Bridgwater 2004, Luo et al. 2004, Dietrich 2012).

Pyrolysis oil as substitutes for phenolics into epoxies is lacking and the OH distribution within PO is currently unknown but is important during crosslinking. Therefore, the objective of this study is to determine the compatibility of whole pyrolysis oil as a substitute for the phenolic component of epoxy resins. Whole pyrolysis oil utilizes both the hydrophobic and hydrophilic phase, increasing the potential yield and industry profits. There may be additional challenges associated with using the resource in this form. Therefore, this research has the potential to

provide interesting results and introduce new possibilities in the field of bio-based industrial adhesives. To explore this question, the stoichiometric ratio for proper pyrolysis oil was determined finding out the optimum mixing ratio of pyrolysis oil and epoxy resin, and the chemistry behind pyrolysis oil and epoxy resin was investigated using both chemical and physical analysis.

6.2. Materials and Method

6.2.1. Materials

Loblolly pine wood chips, *Pinus spp*, (20 mesh), obtained from a local chipping plant in Opelika, AL, USA. All chemicals were purchased from VWR; except phosphorylating agent, 2–chloro–4,4,5,5–tetramethyl–1,3,2–dioxaphospholane (TMDP), which was purchased from Sigma Aldrich. All chemicals were reagent grade and used as received.

6.2.2. Preparation of Pyrolysis Oil

The pyrolysis oil was a combination of four batches produced using an auger style reactor at temperatures ranging from 425 – 500 °C for approximately 10 seconds according to the method reported by Thangalazhy-Gopakumar et al. (2010). The whole pyrolysis oil was methylated using methanol at a rate of 50 % (v/v). The resulting homogenized pyrolysis oil product was vacuum filtered 5 times using #1 Whatman paper in order to make sure that all the ash and char components were removed. Excess methanol was removed by rotary evaporation for 45 min. at 60 °C under 27" Hg vacuum.

6.2.3. ^{31}P NMR Analysis of Pyrolysis Oil

^{31}P-NMR provides great deal of information to determine the content of OH groups present in the pyrolysis oil. In this technique, OH groups belonging to aliphatic, phenolic, carboxylic units are phosphitylated by TMDP followed by quantitative ^{31}P-NMR. In the phosphitylation reaction (Fig. 6.1), TMDP reacts with the free OH groups in the pyrolysis oil, and yields to derivatized compound and hydrochloric acid (HCl). Since HCl may cause to decomposition of derivatized compound, pyridine is used in the solvent system as the based to capture HCl. The reasons of using deuterated chloroform (CDCl$_3$) in the solvent system are (i) to dissolve derivatized sample, (ii) to inhibit precipitation of pyridine-HCl salt, and (iii) to get a deuterium signal for NMR experiment (Pu et al. 2011).
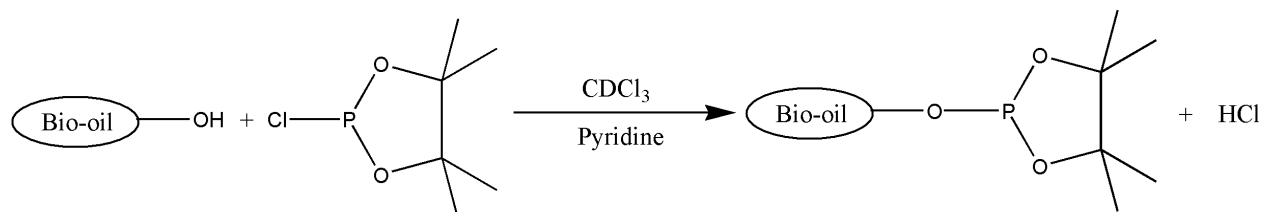
Fig. 6.1. Phosphitylation of free OH group with TMDP in the solvent system of CDCl$_3$/Pyridine.

Phosphitylation of pyrolysis oil was performed as follows: Stock solution was prepared by dissolving 40 mg N-Hydroxy-5-norbornene-2,3-dicarboximide (NHND) as the internal standard, and 40 mg chromium (III) acetylacetonate as the relaxation reagent in a solvent system of pyridine and chloroform (1.6/1, v/v). Approximately 20 ± 2.5 mg of bio-oil was completely dissolved in 500 μL of stock solution at room temperature, and then 150 μL TMDP (derivatization agent) was added to sample vials and vortexed for 2 min. After phosphitylation, the mixture was transferred to an NMR tube for analysis. Peaks were integrated relative to the NHND peak in order to quantitatively calculate the OHN. ^{31}P NMR spectra were acquired with a

Bruker Avance II 250 MHz spectrometer using inverse gated decoupling pulse sequence, 90°

pulse angle, 25 s pulse delay and 128 scans as per the methods of Ben and Ragauskas (Ben and

Ragauskas 2011).

6.2.4. Preparation of Pyrolysis Oil-based Epoxy Resin (POBER)

EPON828 (average molecular weight of ~377g/mole, epoxide equivalent of 185-192

g/eq) was used as the epoxy resin (ER) in this study. Pyrolysis oil was mixed with epoxy resin

until homogenized at ratios of 1:3 to 1:8 (PO:ER, w/w) at one part increments.

Triphenylphosphine (TPP), 0.5% TPP based on EPON828 weight, was added to the mixture to

catalyze the reaction. To aid in the homogenization of the components during mixing,

tetrahydrofuran (THF) was used as the solvent. After blending PO and ER, the mixture was

poured into an aluminum weighing dish (10 cm), and then cured using a temperature ramp of 1h

at 80 °C, 2h at 150 °C, 2h at 200 °C and allowed to cool slowly to 25 °C within the oven as

suggested by Wei et al (2014).

6.2.5. ATR-FT-IR

Attenuated total reflection Fourier Transform Infrared (ATR-FT-IR) spectra of the

pyrolysis oil, epoxy resin (EPON828) and the POBER resin were acquired between 4000 and

650 cm^{-1} with an ATR-FT-IR spectrometer (Model Spectrum400, Perkin Elmer Co., Waltham,

MA) with 4.00 cm-1 resolution and 32 scans to determine the functional groups. All ATR-FT-IR

spectra were collected at room temperature (22 ± 1 °C).

6.2.6. Thermo-mechanical Analysis of POBER Resin

Dynamic mechanical analysis was conducted on a TA Instruments RSAIII Dynamic Mechanical Analyzer (DMA) using samples approximately 26 x 8 x 2 mm according to the method described by Auad et al. (2006). A three-point bending configuration at 1% strain and an oscillating frequency of 1 Hz was utilized. Runs were conducted between 35 and 200 °C with a temperature ramp of 10 °C/min. The number of active chain segments in the network per unit volume (*n*), which is also called crosslink density, was calculated using physical data acquired through DMA analysis according to the following equation:

$$E' = 3nRT$$
(Eqn. 1)

where, *E'* is the storage modulus at rubbery region (Pa) at rubbery plateau region; *n* is the number of active chains (mol/m^3), which is proportional to the crosslinking density of the crosslinked network; *R* is the gas constant (8.31 Pa.m^3/mol.K); *T* is the temperature at rubbery region (K) (Sperling 2005).

6.2.7. Solubility of POBER Resin

POBER resin was grounded to 40 mesh by Wiley Mini Mill (Thomas Scientific, model no: 3383-L10, Swedesboro, NJ.) for acetone extraction. The soxhlet extractor was obtained from Ace Glass Incorporated (Vineland, NJ.). An extraction thimble filled with an appropriate amount of grounded POBER resin was placed into the soxhlet system, and then the extraction flask was filled with 150 mL acetone. The soxhlet system was heated up and allowed to reflux for 4 hours. After extraction, acetone was evaporated and the solid residue was dried in an oven for 1 hour at 105 °C. The weight loss (wt.%) was then calculated by deduction of weight of residue from the weight of starting grounded POBER resin.
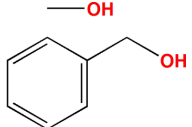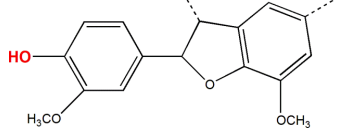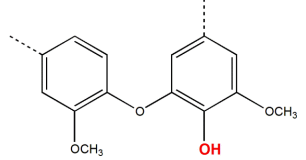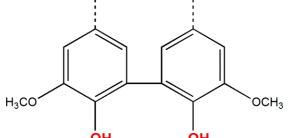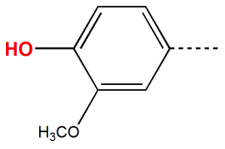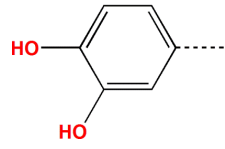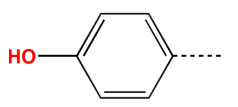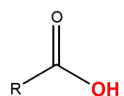
6.3. Results and Discussion

6.3.1. ^{31}P NMR Analysis of Pyrolysis Oil

^{31}P-NMR provides a great deal of information to determine the content and origin of OH groups present in pyrolysis oil. In this technique, OH groups belonging to aliphatic, phenolic and carboxylic units are phosphitylated by TMDP. Quantitative ^{31}P-NMR analysis have been extensively employed by many researchers to characterize the OH groups in lignin (Pu et al. 2011), pyrolysis oil (Ben and Ragauskas 2011), bio-diesel (Nagy et al. 2010), hydrothermal liquefaction oil of algae (Patel and Hellgardt 2013), and bio-oil produced by organic solvent liquefaction (hereafter referred to as liquefaction oil) of biomass (Celikbag et al. 2014). However, no research works could be found in which the OH groups were partitioned into aliphatic, phenolic and acidic categories prior to epoxy reaction. Such understanding is important if we are to overcome the variability and complexity of bio-oil which can complicate and vary the reaction with epoxy.

The hydroxyl number (OHN) of pure ethylene glycol (EG) was also calculated by ^{31}P-NMR in order to confirm the accuracy of the method. OHN of EG was calculated to be 31.75 mmol/g which was quite close to the theoretical OHN value of EG, 32.23 mmol/g. Table 6.1 shows the OHN of pyrolysis oil calculated by quantitative ^{31}P-NMR analysis, the integration region and an example of the chemical structures for each classification. Total OHN of pyrolysis oil was calculated to be 10.83±1.08 mmol/g. High OHN (5.35 – 10.70 mmol/g) is required for a bio-oil to be considered as a high quality bio-based polyol (Zou et al. 2012). Therefore, the pyrolysis oil produced in this study is a good candidate to be used as a bio-based polyol.

Table 6.1. Hydroxyl number (OHN) of the pyrolysis oil determined by quantitative ^{31}P-NMR after derivatization with TMDP.

Type of OH			Example of Chemical Structure	OHN[a] (mmol/g)	Integration Region[b] (ppm)
Aliphatic OH				5.33 ± 0.28	150.0 - 145.5
Phenolic OH	C5 substituded Condensed phenolic OH	β-5		0.04 ± 0.01	144.7 - 142.8
		4-O-5		0.18 ± 0.01	142.8 - 141.7
		5-5		1.28 ± 0.14	141.7 - 140.2
	Guaiacyl phenolic OH			0.44 ± 0.12	140.2 - 139.0
	Catechol type OH			0.76 ± 0.48	139.0 - 138.2
	p-hydroxy-phenyl OH			0.33 ± 0.26	138.2 - 137.3
Acidic OH				2.48 ± 0.31	136.6 - 133.6
Total OHN (mmol/g)				**10.83 ± 1.08**	

[a] OHN values were calculated by integrating of peaks relative to NHND peak. Values are means of three independent replicates, and numbers after ± are the standard deviation.
[b] Integration regions were identified according to ^{31}P-NMR chemical shifts reported by Ben and Ragauskas (2011).

117

It was also found that aliphatic, phenolic and acidic hydroxyl groups accounted for 49%, 28% and 23% of the total OHN, respectively. Aliphatic type of OHs was most likely due to the degradation of cellulose, hemicellulose and lignin (David et al. 2010) while monomeric phenols, guaiacyl, p-hydroxyphenyl and catechol type of OH groups in pyrolysis oil can be attributable to the cleavage of ether bonds in lignin during pyrolysis (Fu et al. 2008, Qu et al. 2011). Phenolic OH groups are important in the synthesis of bio-oil based polymers because aromatic groups provide strength to the resulting polymer system (Hofmann and Glasser 1993). It was previously reported that acids and furfurals were the major component found in the pyrolysis oil of xylan (Qu et al. 2011); thus, it could be conjectured that hemicellulose made more contribution to concentration of acidic OH than cellulose and lignin in the pyrolysis oil produced in our study.

6.3.2. ATR-FT-IR

The IR spectra of POBER (mixing ratio of 1:8), commercial unmodified epoxy resin (EPON828) and pyrolysis oil (PO) are shown in Fig. 6.2, and band assignments are summarized in Table 6.2. The peak at around 3400 cm^{-1} was due to the presence of OH groups, indicating that pyrolysis oil had a significant amount of OH groups, as confirmed by ^{31}P-NMR analysis. The peak at around 1750 cm^{-1} was due to the carbonyl (C=O) groups in the pyrolysis oil which are generated by the decomposition of cellulose and hemicellulose during pyrolysis (Branca et al. 2003). Aromatic components in the pyrolysis oil, which have been previously proved by GC-MS analysis by other researchers (Branca et al. 2003, Thangalazhy-Gopakumar et al. 2010) resulted in the peaks at 1000 – 1150, 1214 – 1233, 1600 and 1500 cm^{-1}. And finally the peak at 910 cm^{-1} is the characteristic peak of epoxide ring.
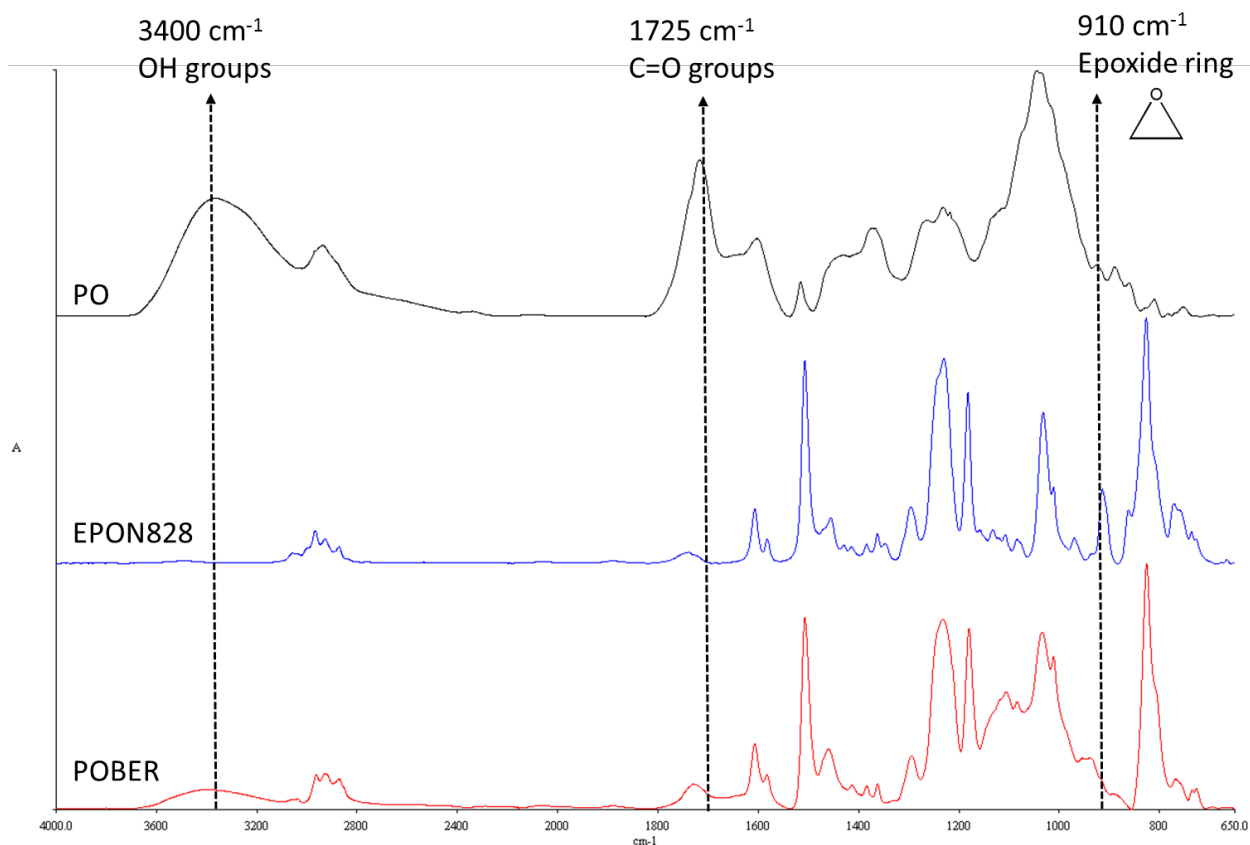
Fig. 6.2. FT-IR spectrum of POBER (mixing ratio of 1:8), EPON828 (commercial unmodified epoxy resin) and pyrolysis oil.

FTIR analysis of the individual components and cured epoxy resin illustrate the completeness of the reaction. As illustrated in Figure 1, pyrolysis oil contains a significant number of hydroxyl groups as indicated by a peak at 3400 cm^{-1}. However, POBER resin exhibited a weak hydroxyl peak at 3400 cm-1. The peak area at 3400 cm^{-1} of the pyrolysis oil and POBER resin was calculated to be 26.0458 and 4.5802 A cm^{-1}, respectively, which clearly indicates that OH groups in the pyrolysis oil was consumed during the curing. On the other hand, the epoxide groups within the EPON828 are indicated by the sharp peak at the 910 cm^{-1}. Following the reaction, both of these groups are nearly completely removed within the cured epoxy spectra. This analysis indicates that the EPON828 and pyrolysis oil provided a complete

119

reaction, consuming these components and thus removing their signatures within the spectra. Another change in the IR spectra was observed at the carbonyl peak (1725 cm^{-1}). As the pyrolysis oil was consumed by EPON828, the peak at 1725 cm^{-1} was not observed in the POBER resin suggesting that carbonyl groups within the pyrolysis oil contributed the curing of EPON828 resin along with the hydroxyl groups.

Table 6.2. Characteristic FT-IR band assignment of **POBER** (mixing ratio of 1:8), **ER** (commercial unmodified epoxy resin, EPON828) and **PO** (pyrolysis oil)

Wavenumber (cm^{-1})	Band Assignment	Sample
3400	O-H stretching vibration	PO
3000 - 3040	Aromatic ring C-H stretching	PO + ER
1725	C=O stretch in unconjugated ketones, carbonyl and ester groups	PO
1600, 1500	C-C stretch (in-ring)	PO + ER + POBER
1214 - 1233	C-C, C-O and C=O stretching	PO + ER + POBER
1000 - 1150	Deformation vibration of C-H bonds in benzene rings	PO + POBER
1050	=C-H bend	ER
910	Epoxide ring	ER

6.3.3. Thermo-mechanical Analysis of POBER Resin

The viscoelastic behavior of POBER resin at different mixing ratios was analyzed by dynamic mechanical analysis (DMA), and the storage modulus and tan δ versus temperature is shown in Fig. 6.3. As shown in Table 6.3, the storage modulus (E') at 30 °C and 160 °C were found to be in the range of 1.03 – 2.85 GPa and 0.006 – 0.018 GPa, respectively, which is in agreement with Qin et al. (2013) and Hu et al. (2014) where epoxy resin was cured with lignin and furan based curing reagents.
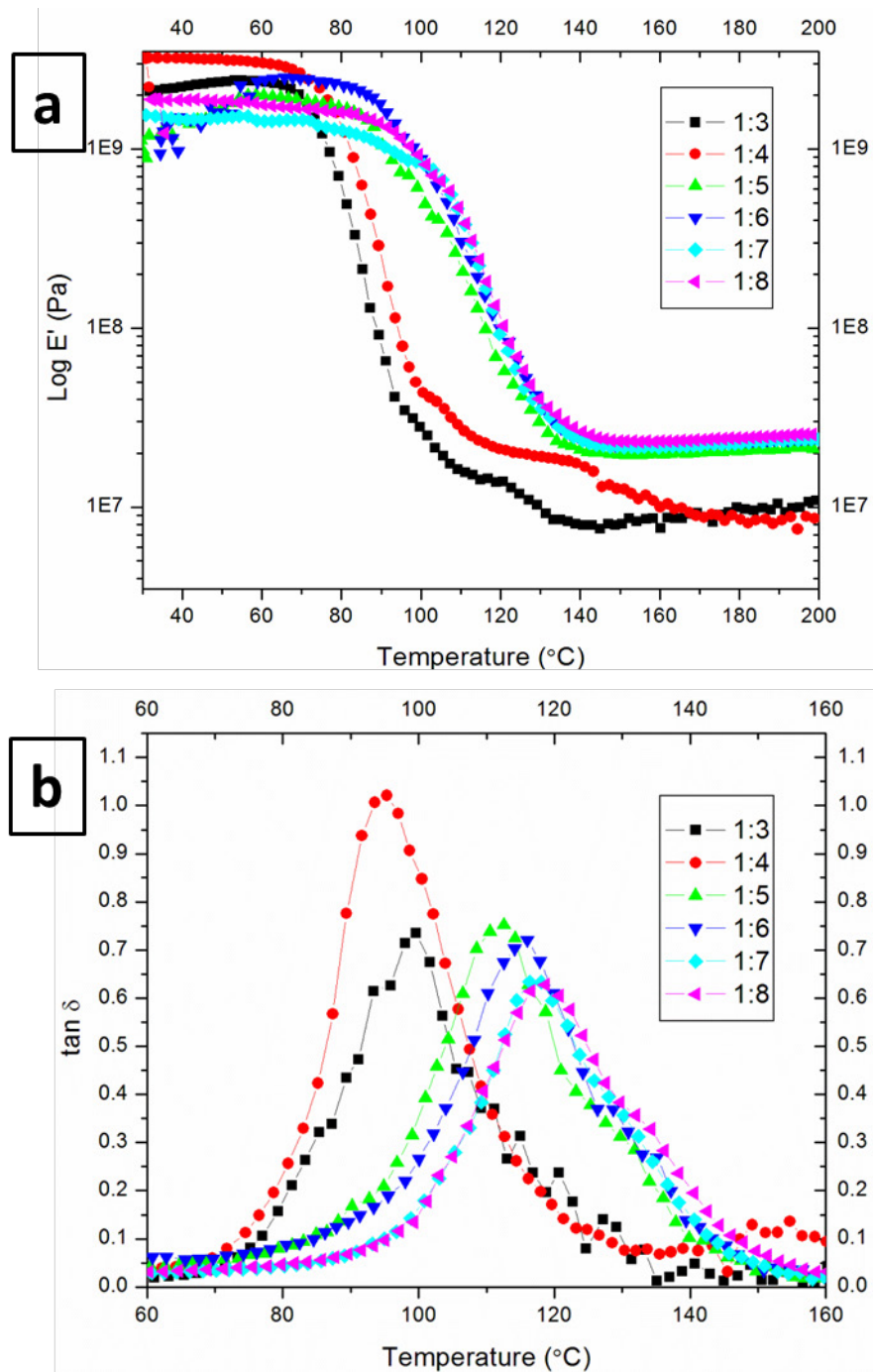
Fig. 6.3. Storage modulus **(a)** and tan δ **(b)** versus temperature for the PO:ER resin at different

mixing ratios.

Glass transition temperature (Tg) is determined by the temperature at maximum tan δ

(Fig. 6.3b) which is measured as the angle between the in-phase and out-of-phase components of

the cyclic motion during DMA analysis (Sperling 2005). Tg of the POBER resin was found to be in the range of 96.5 – 120.1 °C depending on the mixing ratio (Table III) which is comparable to traditional EPON828 resin cured with different curing agents, for instance, 134 °C when cured with diethylenetriamine (Hu et al. 2014), 111 °C with triethylene tetramine (Xie and Chen 2005), 93 °C with aliphatic triamine (Hu et al. 2014). This is a promising finding because pyrolysis oil could be utilized to improve the Tg of epoxy resin without using any petroleum-based curing agent.

The Tg of the POBER resin is also found to be relatively higher as compared to other biooil-based epoxy studies. For example, Wei et al. (2014) modified epoxy resin with a liquefaction oil of switchgrass with diethylene glycol, and the Tg was in the range of 35 – 65 °C. In another study, epoxy resin was synthesized using commercial epoxy resin and the liquefaction oil of Japanese cedar with PEG400/glycerol solvent mixture, and the Tg of the resulting epoxy system was in the range of -40 – 50 °C (Kobayashi et al. 2001). Unlike pyrolysis oil, there is significant amount of unreacted liquefying solvent (24 – 75 % of the bio-oil weight depending on the liquefaction conditions) retained in the liquefaction oil (Celikbag et al. 2014) which acts like a plasticizer when liquefaction oil is used to modify the epoxy resin (Wei et al. 2014). Therefore, unreacted liquefying solvent left in the liquefaction oil is attributed to the low Tg in these studies cited above. Pyrolysis oil, on the other hand, is a solvent free product of pyrolysis process of biomass; thus, a higher Tg can be achieved with pyrolysis oil in epoxy resin systems.

The Tg of the POBER resin synthesized in this study is higher than the lignin-based epoxy systems which could be defined as the epoxy systems that are either cured or modified

with lignin. Lignin has received increased attention for epoxy systems because of its natural aromatic structure and phenolic hydroxyls. Qin et al. (2013) studied the curing behavior of epoxy resin with partially depolymerized lignin, and they reported Tg to be 62.3 – 78.5 °C. In another study, alkaline solution of industrial kraft lignin was utilized to cure two commercial epoxy resins, polyethylene glycol diglycidyl ether (PEGDE) and diglycidyl ether of bisphenol A (DGEBA), and the Tg of the resulting epoxy resins were 30 – 110 °C depending on the resin type used (Nonaka et al. 1997). Delmas et al. (2013) blended PEGDGE epoxy resin with wheat straw Biolignin^{TM} at different ratios, and found the Tg to be 70 °C. Most recently, Mannich-functionlized lignin was incorporated into DGEBA resin to create epoxy composite where authors reported that Mannich-functionlized lignin acted as a plasticizer and decreased the Tg of the epoxy resin (Mendis et al. 2015). Another reason for low Tg of lignin-based epoxy systems might be the unreacted lignin components which cause less oriented crosslinked structures (Pan 2011). One of the main differences between solid lignin powder and pyrolysis oil is the difference in concentration of OH groups which is an important parameter for the curing of epoxies. It is conjectured OH groups in the pyrolysis oil react with the betaine which is the product of ring opening reaction of epoxide in the presence of TPP by nucleophilic attack (Yang February, 1998) (Fig. 6.4a), and then three dimensional crosslinked epoxy matrix is created (Yang February, 1998) (Fig. 6.4b). It should be taken into account that carbonyl groups in the pyrolysis oil contributed to the curing of EPON828 as discussed in the FTIR analysis. In the Figure 3, however, the curing mechanism between epoxy and hydroxyl groups was illustrated in order to simplify the reaction. Pyrolysis oil of previous lignin based feedstock has higher OH numbers than lignin itself because of the cleavage of ether and ester bonds during the pyrolysis process (Fu et al. 2008, Ben and Ragauskas 2011). Therefore, there are more likely less

123

unreacted components in the pyrolysis oil than lignin indicating that more components were incorporated into the epoxy matrix during crosslinking. Thus, the higher Tg in this study, as compared to lignin-based epoxy resins, could be attributable to the higher OH number of pyrolysis oil.
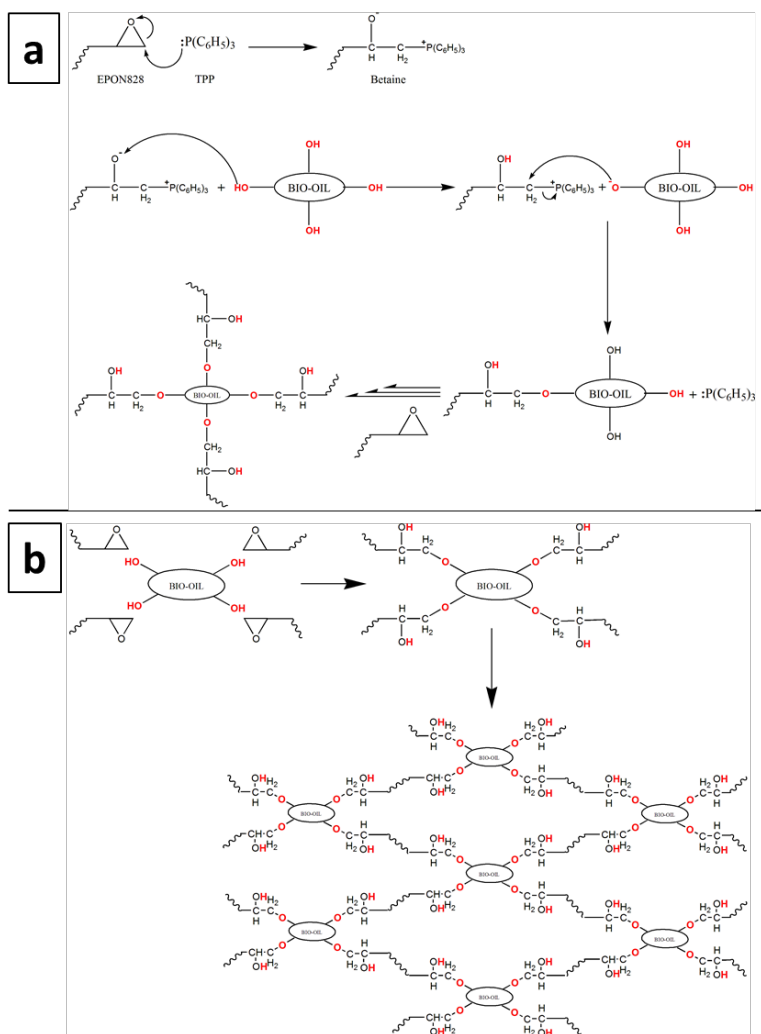
Fig. 6.4. Proposed reaction mechanism between OH groups of pyrolysis oil and epoxide groups of EPON828 in the presence of TPP **(a)**, and the generation of 3-D crosslinked structure **(b).**

Table 6.3. Glass transition temperature (Tg), crosslinking density (*n*), and storage modulus (E')
at 30 °C and 160 °C.[a]

Sample	Tg (°C)	n (mol/m³)	E' (GPa) at 30 °C	E' (GPa) at 160 °C
1:3	96.5 ± 4.4	583 ± 171	2.34 ± 0.46	0.006 ± 0.002
1:4	97.2 ± 2.6	992 ± 90	2.85 ± 0.51	0.011 ± 0.001
1:5	109.2 ± 2.7	1127 ± 110	1.07 ± 0.07	0.015 ± 0.005
1:6	114.7 ± 4.0	1436 ± 135	1.03 ± 0.06	0.015 ± 0.006
1:7	113.6 ± 2.9	1651 ± 46	1.24 ± 0.43	0.016 ± 0.007
1:8	120.1 ± 2.0	1891 ± 125	2.55 ± 0.12	0.018 ± 0.006

[a] Values are mean of repeated analysis and numbers after ± are standard deviation.

Table 6.3 shows how the Tg and crosslinking density increases as the amount of

EPON828 resin is increased. The crosslinking density is defined as the number of active

segments per unit volume (Sperling 2005). As the crosslinking density increased, the chain

mobility was restrained; therefore, an increase in the Tg and the storage modulus at the rubbery

plateau were observed as the crosslinking density increased. The crosslink density was found to

fall in the range of 583 – 1891 mol/m³ depending on the mixing ratio of pyrolysis oil to

EPON828. It was found that the crosslinking density increased in a linear fashion ($R^2 = 0.88$) as

the amount of EPON828 was increased. A similar trend was also observed by Wu and Lee

(2011) where the cure temperature of the epoxy resin increased as more liquefaction oil of

Japanese cedar was introduced into system. Hirose et al. (2003) witnessed an increase in Tg with

increased lignin concentration, contributing this to a disruption in the in the polymer network,

thereby stiffening the matrix. The authors reacted alcoholysis lignin with ethylene glycol and

further reacted the components with dimethylbenzlamine, a crosslinking agent, to form ester

epoxy resins. Additionally, one underlying assumption in this study was that pyrolysis oil

probably resulted in low molecular weight polymers which can probably help to explain the high

reactivity of the epoxy resin to such low levels of bio-oil (1:8). This theory agrees with El-

Mansouri et al. (2011) who found a decreased molecular weight opens up more hydroxyl groups

available for consumption during the cure of bio-based epoxy resins. In order to evaluate the reaction within this system, experiments were conducted using EPON828 and TPP without the addition of pyrolysis oil and a reaction was not achieved, indicating that pyrolysis oil acts as a cross-linking agent within the system.

6.3.4. Solvent Resistance of POBER Resin

Fig. 6.5 illustrates the mass loss of POBER resin synthesized at different PO:ER ratios. To determine the solubility of the POBER resin and determine the minimum epoxide content for stability of the final product, an acetone extraction was conducted. Acetone is an effective solvent for pyrolysis oil and therefore removes unreacted pyrolysis oil from the polymer matrix (Mohan et al. 2006). A decrease in mass loss from 57.74% to 0.49% was observed as the content of EPON828 was increased which indicates that the polymer became more completely reacted, resulting in a less soluble product. Nonaka et al. (1997) supported this observation, where lignin was reacted with epoxide to form a three-dimensional cross-linked network, and a decrease in mass loss was reported as more lignin was incorporated to the epoxy resin. Auad et al. (2007) reacted EPON826 with synthetic phenol at near-stoichiometric ratio, and they observed that no mass loss under acetone extraction occurred at complete crosslinking. In our study, the progressive increase in insolubility, as well as the crosslinking density (Table III), indicates that the stoichiometric ratio was approaching equilibrium and was met at approximately 1:7 to 1:8 PO:ER ratio. At this point, a three-dimensional network (highly crosslinked network) dominated the composite's structure.
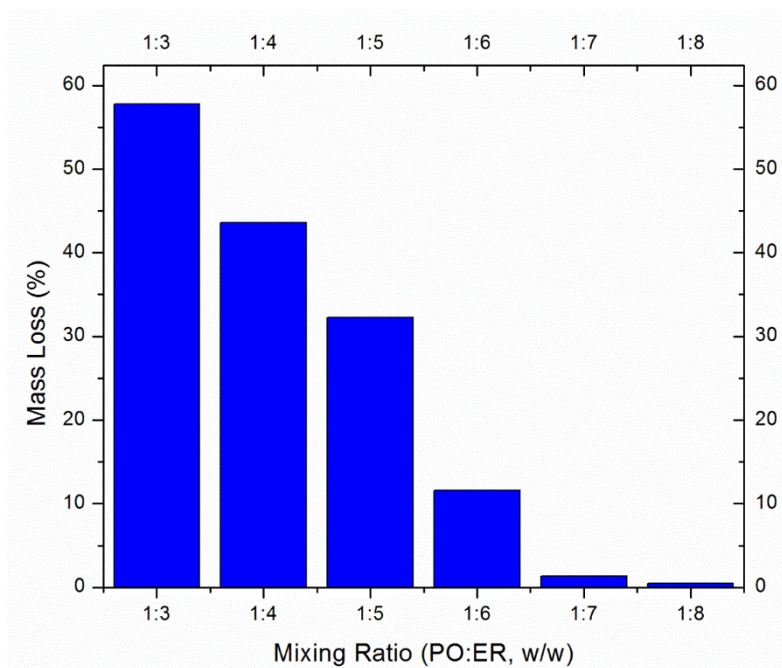
Fig. 6.5. Mass loss (wt%) of POBER resin synthesized at different mixing ratios extracted under acetone for 4 hours.

6.4. Conclusion

Pyrolysis oil-based epoxy resin (POBER) was synthesized by mixing pyrolysis oil with commercial epoxy resin (EPON828) at different mixing ratios of 1:3 – 1:8 (PO:ER, w/w) to investigate the compatibility of pyrolysis oil of loblolly pine as a substitute for phenolic component of epoxy resins. Total hydroxyl number (OHN) of pyrolysis oil was calculated to be 10.83 mmol/g by 31P-NMR analysis. It was also calculated that pyrolysis oil has enough number of aliphatic and phenolic OH numbers 5.33 and 2.87 mmol/g, respectively, which makes it a suitable alternative phenol resource to petroleum-based phenols. FT-IR analysis of pyrolysis oil, EPON828 resin and POBER resin supported that hydroxyl and carbonyl groups in the pyrolysis oil opened up the epoxide rings of EPON828 during curing. DMA analysis of POBER resin suggested that resins synthesized at 1:7 and 1:8 mixing ratios had the highest glass transition

temperatures and crosslinking densities, 113 – 120 °C and 1651 - 1891 mol/m3, respectively. Moreover, acetone extraction supported the superior crosslinked structure at 1:7 and 1:8 mixing ratios since around 0.5% mass loss was observed at those mixing ratios. Overall, the system developed herein has the potential to utilize a naturally derived cross-linking agent.

Acknowledgment

References

1. Amen-Chen, C., H. Pakdel, and C. Roy. 2001. Production of monomeric phenols by thermochemical conversion of biomass: a review. Bioresource Technology **79**:277-299.

2. Auad, M. L., S. R. Nutt, P. M. Stefani, and M. I. Aranguren. 2006. Rheological study of the curing kinetics of epoxy–phenol novolac resin. Journal of Applied Polymer Science **102**:4430-4439.

3. Auad, M. L., L. H. Zhao, H. B. Shen, S. R. Nutt, and U. Sorathia. 2007. Flammability properties and mechanical performance of epoxy modified phenolic foams. Journal of Applied Polymer Science **104**:1399-1407.

4. Auvergne, R., S. Caillol, G. David, B. Boutevin, and J. P. Pascault. 2014. Biobased Thermosetting Epoxy: Present and Future. Chemical Reviews **114**:1082-1115.

5. Ben, H. X. and A. J. Ragauskas. 2011. NMR Characterization of Pyrolysis Oils from Kraft Lignin. Energy & Fuels **25**:2322-2332.

6. Branca, C., P. Giudicianni, and C. Di Blasi. 2003. GC/MS characterization of liquids generated from low-temperature pyrolysis of wood. Industrial & Engineering Chemistry Research **42**:3190-3202.

7. Celikbag, Y., B. K. Via, S. Adhikari, and Y. Wu. 2014. Effect of liquefaction temperature on hydroxyl groups of bio-oil from loblolly pine (Pinus taeda). Bioresource Technology **169**:808-811.

8. Czernik, S. and A. V. Bridgwater. 2004. Overview of applications of biomass fast pyrolysis oil. Energy & Fuels **18**:590-598.

9. David, K., M. Kosa, A. Williams, R. Mayor, M. Realff, J. Muzzy, and A. Ragauskas. 2010. 31P-NMR analysis of bio-oils obtained from the pyrolysis of biomass. Biofuels **1**:839-845.

10. Delmas, G.-H., B. Benjelloun-Mlayah, Y. L. Bigot, and M. Delmas. 2013. Biolignin™ based epoxy resins. Journal of Applied Polymer Science **127**:1863-1872.

11. Dietrich, J. 2012. US spot epoxy prices increase 3.3% on overseas demand.

12. Effendi, A., H. Gerhauser, and A. V. Bridgwater. 2008. Production of renewable phenolic resins by thermochemical conversion of biomass: A review. Renewable and Sustainable Energy Reviews **12**:2092-2116.

13. El Mansouri, N. E., Q. L. Yuan, and F. R. Huang. 2011. Synthesis and Characterization of Kraft Lignin-Based Epoxy Resins. Bioresources **6**:2492-2503.

14. Engelmann, G. and J. Ganster. 2014. Bio-based epoxy resins with low molecular weight kraft lignin and pyrogallol. Page 435 Holzforschung.

15. Fele Žilnik, L. and A. Jazbinšek. 2012. Recovery of renewable phenolic fraction from pyrolysis oil. Separation and Purification Technology **86**:157-170.

16. Ferdosian, F., Z. S. Yuan, M. Anderson, and C. Xu. 2014. Synthesis of lignin-based epoxy resins: optimization of reaction parameters using response surface methodology. Rsc Advances **4**:31745-31753.

17. Fu, D., S. Farag, J. Chaouki, and P. G. Jessop. 2014. Extraction of phenols from lignin microwave-pyrolysis oil using a switchable hydrophilicity solvent. Bioresource Technology **154**:101-108.

18. Fu, Q., D. S. Argyropoulos, D. C. Tilotta, and L. A. Lucia. 2008. Understanding the pyrolysis of CCA-treated wood: Part I. Effect of metal ions. Journal of Analytical and Applied Pyrolysis **81**:60-64.

19. Hirose, S., T. Hatakeyama, and H. Hatakeyama. 2003. Synthesis and thermal properties of epoxy resins from ester-carboxylic acid derivative of alcoholysis lignin. Macromolecular Symposia **197**:157-170.

20. Hofmann, K. and W. G. Glasser. 1993. Engineering Plastics from Lignin. 21.1Synthesis and Properties of Epoxidized Lignin-Poly (Propylene Oxide) Copolymers. Journal of Wood Chemistry and Technology **13**:73-95.

21. Hu, F., J. J. La Scala, J. M. Sadler, and G. R. Palmese. 2014. Synthesis and Characterization of Thermosetting Furan-Based Epoxy Systems. Macromolecules **47**:3332-3342.

22. Islam, M. R., M. D. H. Beg, and S. S. Jamari. 2014. Development of vegetable-oil-based polymers. Journal of Applied Polymer Science **131**. DOI: 10.1002/app.40787.

23. Ismail, T. N. M. T., H. A. Hassan, S. Hirose, Y. Taguchi, T. Hatakeyama, and H. Hatakeyama. 2010. Synthesis and thermal properties of ester-type crosslinked epoxy resins derived from lignosulfonate and glycerol. Polymer International **59**:181-186.

24. Kishi, H., Y. Akamatsu, M. Noguchi, A. Fujita, S. Matsuda, and H. Nishida. 2011. Synthesis of Epoxy Resins from Alcohol-Liquefied Wood and the Mechanical Properties of the Cured Resins. Journal of Applied Polymer Science **120**:745-751.

25. Kobayashi, M., Y. Hatano, and B. Tomita. 2001. Viscoelastic properties of liquefied wood/epoxy resin and its bond strength. Holzforschung **55**:667-671.

26. Koike, T. 2012. Progress in development of epoxy resin systems based on wood biomass in Japan. Polymer Engineering & Science **52**:701-717.

27. Kuo, P. Y., M. Sain, and N. Yan. 2014. Synthesis and characterization of an extractive-based bio-epoxy resin from beetle infested Pinus contorta bark. Green Chemistry **16**:3483-3493.

28. Laurichesse, S., C. Huillet, and L. Averous. 2014. Original polyols based on organosolv lignin and fatty acids: new bio-based building blocks for segmented polyurethane synthesis. Green Chemistry **16**:3958-3970.

29. Liu, Y. L. 2001. Flame-retardant epoxy resins from novel phosphorus-containing novolac. Polymer **42**:3445-3454.

30. Luo, Z., S. Wang, Y. Liao, J. Zhou, Y. Gu, and K. Cen. 2004. Research on biomass fast pyrolysis for liquid fuel. Biomass and Bioenergy **26**:455-462.

31. Manfredi, L. B., M. J. L. Ginés, G. J. Benítez, W. A. Egli, H. Rissone, and A. Vázquez. 2005. Use of epoxy–phenolic lacquers in food can coatings: Characterization of lacquers and cured films. Journal of Applied Polymer Science **95**:1448-1458.

32. Mendis, G. P., I. Hua, J. P. Youngblood, and J. A. Howarter. 2015. Enhanced dispersion of lignin in epoxy composites through hydration and mannich functionalization. Journal of Applied Polymer Science **132**: DOI: 10.1002/app.41263.

33. Mohan, D., C. U. Pittman, and P. H. Steele. 2006. Pyrolysis of wood/biomass for bio-oil: A critical review. Energy & Fuels **20**:848-889.

34. Nagy, M., M. Foston, and A. J. Ragauskas. 2010. Rapid Quantitative Analytical Tool for Characterizing the Preparation of Biodiesel. Journal of Physical Chemistry A **114**:3883-3887.

35. Naik, S. N., V. V. Goud, P. K. Rout, and A. K. Dalai. 2010. Production of first and second generation biofuels: A comprehensive review. Renewable & Sustainable Energy Reviews **14**:578-597.

36. Nonaka, Y., B. Tomita, and Y. Hatano. 1997. Synthesis of lignin/epoxy resins in aqueous systems and their properties. Holzforschung **51**:183-187.

37. Pan, H. 2011. Synthesis of polymers from organic solvent liquefied biomass: A review. Renewable & Sustainable Energy Reviews **15**:3454-3463.

38. Patel, B. and K. Hellgardt. 2013. Hydrothermal upgrading of algae paste: Application of 31P-NMR. Environmental Progress & Sustainable Energy **32**:1002-1012.

39. Perlack, R. D., L. L. Wright, A. F. Turhollow, R. L. Graham, B. J. Stokes, and D. C. Erbach. 2005. Biomass as feedstock for a bioenergy and bioproducts industry: the technical feasibility of a billion-ton annual supply. DTIC Document.

40. Pizzi, A. 2006. Recent developments in eco-efficient bio-based adhesives for wood bonding: opportunities and issues. Journal of Adhesion Science and Technology **20**:829-846.

41. Pu, Y. Q., S. L. Cao, and A. J. Ragauskas. 2011. Application of quantitative P-31 NMR in biomass lignin and biofuel precursors characterization. Energy & Environmental Science **4**:3154-3166.

42. Qin, J., M. Woloctt, and J. Zhang. 2013. Use of Polycarboxylic Acid Derived from Partially Depolymerized Lignin As a Curing Agent for Epoxy Application. Acs Sustainable Chemistry & Engineering **2**:188-193.

43. Qu, T., W. Guo, L. Shen, J. Xiao, and K. Zhao. 2011. Experimental Study of Biomass Pyrolysis Based on Three Major Components: Hemicellulose, Cellulose, and Lignin. Industrial & Engineering Chemistry Research **50**:10424-10433.

44. Raquez, J. M., M. Deléglise, M. F. Lacrampe, and P. Krawczak. 2010. Thermosetting (bio)materials derived from renewable resources: A critical review. Progress in Polymer Science **35**:487-509.

45. Sperling, L. H. 2005. Introduction to Physical Polymer Science. Wiley.

46. Sunitha, K., D. Mathew, and C. P. Reghunadhan Nair. 2015. Phenolic-epoxy matrix curable by click chemistry—synthesis, curing, and syntactic foam composite properties. Journal of Applied Polymer Science **132**: DOI: 10.1002/app.41254.

47. Thangalazhy-Gopakumar, S., S. Adhikari, H. Ravindran, R. B. Gupta, O. Fasina, M. Tu, and S. D. Fernando. 2010. Physiochemical properties of bio-oil produced at various temperatures from pine wood using an auger reactor. Bioresource Technology **101**:8389-8395.

48. Tiimob, B. J., V. K. Rangari, and S. Jeelani. 2014. Effect of reinforcement of sustainable β-CaSiO3 nanoparticles in bio-based epoxy resin system. Journal of Applied Polymer Science **131**:n/a-n/a.

49. Wei, N., B. K. Via, Y. F. Wang, T. McDonald, and M. L. Auad. 2014. Liquefaction and substitution of switchgrass (Panicum virgatum) based bio-oil into epoxy resins. Industrial Crops and Products **57**:116-123.

50. Wu, C.-C. and W.-J. Lee. 2011. Curing behavior and adhesion properties of epoxy resin blended with polyhydric alcohol-liquefied Cryptomeria japonica wood. Wood Science and Technology **45**:559-571.

51. Wu, C. C. and W. J. Lee. 2010. Synthesis and Properties of Copolymer Epoxy Resins Prepared from Copolymerization of Bisphenol A, Epichlorohydrin, and Liquefied Dendrocalamus latiflorus. Journal of Applied Polymer Science **116**:2065-2073.

52. Xie, T. and F. Chen. 2005. Fast liquefaction of bagasse in ethylene carbonate and preparation of epoxy resin from the liquefied product. Journal of Applied Polymer Science **98**:1961-1968.

53. Yang, J. February, 1998. Part I: Synthesis of aromatic polyketones via soluble precursors derived from bis(A-amininitrile)s; Part II: Modifications of epoxy resins with functional

hyperbranched poly(arylene ester). Virginia Polytechnic Institute and State University, Blacksburg, Virginia.

54. Zou, X. W., T. F. Qin, Y. Wang, L. H. Huang, Y. M. Han, and Y. Li. 2012. Synthesis and properties of polyurethane foams prepared from heavy oil modified by polyols with 4,4 '-methylene-diphenylene isocyanate (MDI). Bioresource Technology **114**:654-657.

Chapter 7

Synthesis and Characterization of Bio-oil-based Self-curing Epoxy Resin

Abstract

The purpose of this study was to investigate the utilization of hydrothermal liquefaction (HTL)-bio-oil as a biopolyol for the synthesis of bio-based epoxy resin. Furthermore, the effect of ethanol used as a cosolvent in the HTL process on the properties of resulting bio-oil-based epoxy resin (BOBER) was studied for the first time. Quantitative ^{31}P-NMR analysis of HTL-bio-oil showed that addition of ethanol in HTL process resulted in significant increase in the concentration of aliphatic type OH groups. It was found that not only the total hydroxyl (OH) number of HTL-bio-oil has an effect on the yield and epoxy equivalent weight of BOBER, but the distribution of OH groups within bio-oil (aliphatic, phenolic and acidic OH) also plays an important role for the determination of the optimum amount of catalyst to be used in the synthesis of BOBER. Differential Scanning Calorimetry (DSC) analysis proved the self-curing phenomena of BOBER. Fourier Transform Infrared Spectroscopy (FT-IR) and curing kinetics analysis suggested that etherification reaction was the dominating reaction behind the self-curing of BOBER. Glass transition temperature (Tg), crosslinking density (n), and the storage modulus (E') of self-cured BOBER were calculated to be 63.6 – 96 °C, 8.5 – 58.7 mol/m^3, and 425 – 845 MPa, respectively, using Dynamic Mechanical Analysis (DMA). The BOBER system developed

in this study provided promising results to replace HTL-bio-oil with the petroleum-based phenolic resource in the synthesis of epoxy resins.

7.1. Introduction

Epoxy resins (ERs) are one of the most important thermosets offering superior thermal and mechanical properties, adhesion and chemical resistance. Due to these unique properties, ERs are used for variety of applications such as in paintings and coatings, insulations materials, composites and constructions. The market size of the ER also demonstrates its importance: The North America the epoxy resin market amounted approximately USD 1.0 billion in 2015, and is predicted to be USD 1.4 billion by 2020 (Research 2016); the global epoxy production, on the other hand, is projected to be 3 million tons by 2017 with a market size of USD 21.5 billion (Auvergne et al. 2014).

There are different types of ERs on the market depending on the molecular weight, epoxy equivalent weight (EEW) and viscosity. The most widely used ER is the diglycidyl ether of bisphenol A (DGEBA) which accounts for approximately 75% of the ER in the market today (Pham and Marks 2000). DGEBA is derived from condensation reaction of bisphenol A (BPA) and epichlorohydrin (ECH) in the presence of sodium hydroxide (NaOH). DGEBA owes its thermal resistance, toughness and rigidity to the aromatic ring of BPA, good adhesion properties to the epoxide group of ECH and hydroxyl (OH) groups, and chemical resistance to the ether linkages (Pham and Marks 2000). However, the toxicity of BPA has raised questions and concerns regarding its use in epoxy resins. The U.S. Food and Drug Administration (FDA) and European Union (EU) have banned the use of BPA-based epoxy resins as coatings in infant

formula packaging in 2013 and 2011, respectively (EU 2011, FDA 2013). Therefore, there is an increasing effort to explore bio-based phenolic resources to be used in epoxy synthesis as an alternative to BPA. Moreover, the uncertainty in the price of petroleum as well as the social tendency toward materials from renewable and sustainable resources have also motivated researchers to focus on bio-based materials.

During the past decade, several promising results have been reported in the synthesis of bio-based epoxy resins using lignocellulosic biomass. Comprehensive reviews up to date can be found elsewhere (Raquez et al. 2010, Koike 2012, Auvergne et al. 2014, Baroncini et al. 2016). Lignin has attracted interest as a substiture for BPA (Sen et al. 2015) as well as a bio-based curing agent (Qin et al. 2013, Kai et al. 2016) in epoxy synthesis. Due to poor solubility and reactivity of lignin, it is either depolymerized (Ferdosian et al. 2014, Xin et al. 2016) or modified before epoxidation to enhance the reactivity. Methylation (El Mansouri et al. 2011), glyoxalation (El Mansouri et al. 2011) and alkoxylation (Hofmann and Glasser 1993) are the most common modification techniques which increase the hydroxyl groups of lignin. Although the mechanical and thermal properties of lignin-based ERs were comparable to petroleum-based ERs, high polydispersity index and complex chemical structure of lignin limit its utilization.

Vanillin, commercially produced from lignosulfonates, has also drawn some attentions to be used as an aromatic feedstock as a substitution for BPA (Harvey et al. 2015). Some vanillin derivatives (vanillic acid, methoxyhydroquinone and vanillyl alcohol) have been epoxidized and glycidyl ethers were synthesized without using any solvent (Fache et al. 2014, Fache et al. 2015). However, the low yield of vanillin from lignosulfonates (approximately 10%) (Auvergne et al.

136

2014), and high cost of the purification of vanillin restrain its utilization. Most recently, Fache et al. (2016) proposed purification step could be avoided by using some mixtures of phenolics obtained from G and GS lignin in the vanillin process which were further utilized in bio-based epoxy synthesis. A bio-based epoxy resin which requires less curing activation energy than petroleum-based epoxy has been synthesized using bark extractives (as an alternative to BPA) and ECH in 1,4-dioxane medium (Kuo et al. 2014), and the effect of the reaction parameters (time, temperature, solvent type and catalyst) on the yield and EEW has been studied (Kuo et al. 2016). Most recently, tannin has been used as a phenolic source to produce an epoxy-acrylic resin which was synthesized using acrylic acid (Jahanshahi et al. 2016).

Bio-oil is a term used in the literature for "liquefied biomass" produced by decomposition of lignocellulosic biomass through thermomechanical liquefaction processes, and it could be used as a biopolyol and alternative to BPA to synthesize bio-based epoxy resin due to its high hydroxyl number (OHN). There are mainly three liquefaction processes to obtain bio-oil: (i) organic solvent liquefaction (OSL) – the liquefaction of lignocellulosic biomass using organic solvents such as ethylene glycol at moderate temperature (Celikbag et al. 2014), (ii) fast pyrolysis (FP) – the liquefaction in the absence of oxygen and solvent at elevated temperatures (Thangalazhy-Gopakumar et al. 2010), and (iii) hydrothermal liquefaction (HTL) – the liquefaction using water at high temperature and pressure (Celikbag et al. 2016). It is very important to note that even if the liquid product from OSL, FP and HTL processes is defined as bio-oil, the properties of the bio-oils (OHN, molecular weight and chemical composition) are different from each other. Therefore, utilization of each bio-oil in epoxy synthesis results in an epoxy resin with different properties. OSL-bio-oil has been previously used as a polyol in epoxy

137

synthesis by some researchers (Kishi et al. 2006, Wu and Lee 2010, Kishi et al. 2011, Zhang et al. 2012). It was observed that the resulting epoxy resin suffered from poor mechanical and thermal properties. Since the alcoholic solvents used in the OSL process (such as ethylene glycol, polyethylene glycol and glycerol) have high boiling point, it was found that there was a significant amount of unreacted solvent left in the OSL-bio-oil (Celikbag et al. 2014). In addition, the poor thermal and mechanical properties of epoxy resin were attributed to the unreacted solvent in the OSL-bio-oil which acts as a plasticizer and decreases the thermal and mechanical properties (Wei et al. 2014). Unlike OSL-bio-oil, FP-bio-oil exhibit lower OHN due to the fact that no solvent is used in the FP process. Our research group has previously utilized the FP-bio-oil as a curing agent for a commercial epoxy resin (Celikbag et al. 2015). The glass transition temperature (Tg) of the cured epoxy resin with FP-bio-oil was found to be 120 ℃ which was comparable to the petroleum-based epoxy resins. It was also found that hydroxyl (OH) and carbonyl (C=O) groups played an important role during the curing.

HTL is a promising liquefaction process to produce bio-oil with a significant potential for commercialization in terms of price and life cycle assessment (Elliott et al. 2015). Unlike OSL, in HTL process, lignocellulosic biomass is converted into bio-oil at sub- or super-critical conditions using water as the liquefying solvent. The bio-oil yield was reported to be in the range of 30 – 40 wt.% depending on the HTL parameters (Akhtar and Amin 2011). However, using ethanol as a cosolvent along with the water can increase the bio-oil yield up to 65 wt.% (Cheng et al. 2010). Our group has recently studied the effect of ethanol and HTL temperature on the OH and carbonyl (C=O) groups in HTL-bio-oil, and found that addition of ethanol to HTL process increased the total OHN of HTL-bio-oil, yet decreased the concentration of phenolic type of OH

groups (Celikbag et al. 2016). The total OHN of HTL-bio-oil was found to be in the range of 8.5 – 4.0 mmol/g which suggests that HTL-bio-oil could be utilized as a biopolyol in epoxy synthesis (Celikbag et al. 2016).

To the best of our knowledge, there was no study that utilized the HTL-bio-oil as a biopolyol in epoxy synthesis. Moreover, the studies regarding the utilization of bio-oil (OSL and/or FP) lack specific information regarding the effect of OH groups on the epoxy synthesis. Since the reaction behavior and the mechanical/thermal properties of the resulting epoxy resin as well as the amount of catalyst used in the synthesis depends on the OH groups of bio-oil, it is crucial to design the experiment according to the OHN of bio-oil. Furthermore, in this study, the effect of ethanol used in the HTL process (used as a cosolvent) on the properties of resulting bio-based epoxy resin has been investigated for the first time. Therefore, the objectives of this study were to (i) investigate the effect of OHN of HTL-bio-oil on determining the amount of catalyst in epoxy synthesis, (ii) investigate how the addition of ethanol in HTL process further affects the mechanical and thermal properties of epoxy resin, and (iii) study the curing behavior of the epoxy resin synthesized using HTL-bio-oil.

7.2. Materials and Methods

7.2.1. Materials

Loblolly pine wood chips that are free from bark and leaf were obtained from a local chipping plant in Opelika, AL, USA. Loblolly pine composition (48.5 wt.% cellulose, 31.3 wt.% hemicellulose, 25.8 wt.% lignin and 4.5 wt. % extractives) was determined using standard wet chemistry analysis protocol. All chemicals were purchased from VWR; except the

phosphorylating agent for ^{31}P-NMR analysis, 2-chloro-4,4,5,5-tetramethyl-1,3,2-dioxaphospholane (TMDP), purchased from Sigma Aldrich.

7.2.2. Production and Characterization of HTL-Bio-oil

Bio-oils were produced by HTL process according to the method reported by Celikbag et al. (2016). Two types of bio-oils were used in epoxy synthesis: (i) bio-oil produced in water medium at 350 °C (W-HTL-bio-oil), and (ii) bio-oil produced in water/ethanol medium at 300 °C (W/E-HTL-bio-oil). The HTL temperature was selected based on the highest bio-oil yield which was obtained at 350 °C and 300 °C when water and water/ethanol were used as the liquefying solvent, respectively (Celikbag et al. 2016). OHN of bio-oils were determined by quantitative ^{31}P-NMR according to Celikbag et al. (2015), and ^{31}P-NMR spectra were acquired with a Bruker Avance II 250 MHz spectrometer using inverse gated decoupling pulse sequence, 90° pulse angle, 25 s pulse delay and 128 scans following the methods of Ben and Ragauskas (2011).

7.2.3. Synthesis of Bio-oil-based Epoxy Resin (BOBER)

BOBER was synthesized in two steps: (i) first step at 80 °C for 1 hour using triethylbenzylammonium chloride (TEBAC) as the catalyst in various amounts (TEBAC/OHN=0.05, 0.1 and 0.15 molar ratio); and (ii) second step at room temperature for 2 hours using NaOH as the catalyst (NaOH/OHN=0.5, 1.0 and 1.5 molar ratio). In a typical run, a three-neck round-bottomed flask equipped with condenser and thermometer was charged with 5 g bio-oil and 50 g ECH and placed in an oil bath at 80 °C. The mixture was constantly stirred and TEBAC was slowly added when the mixture reached to 80 °C. After one hour, the flask was placed in a cold water bath, the solution was cooled down to room temperature, and an aqueous

solution of 50% (w/w) NaOH was then added dropwise. The solution was stirred for 2 hours at room temperature after the addition of NaOH. Once the reaction was completed, the solution was diluted with 100 mL acetone and 100 mL ethyl acetate. The byproducts were separated from the solution by vacuum filtration using Whatmann#5 filter paper. Acetone, ethyl acetate and unreacted ECH left in the liquid part were removed by a rotary evaporator at 90 °C under vacuum, and the resulting black viscous liquid was termed as "BOBER". BOBER synthesized using W-HTL-bio-oil and WE-HTL-bio-oil was denoted as BOBER-W and BOBER-WE, respectively. The yield of the BOBER was calculated using Eqn (1) as suggested by Ferdosian et al. (2014) and Kuo et al. (2016):

$$Yield(wt.\%) = \frac{B}{H(1+S)} \times 100 \tag{1}$$

where, B is the weight of BOBER, H is the weight of HTL-bio-oil, and S is the stoichiometric amount of ECH for 1 gram of HTL-bio-oil, which is 0.47 and 0.75 for W-HTL-bio-oil and WE-HTL-bio-oil, respectively.

7.2.4. ATR-FTIR

Attenuated total reflection Fourier Transform Infrared (ATR-FTIR) spectra of the bio-oil and BOBER were acquired between 4000 and 650 cm^{-1} with an ATR-FT-IR spectrometer (Model Spectrum400, Perkin Elmer Co., Waltham, MA) with 4.00 cm^{-1} resolution and 32 scans to determine the functional groups. All ATR-FT-IR spectra were collected at room temperature.

7.2.5. Epoxy Equivalent Weight (EEW) of BOBER

EEW was calculated according to standard test method of ASTM D1652-11 with a slight modification. Briefly, in this method, epoxy resin is dissolved in 10 – 15 mL dichloromethane

(DCM) and 10 mL reagent (tetraethylammonium bromide solution in glacial acetic acid), and then titrated with 0.1 N perchloric acid until the color change was observed. However, color of the resulting solution was black when BOBER was dissolved in 15 mL DCM and 10 mL reagent; therefore, color change during the titration was difficult to observe. Thus, BOBER was dissolved in 100 mL DCM and 20 mL reagent in order to make the solution transparent and the color change visible. EEW of a commercial epoxy resin (EPON 828, EEW of 185 – 192 g/eq) was determined using the modified method (100 mL DCM and 20 mL reagent) and calculated to be 186±5 g/eq which confirmed that using 100 mL DCM and 20 mL reagent to dissolve an epoxy gave a valid result.

7.2.6. Curing Kinetics of BOBER

Differential scanning calorimetry (DSC, TA instruments Q2000) was used to investigate the curing behavior of BOBER. Approximately 10 mg BOBER (without using any curing agent) were placed in an aluminum DSC pan and sealed. The non-isothermal DSC measurement were performed at 2.5, 5, 7.5 and 10 °C/min heating rate over a temperature range of 30 – 350 °C under purging nitrogen gas at 50 mL/min. The curing properties including onset temperature (T_{onset}), the peak temperature (T_p), the end (terminal) temperature (T_{end}), and the heat of cure (ΔH_{total}) were obtained from the DSC curve. The overall activation energy of curing was calculated using Kissinger method which is expressed in Eqn (2) as follows (Ferdosian et al. 2016):

$$\ln(\beta/T_p^2) = \ln(A \times R/E_a) - (E_a/RT_p) \tag{2}$$

where, β is the heating rate, T_p is the peak temperature (K), A is the pre-exponential factor, R is the gas constant (8.314 J mol^{-1} K^{-1}), and E_a is the activation energy (J mol^{-1}) which was obtained

from the slope of the $\ln(\beta_i/T_{p,i}^2)$ vs. $1/T_p$ plot. As can be seen in Eqn (3), Kissenger method takes only T_p into account for each heating rate, and assumes that reaction exhibits nth order mechanism; thus, Kissenger method provides an activation energy of the overall curing process. In order to calculate the activation energy at each degree of curing, Friedman method was also used, as shown in Eqn (3) (Ferdosian et al. 2016):

$$\ln(d\alpha/dt) = \ln(A_\alpha f(\alpha)) - E_\alpha/(RT_\alpha) \tag{3}$$

where, α is the degree of conversion, and $f(\alpha)$ is the differential conversion function. The E_a was obtained from the slope of $\ln(\beta d\alpha/dT)$ vs. $1/T$ at constant degree of conversion (α) for a set of heating rate (β).

7.2.7. Thermomechanical Properties of BOBER

Dynamic mechanical analysis (DMA) was conducted on a TA Instruments RSA III to determine the thermomechanical properties of cured BOBER. Samples were cure prior to DMA testing as follows: 60 °C for 2 h, 80 °C for 2 h, 100 °C for 2 h, 120 °C for 12 h, and 160 °C for 2 h as a post-cure. Cured BOBER-W and BOBER-WE samples were termed as C-BOBER-W and C-BOBER-WE. A three-point bending configuration at 1% strain and an oscillating frequency of 1 Hz was utilized. Runs were conducted between 30°C and 200°C with a temperature ramp of 5 °C/min. The crosslink density (the number of active chain segments in the crosslinked network per unit volume) was calculated using Eqn (4) as follows (Sperling 2005):

$$E' = 3 \times n \times R \times T \tag{4}$$

where, E' is the storage modulus at rubbery region (Pa), n is the crosslink density (mol m^{-3}), R is the gas constant (8.31 Pa m^3 mol^{-1} K^{-1}); T is the temperature at rubbery region (K). Storage

modulus (E') at glassy region at 30 °C was obtained from the DMA curve. Glass transition temperature (Tg) of BOBER was determined by the temperature at maximum tan δ.
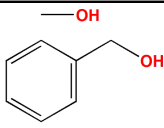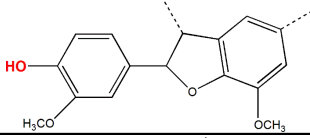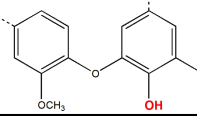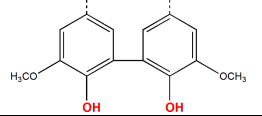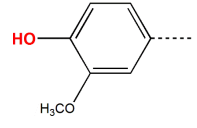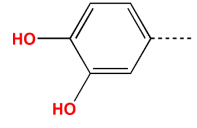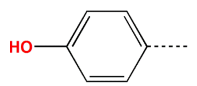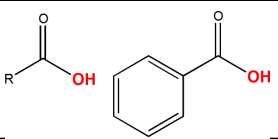
7.3. Results and Discussions

7.3.1. Hydroxyl Group Analysis of Bio-oil: ^{31}P-NMR

Determination of the OH groups of bio-oil plays crucial role in the synthesis of bio-oil based epoxy resins because the amount of catalyst to be used depends on the OHN of the bio-oil. Quantitative ^{31}P-NMR is a strong analytical tool to calculate and partition out the OH groups into aliphatic, phenolic and acidic categories. Table 7.1 shows the OHN of W-HTL-bio-oil and W/E-HTL-bio-oil as well as the example of chemical structures for each classification. Total OHN of W-HTL-bio-oil and W/E-HTL-bio-oil was calculated to be 5.10±0.05 and 8.11±0.10 mmol/g, respectively. A significant difference was observed in the aliphatic type of OH between the bio-oils (p-value<0.0001) which were calculated to be 0.07±0.02 and 3.28±0.03 mmol/g for W-HTL-bio-oil and W/E-HTL-bio-oil, respectively. Higher OHN of bio-oil produced in W/E-HTL could be attributable to the synergy effect of water and ethanol which enhances the degradation of biomass during the HTL process due to good hydrogen donor capability of ethanol and provides more side groups (Vasilakos and Austgen 1985). As can be seen in Table 1, both bio-oils contained all types of phenolic OH groups including condensed phenolic, guaiacyl phenolic OH, catechol typeOH and p-hydroxy-phenyl OH which are important components in epoxy resin synthesis because phenolics provide strength to the resin (Pham and Marks 2000). However, addition of ethanol significantly decreased the total phenolic concentration from 4.48 to 4.05 mmol/g (p-value=0.018). The decrease in phenolic OH could be attributable to condensation

reaction between ethanol and phenolic fragments originating from the degradation of lignin

(Celikbag et al. 2016).

Table 7.1. Hydroxyl number (OHN) of the bio-oil produced by W-HTL and W/E-HTL determined by quantitative ^{31}P-NMR phosphilated with TMDP.

Type of OH group		Example of Chemical Structure	Integration Region[b] (ppm)	OHN (mmol/g)[a]	
				W-HTL	W/E-HTL
Aliphatic OH			150.0 - 145.5	0.07 ± 0.02	3.28 ± 0.03
Phenolic OH	C5 substituded Condensed phenolic OH	β-5	144.7 - 142.8	0.21 ± 0.01	0.37 ± 0.01
		4-O-5	142.8 - 141.7	0.24 ± 0.01	0.39 ± 0.01
		5-5	141.7 - 140.2	0.36 ± 0.03	0.72 ± 0.02
	Guaiacyl phenolic OH		140.2 - 139.0	1.82 ± 0.06	1.62 ± 0.03
	Catechol type OH		139.0 - 138.2	1.10 ± 0.05	0.55 ± 0.02
	p -hydroxy-phenyl OH		138.2 - 137.3	0.77 ± 0.03	0.39 ± 0.02
		Total Phenolic OH		4.48 ± 0.18	4.05 ± 0.07
Acidic OH			136.6 - 133.6	0.54 ± 0.05	0.78 ± 0.14
Total OHN (mmol/g)				5.10 ± 0.21	8.11 ± 0.10

[a]OHN values were calculated by integrating of peaks relative to NHND peak. Values are means of three independent replicates, and numbers after ± are the standard deviation.
[b]Integration regions and chemical structures were identified according to ^{31}P-NMR chemical shifts reported by Ben and Ragauskas (2011).

7.3.2. Yield and Epoxy Equivalent Weight (EEW) Analysis of BOBER

Fig. 7.1 shows the yield and EEW of BOBER synthesized in various TEBAC/OHN and NaOH/OHN molar ratios, and the reaction mechanism between bio-oil and ECH is illustrated in Fig. 7.2. It should be noted that some unavoidable side reactions such as hydrolysis of epoxide groups, abnormal addition of ECH and formation of bound chlorides were not shown in the Fig. 7.2 for simplicity. As can be seen in Fig. 7.1, the yield of BOBER-W and BOBER-W/E increased as the amount of TEBAC was increased. The role of TEBAC in the first step of the synthesis is to form ion pairs (Pielichowski and Czub 1997, Fache et al. 2014) which further underwent addition reaction with ECH to form BOBER (Fig. 7.2). Thus, the increase in BOBER yield with the increase in TEBAC may be attributable to more formation of ion pair. It was hypothesized that a bio-oil with higher OHN value yields more BOBER since ECH undergoes addition reaction with OH groups in bio-oil. Therefore, higher BOBER-WE yield was expected when W/E-HTL-bio-oil was used due to its higher OHN value. However, higher BOBER-W yield was obtained when W-HTL-bio-oil was used. As discussed before (see above, section 3.1. Hydroxyl Group Analysis of Bio-oil: ^{31}P-NMR), the main difference between these two bio-oils was their concentration of aliphatic OH groups (OHN of aliphatic OH of W/E-HTL-bio-oil and W-HTL-bio-oil is 3.28 and 0.07 mmol/g, respectively). Aliphatic OHs are less reactive than phenolic and acidic OHs (Kuo et al. 2016), and may not always form an ion pair in the presence of TEBAC (Fache et al. 2014). Thus, it could be conjectured that aliphatic OHs in W/E-HTL-bio-oil were not completely utilized in the formation of ion pair which resulted in less BOBER-WE yield as compared to the BOBER-W system.
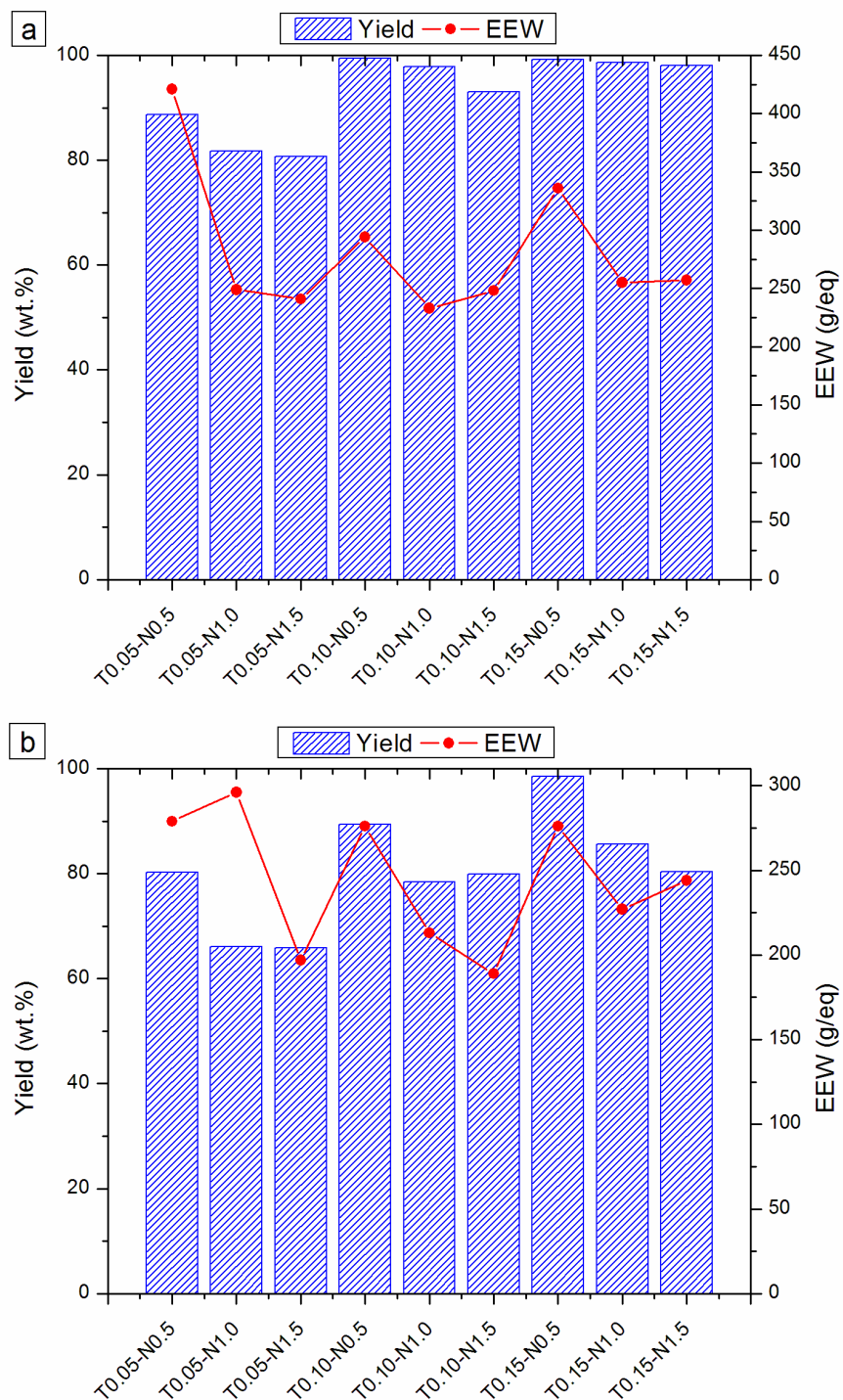
Fig. 7.1. Yield and EEW of BOBER-W **(a)**, and BOBER-WE **(b)** synthesized using various amount of catalyst. Numbers after T and N indicate the molar ratio of TEBAC and NaOH over OHN, respectively (for example, T0.05-N1.5 means TEBAC/OHN=0.05, and NaOH/OHN=1.5).

147

In the second step of the reaction, NaOH was used as the catalyst due to the fact that TEBAC is not a strong enough base for dehydrochlorination (Pham and Marks 2000). The roles of the NaOH are to dehydrochlorinate the intermediates (ring closing) and neutralize HCl (Lee and Neville 1967). During the second step, two possible mechanisms may occur: (i) complete dehydrochlorination, and (ii) incomplete dehydrochlorination, as illustrated in Fig. 7.2. The amount of NaOH used in this step is crucial because excess or insufficient amount of NaOH results in a decrease in BOBER yield. An excess amount of NaOH causes hydrolysis of ECH and increases the side reactions (Pielichowski and Czub 1997) which results in a decrease in the yield of BOBER. When there is not sufficient amount of NaOH in the system, incomplete dehydrochlorination may occur (Fig. 7.2). As can be seen in Fig. 7.1, in both of the systems, BOBWE-W and BOBER-WE, a decrease in BOBER yield was observed as the amount of NaOH increased which may be attributable to hydrolysis of ECH and incomplete dehydrochlorination.

Yield is an important consideration for the economic viability of the process. However, EEW should also be taken into the account as it represents the reactivity of BOBER. EEW is by definition the weight of resin in grams that contains 1-gram equivalent of epoxide group (Lee and Neville 1967). For instance, if there are 3 epoxide groups, then EEW is the one-third of the average molecular weight of the resin. That is to say, lower EEW is desirable as it means higher concentration of epoxide group attached to the resin. Thus, the optimum amount of catalyst was determined according to the lowest EEW at highest BOBER yield. As can be seen in Fig.7.1, T0.10-N1.0 and T0.10-N1.5 were chosen as the optimum catalyst/OHN molar ratios for BOBER-W and BOBER-WE, respectively. This finding suggests that not only the total OHN of bio-oil has an effect on the yield and EEW of BOBER, but the distribution of OH groups within

bio-oil (aliphatic, phenolic and acidic OH) also plays an important role for the determination of the optimum amount of catalyst to be used in the synthesis of BOBER.
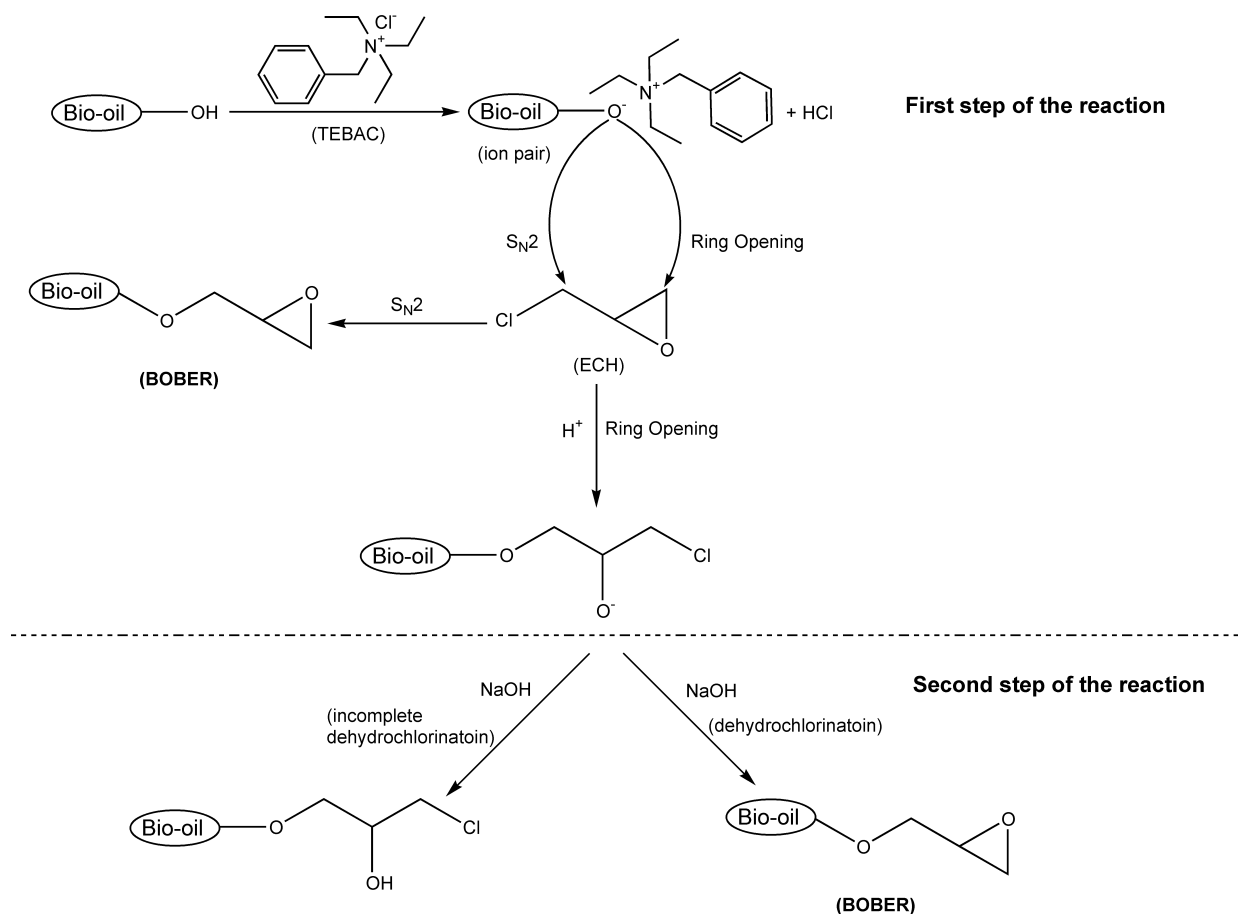
Fig. 7.2. Illustration of the formation of BOBER in two steps using bio-oil and ECH in the presence of TEBAC and NaOH (Auvergne et al. 2014, Fache et al. 2014).

7.3.3. Curing Kinetics of BOBER

The DSC diagram of BOBER at different heating rates and the curing properties are shown in Fig. 3 and Table 2, respectively. The exothermic DSC peaks shown in Fig. 3 clearly indicate that both epoxy resins, BOBER-W and BOBER-WE, cured without the help of a curing
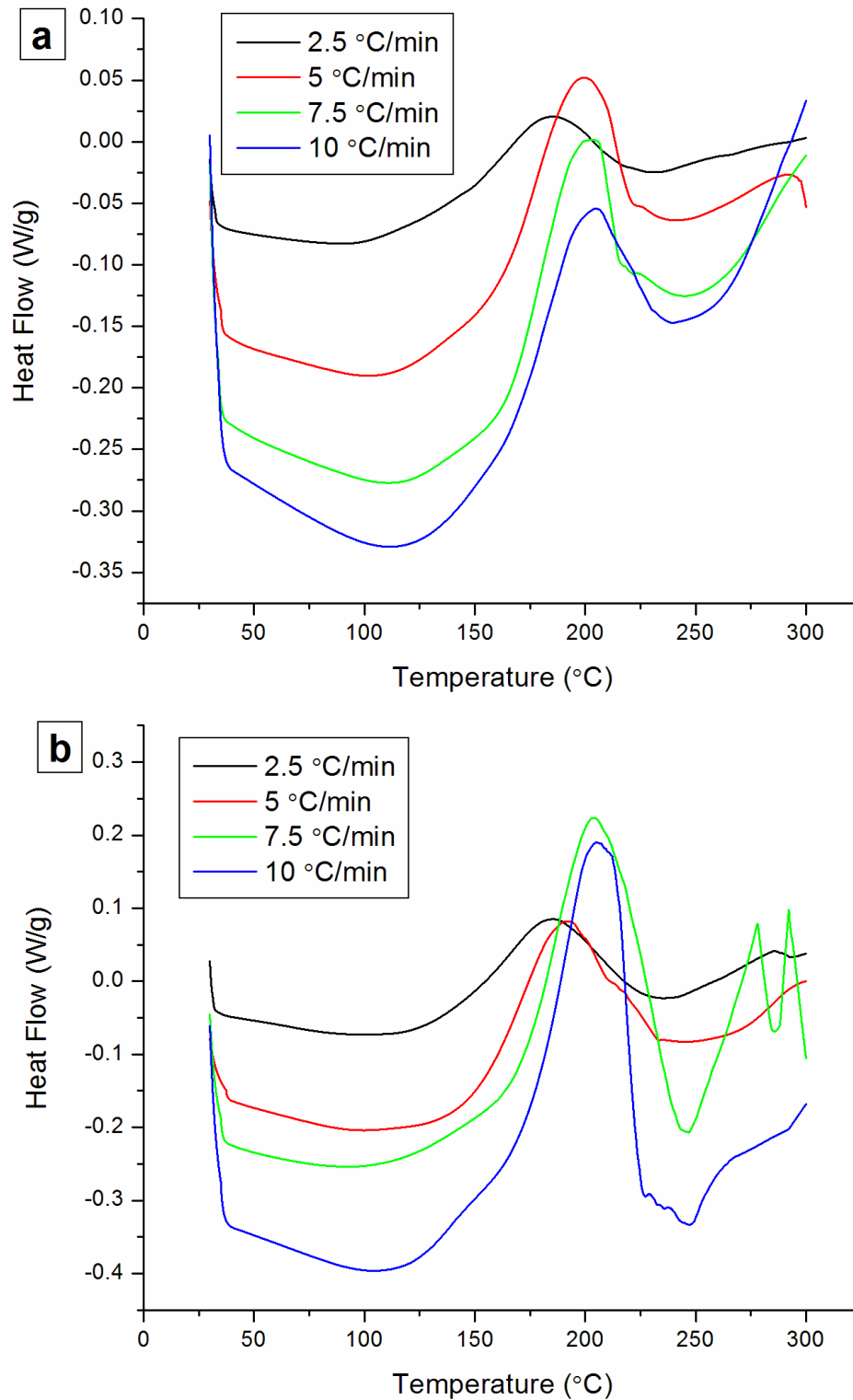
Fig. 7.3. DSC curves of BOBER-W **(a)** and BOBER-WE **(b)** at different heating rates.

agent. In both systems, the exothermic peaks were slightly shifted toward higher temperatures as

the heating rate was increased (Fig. 7.3) which resulted in an increase in the T_{onset}, T_p, and T_{end}

(Table 2). This increase is most likely due to the fact that BOBER had less time at a specific

temperature at a higher heating rate, and thus generated more heat per unit time (Ferdosian et al.

2016, Zhang et al. 2016).

As shown in Table 7.2, there was no significant difference observed between curing

properties (T_{onset}, T_p, T_{end}) of BOBER-W and BOBER-WE which are important parameters to set

the curing temperature and activation energy (Zhang et al. 2016). Thus, data in Table 7.2

suggests that both of the epoxy systems can be cured using the same curing profile (curing time

and temperature). However, depending on the heating rate, the heat of curing (ΔH_{total}) of

BOBER-W (129 – 184 J/g) was found to be in a higher range than that of BOBER-W/E (46 – 94

J/g). This suggests that BOBER-W has released more heat and therefore is more sensitive to

curing than BOBER-WE (Jubsilp et al. 2006).

Table 7.2. Curing characteristics and the overall activation energy of BOBER synthesized using W-HTL-bio-oil (BOBER-W) and W/E-HTL-bio-oil (BOBER-WE).

Sample ID	Heating rate (ºC/min)	T_{onset} (ºC)	T_p (ºC)	T_{end} (ºC)	ΔH_{total} (J/g)	Ea (kJ/mol)[a]
BOBER-W	2.5	136.2	184.0	235.5	166.5	95
	5	149.0	190.5	245.0	129.9	
	7.5	164.7	203.8	246.1	184.4	
	10	165.1	205.2	247.2	149.3	
BOBER-WE	2.5	130.6	182.5	231.9	92.9	98
	5	154.3	197.1	242.3	94.1	
	7.5	160.6	203.0	246.0	62.0	
	10	157.1	204.3	204.3	46.4	

[a] Overall activation energy was calculated using Kissenger method.

The overall activation energy indicates the energy required to initiate the curing reaction which was calculated to be 95 and 98 kJ/mol for BOBER-W and BOBER-WE, respectively, using Kissenger method. It could be conjectured that both epoxy systems might have similar curing mechanisms since their activation energy values were not significantly different (Jubsilp et al. 2006). However, relatively higher activation energy of BOBER-WE may be attributable to the lower EEW which indicates more epoxide groups attached to the resin (see above, section 3.2. Yield and Epoxy Equivalent Weight (EEW) Analysis of BOBER); thus, BOBER-WE required relatively more energy for curing. The overall activation energy of BOBER is higher than the commercial epoxy resin cured with amine type curing agent 55 – 60 kJ/mol (Sbirrazzuoli et al. 2006). However, it should be noted that no curing agent was used to cure BOBER in this study; therefore, higher activation energy was needed due to the absence of a curing agent in the system. The overall activation energy of BOBER system (95 – 98 kJ/mol) could also provide information about the type of reaction that took place during the curing step. Sbirrazzuoli et al. (2006) studied the kinetics of curing reactions of an epoxy-amine system, and they found the activation energy of primary amine epoxy reaction and etherification reaction to be 55-60 and 104 kJ/mol, respectively. Thus, it could be speculated that the etherification reaction was the dominating reaction during the curing of BOBER system. Etherification is discussed in detail in FT-IR analysis (see the section 7.3.4).

Fig. 7.4 shows the required activation energy for a given degree of curing calculated using Friedman method. As can be seen in Fig. 7.4, the activation energy for both of the epoxy systems increased as the degree of curing increased, suggesting that the curing mechanism of the BOBER changed during this step. Increasing activation energy with the extend of curing could

indicate the self-curing of BOBER (etherification). As also noted by Ferdosian et al. (2015), when an epoxy matrix is exposed to self-curing, the rigidity and viscosity of the matrix increases; thus, restraining the self-curing process. As a result, the activation energy of curing increases with the extend of curing. Another approach was taken for an increasing activation by Alonso et al. (2006) where the authors studied the curing kinetics of lignin-based PF resin. They found that different reactions took place during the curing, and caused an increase in the activation energy. A similar rational can be applied to the curing of BOBER. Therefore, increasing activation energy with the extend of curing may be attributable to (i) different types of reactions taking place during the curing, and (ii) limitation of self-curing reactions due to the increase in the crosslink density and viscosity.
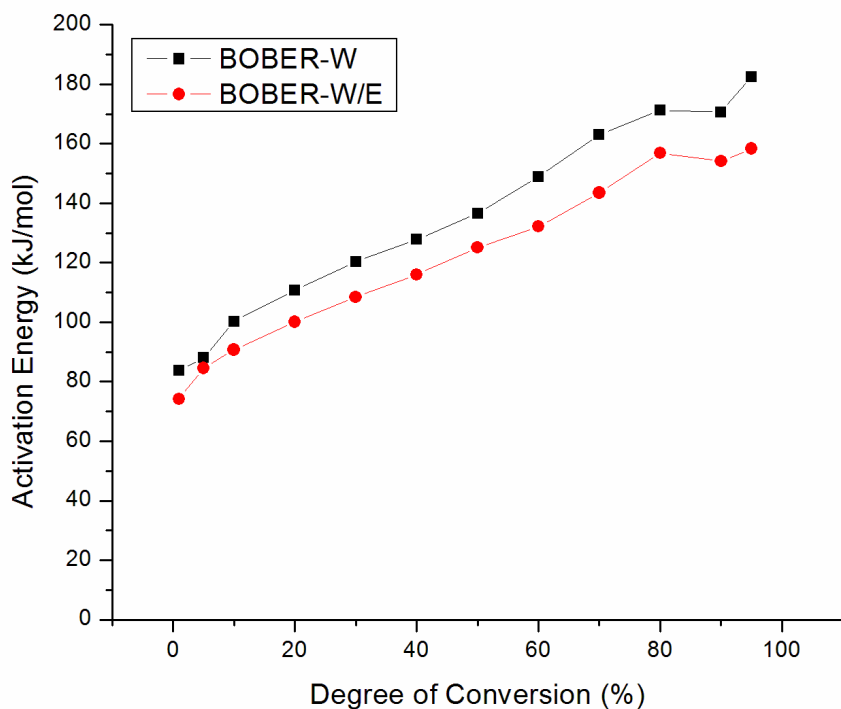

Fig. 7.4. Variation of the activation energy of BOBER with respect to the degree of conversion calculated according to Friedman method.

7.3.4. ATR-FT-IR

FT-IR analysis was performed to obtain an insight about the reactions taking place in the synthesis and curing of BOBER. The IR spectra of HTL-bio-oil, BOBER and C-BOBER is shown in Fig. 7.5, and the band assignments are summarized in Table 3.1. The broad peak at around 3300 cm^{-1} was due to the presence of OH groups, and the peak at 908 cm^{-1} is the characteristic peak of oxirane ring. As can be seen in Figs. 7.5a and b, the intensity of the OH peak at 3300 cm^{-1} of HTL-bio-oils decreased while oxirane peak appeared in the IR spectra of BOBER. This could be evidence of the glycidylation reaction during the synthesis of BOBER which suggests that OH groups in the HTL-bio-oil were consumed by ECH. When both BOBER-W and BOBER-WE were cured, the oxirane peak disappeared, and the intensity of the OH peak at 3300 cm^{-1} increased. The absence of the oxirane peak in the IR spectra of C-BOBER-W and C-BOBER-WE indicates that a ring opening reaction took place during the curing which resulted in the increase of the intensity of the peak at 3300 cm^{-1}.

One of the possible reactions taking places during the curing of an epoxy resin is an etherification (also called homopolymerization) which is the reaction between an oxirane ring and a hydroxyl group at elevated temperature or in the presence of a catalyst (Xu and Schlup 1998). Hydroxyl groups, on the other hand, have been found to promote the autocatalytic network formation during curing (Kuo et al. 2014) and accelerate the etherification reaction (Petrie 2005). As can be seen in Fig. 5, a peak at around 1140 cm^{-1} was observed in the IR spectra of BOBER-W and BOBER-WE which was due to the secondary OH groups (Guo et al. 2011, Zhang et al. 2016). When BOBER-W and BOBER-WE were cured, the peak at 1140 cm^{-1} disappeared, and a new peak at 1085 cm^{-1} appeared which was reported to be an ether band in an
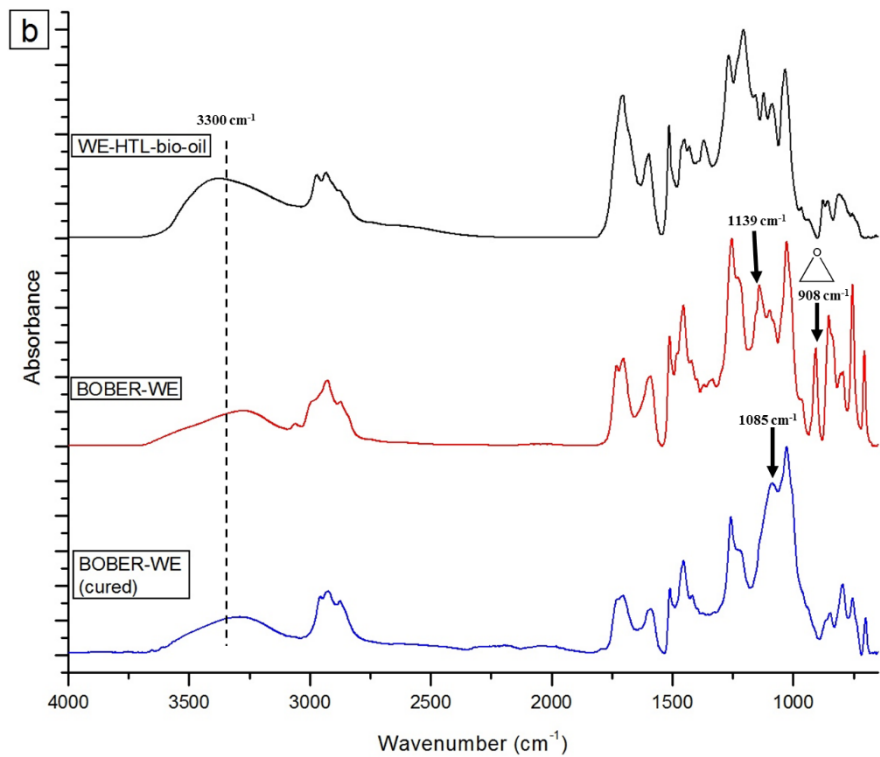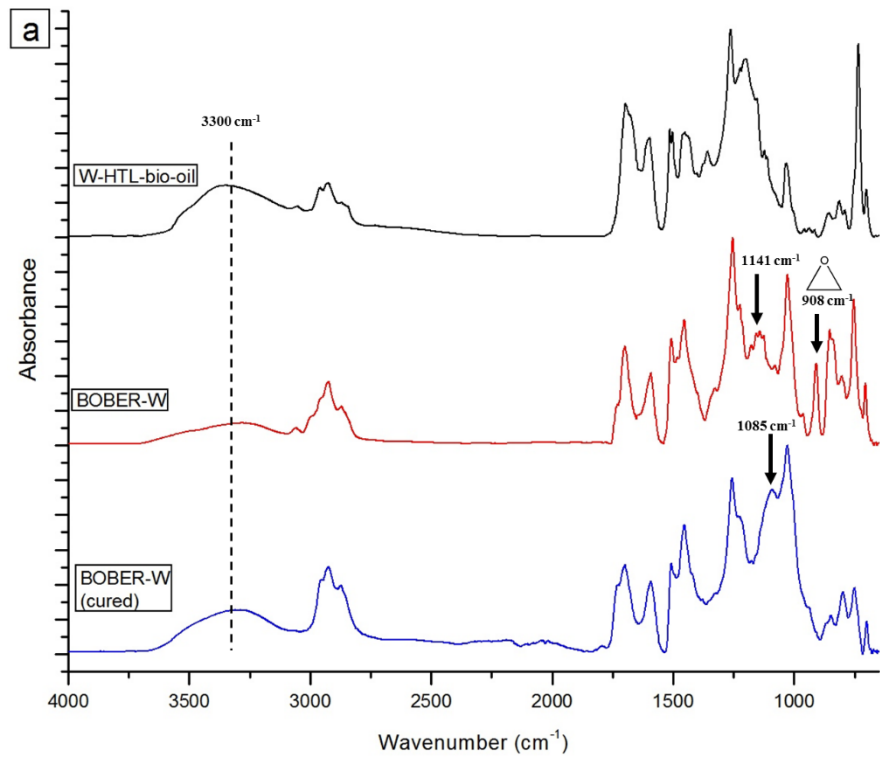
Fig. 7.5. FT-IR spectra of BOBER-W **(a)**, and BOBER-WE **(b)**.

155

epoxy resin (Riccardi and Williams 1986). In addition, the peaks at 1258 and 1027 cm^{-1} confirm

the presence of ether groups in the C-BOBER as well. Therefore, the self-curing phenomena in

this study could be attributable to the etherification reaction between the oxirane ring and OH

groups, as illustrated in Fig. 7.6.

Table 7.3. Characteristic FT-IR band assignments of HTL-bio-oils and BOBER

Wavenumber (cm^{-1})	Band Assignment
3300	O-H stretching
2927	Methyl groups
2873	Methylene groups
1734	C=O stretch (saturated carbonyl)
1698	C=O stretch (α, β-unsaturated carbonyl)
1593 - 1453	C-C stretch in aromatic ring
1258, 1085, 1027	C-O-C stretch (ether groups)
1140	O-H bend
910	Epoxide group

Due to the complex nature of lignocellulosic biomass, HTL-bio-oil contains variety of

compounds such as aromatics, aldehydes, anhydrides, ketones, alcohols, esters and carboxylic

acids (Cheng et al. 2010). Thus, the BOBER system synthesized using HTL-bio-oil is assumed

to contain some derivatives of these compounds. Among them, alcohols, carboxylic acids and

anhydrides may accelerate the ring opening of oxirane at elevated temperature which most likely

resulted in the etherification reaction during the curing, and which allows the BOBER react with

each other to form a solid structure. Curing kinetics of BOBER also supported that the

etherification reaction took place when BOBER was cured, as discussed before. Finally, it should

be mentioned that due to the complex structure of BOBER, different types of reactions besides

etherification could also be anticipated to take place during the curing of BOBER. More analysis is required for a deeper understanding.
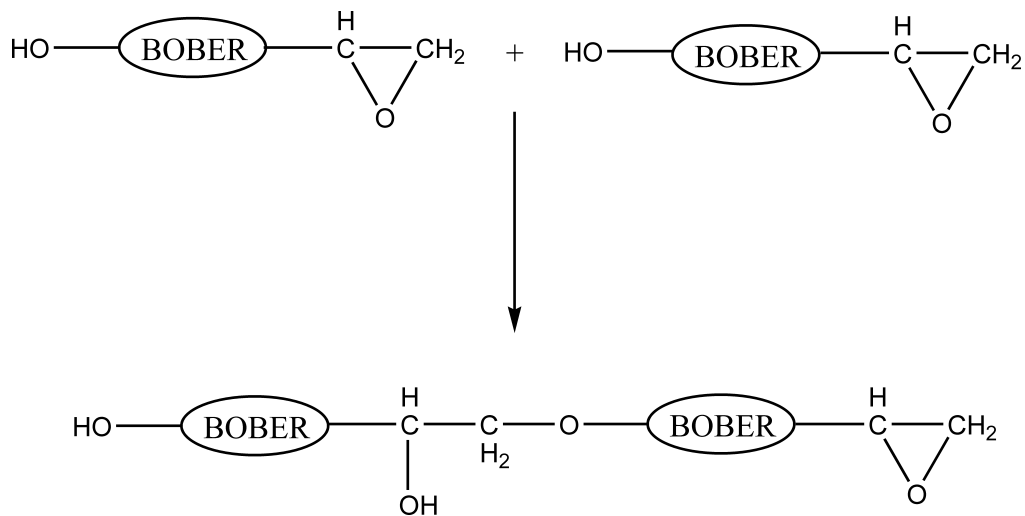

Fig. 7.6. Proposed reaction mechanism (etherification) for curing of BOBER.

7.3.5. Thermomechanical Properties of BOBER

The viscoelastic behavior of C-BOBER was investigated by DMA, and the storage modulus (E') and tan δ versus temperature is shown in Figs. 7.7a and b, respectively. E' of C-BOBER-W and C-BOBER-WE at 30 °C was found to be 425 and 845 MPa, respectively (Table 7.4) which indicates that C-BOBER-WE was stiffer than cured BOBER-W at ambient condition. E' of C-BOBER was also comparable with a lignin-based epoxy nanocomposite whose E' at room temperature was reported to be 175 – 250 MPa (Zhao and Abu-Omar 2015). As can be seen in Fig. 7.7, when the temperature increased, the storage modulus initially decreased, and then exhibited the rubbery plateau which is an evidence for the crosslinked structure. The crosslink density of C-BOBER-WE (58.7 mol/m^3) was also found to be higher than that of C-BOBER-W
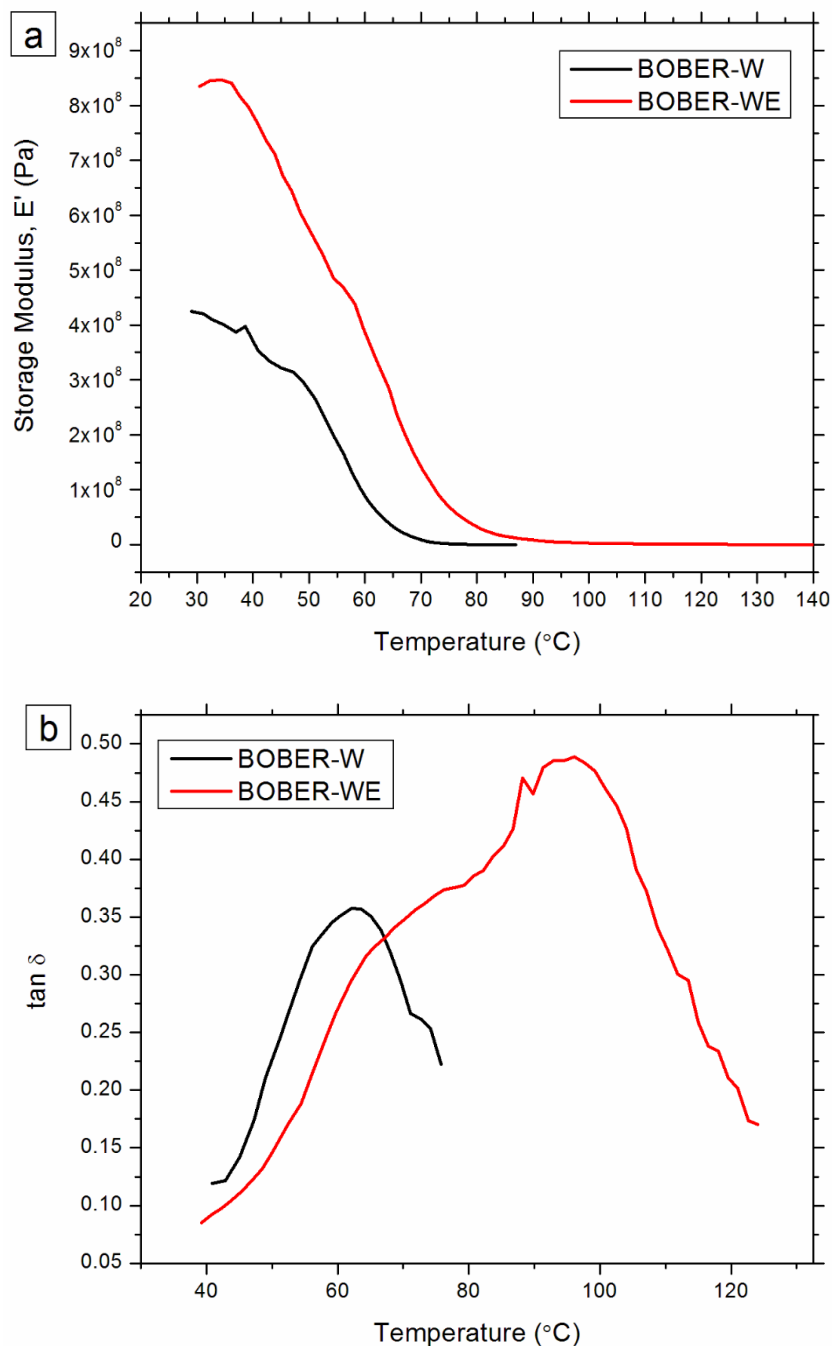
Fig. 7.7. Storage modulus **(a)** and tan delta **(b)** as a function of temperature of the cured BOBER. (8.5 mol/m^3). The higher storage modulus and crosslink density of C-BOBER-WE could be attributable to lower EEW of BOBER-WE. As discussed before (see the section 3.2. Yield and Epoxy Equivalent Weight (EEW) Analysis of BOBER), lower EEW indicates that BOBER-WE

158

has more epoxide groups in the system; thus, provided a higher degree of homopolymerization when BOBER-WE was cured.

Table 7.4. Glass transition temperature (Tg), crosslinking density (n) and storage modulus (E') of cured BOBER-W and BOBER-WE.

Sample	Tg (°C)	n (mol/m^3)	E' (MPa) at 30 °C
C-BOBER-W	63.6	8.5	425
C-BOBER-WE	96.0	58.7	845

The Tg was determined by the peak temperature of tan δ versus temperature thermogram (Fig. 7b), and found to be 63.6 and 96 °C for C-BOBER-W and C-BOBER-WE, respectively. Tg is influenced by the chain mobility, and the increase in the crosslink density results in a decrease in chain mobility (Sperling 2005). Thus, the higher Tg of C-BOBER-WE could be attributable to a higher crosslink density. Moreover, a broader tan δ peak was also observed in C-BOBER-WE (Fig. 7b) which could indicate to a less uniform crosslinked structure. Tg of both C-BOBER-W and C-BOBER-WE are promising as compare to the bio-based epoxy resin reported in the literature. For instance, Tg of 62.3 – 78.5 °C for an epoxy resin cured with depolymerized kraft lignin (Qin et al. 2013), 94.3 °C for partially depolymerized lignin-based epoxy resin (Xin et al. 2016), 4.6 – 91.6 °C for vegetable oil-based epoxy resin (Liu et al. 2016), 30 – 38 °C for castor oil-based epoxy resin (Park et al. 2005), 55 – 88 °C for furan-based epoxy resin (Hu et al. 2014), 83 – 100 °C for organasolv and kraft lignin-based epoxy resin (blended with DGEBA) (Ferdosian et al. 2016), and 104 °C for vanillyl alcohol-based epoxy resins (Hernandez et al. 2016) have been previously reported. It is noteworthy to mention that either petroleum- or bio-based curing agents were used to cure the epoxy resins in these studies. In this present study,

however, no curing agent was used. Therefore, it could be concluded that the C-BOBER system, especially C-BOBER-WE, would be a highly competitive candidate in the field of bio-based epoxy resins.

7.4. Conclusion

In this study, the utilization of two different HTL-bio-oils (W-HTL-bio-oil and WE-HTL-bio-oil) was investigated for the synthesis of BOBER. ^{31}P-NMR analysis were performed to characterize the hydroxyl (OH) groups in bio-oils, and it was found that WE-HTL-bio-oil contains a significantly higher concentration of aliphatic OH than W-HTL-bio-oil which resulted in lower BOBER yield and EEW. The optimum amount of catalyst was found to be T0.10-N1.0 and T0.10-N1.5 for BOBER-W and BOBER-WE, respectively. DSC analysis of BOBER was confirmed the self-curing phenomena. The activation energy for curing of BOBER-W and BOBER-WE was calculated to be 95 and 98 kJ/mol, respectively, using Kissinger method, suggesting that curing of BOBER was mainly controlled by etherification reaction. FT-IR analysis provided evidence for (i) the glycidylation reaction that took place during the synthesis of BOBER, and (ii) etherification reaction during the curing of BOBER. DMA analysis showed that BOBER-WE had a higher storage modulus (845 MPa), glass transition temperature (96 °C), and crosslink density (58.7 mol/m3) than BOBER-W (425 MPa, 63.6 °C, and 8.5 mol/m3), suggesting that addition of ethanol in HTL process improved the thermomechanical properties of BOBER. The bio-based epoxy resin system developed in this study provided promising results to replace the petroleum-based phenolic resource with HTL-bio-oil in the synthesis of epoxy resins.

Acknowledgment

References

1. Akhtar, J. and N. A. S. Amin. 2011. A review on process conditions for optimum bio-oil yield in hydrothermal liquefaction of biomass. Renewable and Sustainable Energy Reviews **15**:1615-1624.

2. Alonso, M. V., M. Oliet, J. García, F. Rodríguez, and J. Echeverría. 2006. Gelation and isoconversional kinetic analysis of lignin–phenol–formaldehyde resol resins cure. Chemical Engineering Journal **122**:159-166.

3. Auvergne, R., S. Caillol, G. David, B. Boutevin, and J. P. Pascault. 2014. Biobased Thermosetting Epoxy: Present and Future. Chemical Reviews **114**:1082-1115.

4. Baroncini, E. A., S. Kumar Yadav, G. R. Palmese, and J. F. Stanzione. 2016. Recent advances in bio-based epoxy resins and bio-based epoxy curing agents. Journal of Applied Polymer Science **133.** DOI: 10.1002/app.44103.

5. Ben, H. X. and A. J. Ragauskas. 2011. NMR Characterization of Pyrolysis Oils from Kraft Lignin. Energy & Fuels **25**:2322-2332.

6. Celikbag, Y., T. J. Robinson, B. K. Via, S. Adhikari, and M. L. Auad. 2015. Pyrolysis oil substituted epoxy resin: Improved ratio optimization and crosslinking efficiency. Journal of Applied Polymer Science **132**.

7. Celikbag, Y., B. K. Via, S. Adhikari, G. Buschle-Diller, and M. L. Auad. 2016. The effect of ethanol on hydroxyl and carbonyl groups in biopolyol produced by hydrothermal liquefaction of loblolly pine: 31P-NMR and 19F-NMR analysis. Bioresource Technology **214**:37-44.

8. Celikbag, Y., B. K. Via, S. Adhikari, and Y. Wu. 2014. Effect of liquefaction temperature on hydroxyl groups of bio-oil from loblolly pine (Pinus taeda). Bioresource Technology **169**:808-811.

9. Cheng, S., I. D'cruz, M. Wang, M. Leitch, and C. Xu. 2010. Highly Efficient Liquefaction of Woody Biomass in Hot-Compressed Alcohol−Water Co-solvents. Energy & Fuels **24**:4659-4667.

10. El Mansouri, N.-E., Q. Yuan, and F. Huang. 2011. SYNTHESIS AND CHARACTERIZATION OF KRAFT LIGNIN- BASED EPOXY RESINS. Bioresources **6**:2492-2503.

11. Elliott, D. C., P. Biller, A. B. Ross, A. J. Schmidt, and S. B. Jones. 2015. Hydrothermal liquefaction of biomass: Developments from batch to continuous process. Bioresource Technology **178**:147-156.

12. EU. 2011. The restriction of use of Bisphenol A in plastic infant feeding bottles. http://eur-lex.europa.eu/LexUriServ/LexUriServ.do?uri=OJ:L:2011:026:0011:0014:EN:PDF (accessed September 2016).

13. Fache, M., B. Boutevin, and S. Caillol. 2016. Epoxy thermosets from model mixtures of the lignin-to-vanillin process. Green Chemistry **18**:712-725.

14. Fache, M., E. Darroman, V. Besse, R. Auvergne, S. Caillol, and B. Boutevin. 2014. Vanillin, a promising biobased building-block for monomer synthesis. Green Chemistry **16**:1987-1998.

15. Fache, M., A. Viola, R. Auvergne, B. Boutevin, and S. Caillol. 2015. Biobased epoxy thermosets from vanillin-derived oligomers. European Polymer Journal **68**:526-535.

16. FDA. 2013. Indirect Food Additives: Adhesives and Components of Coatings. https://www.gpo.gov/fdsys/pkg/FR-2013-07-12/pdf/2013-16684.pdf (accessed September 2016).

17. Ferdosian, F., Z. Yuan, M. Anderson, and C. Xu. 2015. Sustainable lignin-based epoxy resins cured with aromatic and aliphatic amine curing agents: Curing kinetics and thermal properties. Thermochimica Acta **618**:48-55.

18. Ferdosian, F., Z. S. Yuan, M. Anderson, and C. Xu. 2014. Synthesis of lignin-based epoxy resins: optimization of reaction parameters using response surface methodology. Rsc Advances **4**:31745-31753.

19. Ferdosian, F., Y. Zhang, Z. Yuan, M. Anderson, and C. Xu. 2016. Curing kinetics and mechanical properties of bio-based epoxy composites comprising lignin-based epoxy resins. European Polymer Journal **82**:153-165.

20. Guo, Y., C. Bao, L. Song, B. Yuan, and Y. Hu. 2011. In Situ Polymerization of Graphene, Graphite Oxide, and Functionalized Graphite Oxide into Epoxy Resin and Comparison Study of On-the-Flame Behavior. Industrial & Engineering Chemistry Research **50**:7772-7783.

21. Harvey, B. G., A. J. Guenthner, H. A. Meylemans, S. R. L. Haines, K. R. Lamison, T. J. Groshens, L. R. Cambrea, M. C. Davis, and W. W. Lai. 2015. Renewable thermosetting resins and thermoplastics from vanillin. Green Chemistry **17**:1249-1258.

22. Hernandez, E. D., A. W. Bassett, J. M. Sadler, J. J. La Scala, and J. F. Stanzione. 2016. Synthesis and Characterization of Bio-based Epoxy Resins Derived from Vanillyl Alcohol. Acs Sustainable Chemistry & Engineering **4**:4328-4339.

23. Hofmann, K. and W. G. Glasser. 1993. Engineering Plastics from Lignin. 21.1Synthesis and Properties of Epoxidized Lignin-Poly (Propylene Oxide) Copolymers. Journal of Wood Chemistry and Technology **13**:73-95.

24. Hu, F., J. J. La Scala, J. M. Sadler, and G. R. Palmese. 2014. Synthesis and Characterization of Thermosetting Furan-Based Epoxy Systems. Macromolecules **47**:3332-3342.

25. Jahanshahi, S., A. Pizzi, A. Abdulkhani, and A. Shakeri. 2016. Analysis and Testing of Bisphenol A—Free Bio-Based Tannin Epoxy-Acrylic Adhesives. Polymers **8**:143.

26. Jubsilp, C., S. Damrongsakkul, T. Takeichi, and S. Rimdusit. 2006. Curing kinetics of arylamine-based polyfunctional benzoxazine resins by dynamic differential scanning calorimetry. Thermochimica Acta **447**:131-140.

27. Kai, D., M. J. Tan, P. L. Chee, Y. K. Chua, Y. L. Yap, and X. J. Loh. 2016. Towards lignin-based functional materials in a sustainable world. Green Chemistry **18**:1175-1200.

28. Kishi, H., Y. Akamatsu, M. Noguchi, A. Fujita, S. Matsuda, and H. Nishida. 2011. Synthesis of Epoxy Resins from Alcohol-Liquefied Wood and the Mechanical Properties of the Cured Resins. Journal of Applied Polymer Science **120**:745-751.

29. Kishi, H., A. Fujita, H. Miyazaki, S. Matsuda, and A. Murakami. 2006. Synthesis of wood-based epoxy resins and their mechanical and adhesive properties. Journal of Applied Polymer Science **102**:2285-2292.

30. Koike, T. 2012. Progress in development of epoxy resin systems based on wood biomass in Japan. Polymer Engineering & Science **52**:701-717.

31. Kuo, P.-Y., L. de Assis Barros, M. Sain, J. S. Y. Tjong, and N. Yan. 2016. Effects of Reaction Parameters on the Glycidyl Etherification of Bark Extractives during Bioepoxy Resin Synthesis. Acs Sustainable Chemistry & Engineering **4**:1016-1024.

32. Kuo, P.-Y., M. Sain, and N. Yan. 2014. Synthesis and characterization of an extractive-based bio-epoxy resin from beetle infested Pinus contorta bark. Green Chemistry **16**:3483-3493.

33. Lee, H. and K. Neville. 1967. Handbook of epoxy resins. McGraw-Hill.

34. Liu, R., X. Zhang, S. Gao, X. Liu, Z. Wang, and J. Yan. 2016. Bio-based epoxy-anhydride thermosets from six-armed linoleic acid-derived epoxy resin. Rsc Advances **6**:52549-52555.

35. Park, S.-J., F.-L. Jin, J.-R. Lee, and J.-S. Shin. 2005. Cationic polymerization and physicochemical properties of a biobased epoxy resin initiated by thermally latent catalysts. European Polymer Journal **41**:231-237.

36. Petrie, E. 2005. Epoxy Adhesive Formulations. McGraw-Hill Education.

37. Pham, H. Q. and M. J. Marks. 2000. Epoxy Resins. Ullmann's Encyclopedia of Industrial Chemistry. Wiley-VCH Verlag GmbH & Co. KGaA.

38. Pielichowski, J. and P. Czub. 1997. Application of phase transfer catalysis in the synthesis of low-molecular-weight epoxy resins. Die Angewandte Makromolekulare Chemie **251**:1-12.

39. Qin, J., M. Woloctt, and J. Zhang. 2013. Use of Polycarboxylic Acid Derived from Partially Depolymerized Lignin As a Curing Agent for Epoxy Application. Acs Sustainable Chemistry & Engineering **2**:188-193.

164

40. Raquez, J. M., M. Deléglise, M. F. Lacrampe, and P. Krawczak. 2010. Thermosetting (bio)materials derived from renewable resources: A critical review. Progress in Polymer Science **35**:487-509.

41. Research, G. V. 2016. Epoxy Resin Market Analysis By Application (Paints & Coatings, Wind Turbine, Composites, Construction, Electrical & Electronics, Adhesives) And Segment Forecasts To 2024. http://www.grandviewresearch.com/industry-analysis/epoxy-resins-market, (accessed September 2016)

42. Riccardi, C. C. and R. J. J. Williams. 1986. A kinetic scheme for an amine-epoxy reaction with simultaneous etherification. Journal of Applied Polymer Science **32**:3445-3456.

43. Sbirrazzuoli, N., A. Mititelu-Mija, L. Vincent, and C. Alzina. 2006. Isoconversional kinetic analysis of stoichiometric and off-stoichiometric epoxy-amine cures. Thermochimica Acta **447**:167-177.

44. Sen, S., S. Patil, and D. S. Argyropoulos. 2015. Thermal properties of lignin in copolymers, blends, and composites: a review. Green Chemistry **17**:4862-4887.

45. Sperling, L. H. 2005. Introduction to Physical Polymer Science. Wiley.

46. Thangalazhy-Gopakumar, S., S. Adhikari, H. Ravindran, R. B. Gupta, O. Fasina, M. Tu, and S. D. Fernando. 2010. Physiochemical properties of bio-oil produced at various temperatures from pine wood using an auger reactor. Bioresource Technology **101**:8389-8395.

47. Vasilakos, N. P. and D. M. Austgen. 1985. Hydrogen-donor solvents in biomass liquefaction. Industrial & Engineering Chemistry Process Design and Development **24**:304-311.

48. Wei, N., B. K. Via, Y. F. Wang, T. McDonald, and M. L. Auad. 2014. Liquefaction and substitution of switchgrass (Panicum virgatum) based bio-oil into epoxy resins. Industrial Crops and Products **57**:116-123.

49. Wu, C. C. and W. J. Lee. 2010. Synthesis and Properties of Copolymer Epoxy Resins Prepared from Copolymerization of Bisphenol A, Epichlorohydrin, and Liquefied Dendrocalamus latiflorus. Journal of Applied Polymer Science **116**:2065-2073.

50. Xin, J., M. Li, R. Li, M. P. Wolcott, and J. Zhang. 2016. Green Epoxy Resin System Based on Lignin and Tung Oil and Its Application in Epoxy Asphalt. Acs Sustainable Chemistry & Engineering **4**:2754-2761.

51. Xu, L. S. and J. R. Schlup. 1998. Etherification versus amine addition during epoxy resin amine cure: An in situ study using near-infrared spectroscopy. Journal of Applied Polymer Science **67**:895-901.

52. Zhang, D., R. Wang, S. Farhan, H. Jiang, N. Wang, and L. Yuan. 2016. Curing kinetics, thermal and mechanical properties of TDE-85 modified by bicyclo-benzoxazine. Rsc Advances.

53. Zhang, W., Y. Zhang, and D. Zhao. 2012. Synthesis of liquefied corn barn-based epoxy resins and their thermodynamic properties. Journal of Applied Polymer Science **125**:2304-2311.

54. Zhao, S. and M. M. Abu-Omar. 2015. Biobased Epoxy Nanocomposites Derived from Lignin-Based Monomers. Biomacromolecules **16**:2025-2031.

166

Chapter 8

General Conclusions and Future Work

8.1. General Conclusions

Source and variation of OH groups in bio-oils obtained from organic solvent liquefaction (OSL) and hydrothermal liquefaction (HTL) was investigated in order to improve the utilization of bio-oil in epoxy resin (ER) synthesis. As a result, bio-oil were utilized as a curing agent for a commercial epoxy resin (EPON828), and a biopolyol to synthesize a self-curing epoxy resin. Major findings are summarized as follows:

- OSL is considered as an effective liquefaction process due to the high hydroxyl number (OHN) of resulting bio-oil (OSL-bio-oil). However, it was found that unreacted liquefying solvent retained in OSL-bio-oil was the major source for OH groups, and accounted for 70 – 95 % of the total OHN depending on liquefaction temperature. Aliphatic OHs accounted for the majority of hydroxyl groups as evidenced by ^{31}P-NMR analysis.

- ^{31}P-NMR analysis revealed that OSL-bio-oil lacks phenolic type of OH groups due to the condensation reaction between lignin fragments and liquefying solvent.

- OHN of OSL-bio-oil was found to be stable over 2 months when stored in a freezer. OHN stability was attributed to (i) lower storage temperature which reduces the aging rate, and (ii) stabilizing effect of EG present in the bio-oil.

- OSL process in atmospheric reactor and sealed Parr® reactor was compared. Residue content (RC) was found to be 47 and 25 wt.% at 150 °C for 60 min. when OSL was performed in atmospheric reactor and sealed Parr® reactor, respectively. The atmospheric reactor was determined to be less efficient and lower in RC. Less RC when using a sealed Parr® reactor was attributed to the pressurized effect, which facilitates the penetration of liquefying solvent through biomass so that more biomass undergoes decomposition, resulting in less residue.

- HTL process in water and water/ethanol was studied at sub- and super-critical conditions. For the first time, ^{31}P-NMR and ^{19}F-NMR were employed to understand the effect of ethanol on the OHN of bio-oil.

- ^{31}P-NMR analysis of HTL-bio-oil revealed that addition of ethanol significantly increased the bio-oil yield from 25 to 68 wt.%, and OHN from 3.91 to 7.42 mmol/g. Improved bio-oil yield and OHN was attributed to the hydrogen donation capability of ethanol which stabilizes the free radicals generated during HTL.

- ^{19}F-NMR analysis of HTL showed that carbonyl concentration of HTL-bio-oil decreased from 3.46 to 2.53 mmol/g when ethanol was used as a co-solvent. The decrease in carbonyl concentration was attributed to (i) the stabilization of carbonyl groups to acetal

groups by ethanol, and (ii) the shift of keto–enol tautomerism toward the enol form. It was conjectured that HTL-bio-oil produced using water/ethanol solvent would be more stable since carbonyl group containing compounds are main reason for bio-oil aging.

- Bio-oil could can be utilized as a bio-based curing agent for ERs. A commercial ER (EPON828) was cured with pyrolysis bio-oil. FT-IR analysis showed that OH groups in bio-oil opened the epoxide ring in ER, and created crosslinked structure. The crosslinked structure of bio-oil cured ER was confirmed by DMA analysis which also used to calculate the Tg (120 °C), crosslink density (1891 mol/m^3), and storage modulus at room temperature (2.55 GPa).

- Bio-oil cured ER exhibited only 0.49 wt.% mass loss when extracted with acetone for 4 hours which suggested that the resulting ER had a superior chemical resistance.

- Two different HTL-bio-oils were utilized as a biopolyol in bio-oil-based epoxy resin (BOBER) synthesis: a bio-oil obtained from HTL in water (W-HTL-bio-oil), and water/ethanol HTL (WE-HTL-bio-oil); and for the first time investigated how the addition of ethanol in HTL process further affects the mechanical and thermal properties of epoxy resin.

- The yield of BOBER synthesized using W-HTL was higher than that of WE-HTL; however, equivalent weight (EEW) was lower. The yield of BOBER was found to be up to 99 wt.% with an epoxy equivalent weight (EEW) of 190 g/eq depending on the amount of catalyst used.

169

- BOBER synthesized using WE-HTL exhibited better thermomechanical properties than that of W-HTL. Tg and crosslink density of BOBER from WE-HTL and W-HTL was calculated to be 96 and 63.6 °C; and 58.7 and 8.5 mol/m^3, respectively.

- Finding suggested that not only the total OHN of bio-oil has an effect on the yield and EEW of BOBER, but the distribution of OH groups within bio-oil (aliphatic, phenolic and acidic OH) also plays an important role for the determination of the optimum amount of the catalyst to be used in the synthesis of BOBER.

- BOBER was a self-curing resin which means that when it is heated, it could be cured without help of a curing agent. Self-curing phenomena of BOBER was proved by DSC analysis, and the activation energy of curing calculated to be 95 – 98 kJ/mol, using Kissinger model of kinetic analysis.

- Self-curing phenomena was attributed to etherification reaction which was evidenced by FTIR analysis.

8.2. Future Work

- One of the challenges in epoxy market today is the toxicity problem due to the use of bisphenol-A (BPA). It would be worthwhile to perform toxicity analysis of BOBER. In addition, life cycle assessment (LCA) of BOBER is also needed in order to increase the use of BOBER. LCA is a useful procedure to evaluate the environmental impact of a new

product and it is an internationally accepted method to analyze systematic impacts and outputs of a new product and the consequences to the environment.

- Biodegradability is another concern for our world. There have been a lot of efforts to produce bio-based epoxy resins. To the best of our knowledge, no biodegradability analysis of bio-based epoxy resin has been reported. Therefore, the field of bio-based epoxy resins is in need of biodegradability analysis.

- A comprehensive cost analysis of bio-based epoxy resins is a must. The majority of research focuses on the technical aspects of bio-oil production and synthesis of bio-based epoxy resin. Cost analysis would provide an insight about the future of BOBER.

- Besides epoxy resins, bio-oil could be used as a biopolyol for the synthesis of other widely used polymers such as polyurethane and polyester. It would be very beneficial for the biorefinery process if bio-oil could be utilized in the synthesis of variety of polymers. In order to achieve this, the variation of OH in bio-oil should be dealt with since the OH groups in bio-oil react with the other monomers in the polymer synthesis. Due to the complex nature of lignocellulosic biomass, bio-oil contains aliphatic, aromatic and acidic type of OH groups. It is known that aliphatic OHs are not as reactive as aromatic and acidic types. Thus, incomplete reaction is inevitable. Modification of bio-oil to produce a bio-oil with uniform OH groups would increase the utilization of bio-oil in the synthesis of different polymers which will enhance the feasibility of biorefinery process.

- Although commercial epoxy resins exhibit excellent adhesive properties, they are not used in the wood composite market due to the poor epoxy-wood bond upon water exposure. However, this may not be the case for BOBER because bio-oil could improve the wood stability under excessive swelling and shrinkage. Introducing BOBER to the wood composite market will open new avenues for the epoxy resins.